ACARP

Australian Coal Association Research Program

FINAL REPORT

Post Mining Landscape Parameters for Erosion and Water Quality Control

C4011 and C5009

November 1998

ACARP

Australian Coal Association Research Program

"Post Mining Landscape Parameters for Erosion and Water Quality Control "

H.B. So, G.J. Sheridan, R.J. Loch, C. Carroll, G.Willgoose,
M. Short, A. Grabski

Final Report Projects 1629 & 4011
November 1998

THE UNIVERSITY OF QUEENSLAND

A COLLABORATIVE PROJECT BETWEEN

School of Land and Food

THE UNIVERSITY OF QUEENSLAND

CENTER FOR MINED LAND REHABILITATION

The UNIVERSITY of NEWCASTLE AUSTRALIA

NATURAL RESOURCES

ACIRL

and

INDUSTRY

Environmental Officers from 15 minesites

The research was supported & funded by:

ACARP
Australian Coal Association Research Program

BHP

MIM
HOLDINGS
LIMITED

CAPCOAL

CURRAGH

CALLIDE
COALFIELDS

PACIFIC COAL
PTY. LIMITED
A.C.N. 010 542 140

ARCO Coal Australia Inc.

Table of Contents

List of Tables

List of Figures

Executive summary

This report covers the achievements of two successive ACARP projects, C1629 (1992-1994), and C4011 (1995-1997), entitled ***'Postmining Landscape Parameters for Erosion and Water Quality Control'*** (PLPEWC). In addition, this report will also cover ACARP project C5009 which is an extension of Field Plot monitoring in this project. The project is a result of close consultations with the mining industry over a considerable time prior to the commencement of the project in 1992. The project combined the skills and expertise of researchers from the School of Land and Food & the Centre for Mined Land Rehabilitation of the University of Queensland, the Queensland Department of Natural Resources, the University of Newcastle and the Australian Coal Industry Research Laboratories in Ipswich, with the skills and experience of environmental officers from 15 open cut coal mines in the Bowen Basin. Close collaboration and consultation between the project partners was maintained throughout the project through a steering committee comprised of representatives from each of the contributing mining companies and research staff. The steering committee reviewed the project at 3 monthly intervals and provided feedback and direction. This represented continuous monitoring by industry, in a co-operative spirit, to ensure that research maintained its focus on issues relevant to the mining industry.

The PLPEWC project addressed a major problem of the open-cut coal mining industry, ***viz. 'how to achieve economic postmining reconstruction which meets the criteria of acceptable erosion and runoff water quality'***. The project was jointly funded by the Australian Coal Association Research Program (ACARP) and the 6 major coal mining companies, BHP Coal Pty Ltd, MIM Holdings Ltd, Pacific Coal Pty Ltd, Curragh Queensland Mining Ltd, Callide Coalfields Pty Ltd, and Capricorn Coal Management Pty Ltd.

Objectives of the project :

The major objectives of the PLPEWC project were:

(i) to develop appropriate methodologies to determine the critical range of degree of slope - length of slope - vegetative cover combinations for acceptable control of erosion and salt generation, as an aid towards the design of stable and sustainable postmining landforms;

(ii) to survey and determine the success of existing rehabilitation/revegetation strategies as an aid towards the validation of the above mentioned design criteria;

(iii) to provide training and technology transfer to allow the integration of research outcomes into the development of efficient environmental management practices on minesites.

The first two objectives were pursued through a series of experimental programs at 4 different scales: the laboratory flume, the field rainfall simulation plots, the field erosion plots and the field catchments. An erosion survey of existing rehabilitated sites was initiated during the latter part of the project, while a substantial effort was devoted into the integration of the results into computer models that are useful in the landscape design process at the mine. These models are supplied on a CD rom with the main report.

There were 7 component projects within this program and details of these are contained in the main report. These components and the institutions responsible for each component are:

1. Laboratory erosion experiments using the tilting flume-rainfall simulation facility at the Erosion Processes Laboratory (EPL) of the University of Queensland, and the development of a methodology to predict potential erosion in the field from laboratory derived parameters (The University of Queensland);
2. Laboratory experiments on salt generation using the EPL and the development of a model to predict salt generation from eroding surfaces (The University of Queensland);
3. Field rainfall simulation and the development of a methodology to determine the optimal slope-slope length-vegetative cover combinations required for effective erosion control (Queensland Dept of Natural Resources Toowoomba & The University of Queensland);
4. Field erosion plots to determine the extent of erosion and salt generation for a limited set of treatments (bare spoil and soil, spoil and soil with grasses and native vegetation developed on 10, 20 and 30% slopes) under natural rainfall (Queensland Dept of Natural Resources, Emerald). Project C5006 was originally conceived as an extension of the main project, to monitor the water relations of these plots and derive the Plant Available Water Capacity (PAWC) of the soils and spoils in these field plots. However, approval was not received for an increase in the commitments required from our QDNR collaborators, and the steering committee decided to move this project to the University of Queensland and expand the determination of PAWC to all soils and spoils. Results of this work are reported as part of the material characteristics (Table 3.1);
5. Field catchments to determine the extent of erosion and salt generation from a series of small catchments, to be used for the adaptation and calibration of the Landscape Evolution Model SIBERIA for use on the materials from the Bowen Basin (Queensland Dept of Natural Resources Emerald & The University of Newcastle);
6. Development of a computer package which links SIBERIA to existing landscape design packages such as ARGUS, MINCOM, VULCAN etc. This package is intended to predict the effect of erosion on future designed landscapes (The University of Newcastle & ACIRL);
7. Field erosion survey to determine the success of existing rehabilitation strategies for the prevention of erosion, and to examine the factors responsible for erosion on these sites (The University of Queensland).

Experimental Strategy:

The 7 components of the project represent the collective approach adopted by the research team and the relationship between them is shown diagrammatically in Figure 1-1. The essential components of the strategy are:

1. Field plots of 20 m x 5 m (100m^2) and catchments (up to 2.5 ha) under natural rainfall were designed to measure field parameters most relevant to the erosive events expected on these soils/spoils. These parameters are required for the prediction of potential soil loss that may occur on soil/spoil under a set of environmental conditions which will be unique for each mine. However, the cost of these field plots/catchments are very high, hence it was not possible to cover all mines, nor was it possible to cover all possible

treatments. Therefore, these plots were located on 3 representative mines covering the range of materials from the Bowen Basin, with a limited range of treatments. Monitoring of erosion parameters will have to be conducted over a sufficiently long period that is representative of the range of conditions expected in the region;

2. Due to the large variability between materials, determination of field parameters for all other materials was conducted with the portable field rainfall simulator on 12 m x 1.5 m (18 m^2) plots. Erosion parameters were determined under similar conditions with rainfall of 100 mm/h for 30 minutes considered to be representative of the intensity of rainstorms that can be expected in the Bowen Basin. Therefore, these erosion parameters represented valid comparisons between mine materials. An additional advantage of the simulator is that vegetated plots can be investigated to derive relevant vegetative cover functions. The Modified Universal Soil Loss Equation (MUSLE) was selected for extrapolation beyond the experimental conditions, due to its simplicity and robust nature;

3. Laboratory techniques, using a tilting flume and rainfall simulator combination, were investigated to determine whether potential erosion in the field can be predicted from laboratory measurements, as field rainfall simulations are expensive to conduct. An appropriate robust and rapid laboratory based methodology could significantly reduce future cost to the industry for the determination of the relevant erosion parameters. Furthermore planning postmining landscapes can be initiated prior to the mining operation. This facility was also used to develop the necessary parameters for a salt generation model;

4. In anticipation of the possible need to predict future landscapes after mining, the landscape evolution model SIBERIA was adapted and calibrated for the materials from the Bowen Basin. The University of Newcastle developed the landscape evolution model;

5. However, the ultimate test of the sustainability of rehabilitation strategies will be in the field itself. The spatial, temporal and material variability in the field could not be represented by the materials used to derive the erosion parameters for the models. Therefore, a field survey was initiated during the last two years of the project to determine potential site factors and the probability of erosion events on existing rehabilitated sites, and to provide data for the validation of model results. Furthermore, this survey may provide relevant information on the industries' best practice.

During the early years of the project, each individual project component operated independently. Contact was maintained between these components to ensure that the results would be integrated. The first two years following installation of instruments in the field were drought years in central Queensland and progress on the field plot and catchment components was very slow. Much of the work was concentrated in the laboratory and in the field with the field rainfall simulator. Integration between the various components was conducted during the last two years through informal meetings and two formal workshops amongst the researchers. At the last workshop, industry members of the steering committee participated to put forward the industry viewpoints and to maintain an industry focus during the integration process.

The results showed good agreement in the values of erodibility and sediment delivery rates measured at the different levels. However a lack of representative data from field plots allowed only limited comparisons to be made between the field plots and the field/laboratory simulator plots. The comparison with field data is expected to be revisited at the end of the year 2000 when the current monitoring program of the field plots will be completed and data collection can be expected to cover a representative range of climatic conditions for Central Queensland. Currently, the most extensive and immediately useful data for the design of postmining landforms are derived from the field and laboratory rainfall simulator components of the project.

The results from the field rainfall simulation part of the project indicated that in general, the materials studied (topsoils and spoils) showed relatively low infiltration capacities. Therefore infiltration of rain will initially be poor, making establishment of vegetation difficult. Erodibilities (susceptibility to erosion) vary considerably, and effective erodibilities (with surface rock cover taken into account) will be low for some spoils in particular. However, the low water holding capacity of rocky materials is likely to impose limitations on the potential productivity and stability of rehabilitated areas based on those materials, unless the rock weathers to produce finer-grained minerals within a reasonably short period.

The potential impact of vegetation on erosion from rehabilitated soils is enormous. Under vegetation, infiltration capacities increase greatly, soil structure is improved and erosion can be greatly reduced. The type of vegetation established and its productivity can impact on the effectiveness of site stabilization. As a general rule, 30 to 40% vegetation cover will be required to reduce erosion to acceptable levels. For that reason, the *PGM* model, a combination of 3 existing public domain models *Perfect-Grasp-Musle*, was specifically designed to focus on impacts of vegetation on runoff and erosion, while giving information on slope gradients and length that would guide the design and management of rehabilitated sites. *Perfect* models the hydrology of the soil/spoil and determines the amount of plant available water, which is used by *Grasp* to determine the grass biomass and the vegetative cover. This vegetative cover is then used as the input into *Musle* to determine the slope gradient-length-vegetative cover that will result in erosion of a particular desired magnitude. The PGM modeling package represents the simplest and most relevant way for the extensive database (rainfall simulator data and physical-chemical data of all materials) from this study to be accessed by environmental officers at the participating minesites. Like all models, it will gradually become obsolete or in need of upgrade. However, in the short term it presents a powerful tool for assessing many aspects of mine rehabilitation.

The PGM module should be useful for deriving appropriate criteria for designing suitable post-mining landscapes specific to each minesite. However should the mine be interested in what the future landscape will look like, after it has been subjected to erosion, it can gain an appreciation of that future landscape through the *EAMS* (Environmental Assessment Management System) module. If the designed landscape is not likely to be sustainable, EAMS can be used to derive a more acceptable set of criteria as a feedback to the PGM module, which can produce a final acceptable design criteria for landscape design.

Extrapolation to other soil-climate combinations from the current field rainfall simulation and field plot data may not be appropriate and may require additional field measurements which are expensive and resource intensive. If potential field erosion can be predicted from laboratory based measurements, additional data collection necessary for future rehabilitation activities will be faster and less costly. Landscape design can be initiated and potential failures predicted prior to mine construction. The laboratory research demonstrated that potential soil losses from bare unconsolidated hillslope surfaces associated with the combined processes of rill and interill erosion, could successfully be predicted from laboratory scale measurements of erodibility. This project has also shown that material erodibility parameters can be predicted from the physical and chemical properties of the media, which are readily available from routine soil analysis. Relevant analyses are texture (clay and fine sand contents), organic carbon contents, pH, bulk density, dispersed silt and clay contents, Exchangeable Sodium Percentage (ESP) and the electrical conductivity (EC) of the soil solution. A user-friendly Windows based application of the MINE*rosion* model should enable these research findings to be utilized by the mining industry as an aid towards the successful design of stable post-mining landforms.

The major potential offsite pollutant associated with erosion is salt generated by run-off from postmining landscapes. This project has successfully developed the *SaltRO* model, which predicts potential salt generation associated with erosion from these landscapes. A library of the relevant parameters has been completed for 8 minesites. Work is continuing to complete this library for the other 7 minesites and results will be made available to all participating mines.

Field experience at minesites indicated that successfully revegetated minesites may still erode at significant rates. Similarly, minesites designed using the methodology developed in this project may still be subject to erosion after successful revegetation. A simple methodology was developed towards the latter part of the project to estimate the degree of erosion that had occurred on rehabilitated minesites, to relate these erosion rates to relevant site factors, and to provide information on the potential best practice in rehabilitation of opencut coal mines. This information may also be useful for the validation of the model outcomes. This component of the project is continuing and results will be made available to all participating mines.

During the life of the project, all environmental officers of the participating mines and officers of the Department of Mines and Energy, were briefed annually at workshops held for this purpose. Other interested parties also attended these workshops. On the 30 October-1 November 1997 a two day workshop was held as a training workshop for environmental officers in the use of the models developed in this project.

Outcomes from the project :

Overall the project has achieved its major objective of providing the industry with methodologies and design packages that will be useful for the prediction, prevention or minimisation of erosion from postmining landscapes. Optimal landscape design can now be achieved using data derived from field plots, field catchments and field rainfall simulator plots. It can also be achieved using laboratory flume data and data derived from routine soil analysis, but is currently limited to bare, unconsolidated materials only. Similarly, salt generation can be predicted from data derived from the laboratory for bare, unconsolidated materials only.

Further work will be necessary if these results are to be extrapolated to other regions or soils, and to further develop the laboratory components of the project, if they are needed to cover a wider range of conditions in the field. The field erosion plots and catchments and the field erosion survey are currently incomplete and this part of the project is on-going with continued ACARP funding for the field plots and catchments.

The major outcomes from this project are:

1. An extensive database of physical and chemical properties for 34 materials from the Bowen Basin covering spoil and topsoil;

2. A user-friendly Windows - based PGM (PERFECT/GRASP/MUSLE) design package to determine the optimal combination of slope, slope length and vegetative cover that will limit erosion to acceptable levels;
3. A Windows-based EAMS (Environmental Assessment Management System) package that predicts future landscapes subjected to erosion under a selected set of climatic conditions;
4. A user friendly Windows-based MINE*rosion* model to predict the potential soil loss from laboratory rainfall simulator-tilting flume derived parameters;
5. A SaltRO model to predict potential salt generation from eroding surfaces; and
6. A simple survey methodology to determine the extend of erosion on rehabilitated minesites.

The database of soil/spoil properties and the models are included as a CD-Rom with the main report and a 22 minutes video report of the project.

Finally, we would like to thank the Australian Coal Association Research Program (ACARP), BHP Coal Pty Ltd, MIM Holdings Ltd, Pacific Coal Pty Ltd, Curragh Queensland Mining Ltd, Callide Coalfields Pty Ltd, and Capricorn Coal Management Pty for their generous and continuous financial, technical, operational and moral support. Thanks also to the many Environmental Officers who supported the work on-site, and particularly the officers who participated in the management of the project through the steering committee. We would also like to express our appreciation to Professor L.C. Bell, who was responsible for initiating this project and was chairman of the steering committee for the first two years.

1. Project overview

This report covers the achievements of two successive ACARP projects, C1629 (1992-1994), and C4011 (1995-1997), entitled ***'Postmining Landscape Parameters for Erosion and Water Quality Control'*** (PLPEWC). In addition, this report will also cover ACARP project C5009 which is an extension of Field Plot monitoring in this project. This report will also cover ACARP project C5009 which is an extension of Field Plot monitoring in this project. The project is a result of close consultations with the mining industry over a considerable time prior to the commencement of the project in 1992. The project combined the skills and expertise of researchers from the School of Land and Food & the Centre for Mined Land Rehabilitation of the University of Queensland, the Queensland Department of Natural Resources in Toowoomba and Emerald, the University of Newcastle and the Australian Coal Industry Research Laboratories in Ipswich, with the skills and experience of environmental officers from 15 open cut coal mines in the Bowen Basin. Close collaboration and consultation between the project partners was maintained throughout the project through a steering committee comprised of representatives from each of the contributing mining companies and research staff. The steering committee reviewed the project at 3 monthly intervals and provided feedback and direction. This represented continuous monitoring by industry, in a co-operative spirit, to ensure that research maintained its focus on issues relevant to the mining industry.

Open-cut coal mining and associated activities necessitate the disturbance of large areas of land, which must be stabilized and rehabilitated following mining operations. In central Queensland, the area disturbed by open-cut coal operations exceeds 50,000 ha (Welsh *et al.* 1994). The first step during mine-site rehabilitation is the design of the post-mining landform. This is also the most expensive component of the rehabilitation process as it involves extensive earthworks requiring heavy plant and equipment. In 1993, the cost of rehabilitation was estimated to range from $5,000 to $25,000 per hectare (Bell *et al.* 1993). The primary aim of the earthworks is to produce a post-mining landscape that is resistant to geo-technical failure and surface erosion processes, and which will be able to support vegetation for a sustainable and maintenance free post-mining land use. The extent and cost of earthworks may be minimised, and rehabilitation failures avoided, if soil erosion from post-mining landforms can be predicted prior to construction.

The PLPEWC project addressed a major problem of the open-cut coal mining industry, ***viz.*** ***'how to achieve economic postmining reconstruction which meets the criteria of acceptable erosion and runoff water quality'***. Therefore, the principle objective of this research program was to provide the necessary information and tools to assist the open-cut coal mining industry to design stable post-mining landforms with acceptable levels of erosion and runoff water quality. The project was jointly funded by the Australian Coal Association Research Program (ACARP) and the 6 major coal mining companies, BHP Coal Pty Ltd, MIM Holdings Ltd, Pacific Coal Pty Ltd, Curragh Queensland Mining Ltd, Callide Coalfields Pty Ltd, and Capricorn Coal Management Pty Ltd.

Soil erosion prediction models have mostly been developed for solving erosion problems associated with agricultural conditions. The surface media, topography and management practices on minesites are very different to those found in agricultural settings, and hence it is unclear whether these models will work satisfactorily under these different conditions. Current erosion models were largely developed on low slopes, generally <15%, and were derived from data collected under temperate rainfall patterns. They are not suitable for use on the steep slopes of the Central Queensland postmining landscapes, which are exposed to intense tropical rainstorms during the summer period.

The specific objectives of the project are therefore:

(i) to develop appropriate methodologies to determine the critical range of degree of slope - length of slope in combination with vegetative cover for acceptable control of erosion and salt generation, as an aid towards the design of stable and sustainable postmining landforms;

(ii) to survey and determine the success of existing rehabilitation/revegetation strategies as an aid towards the validation of the above mentioned design criteria;

(iii) to provide training and technology transfer to allow the integration of research outcomes into the development of efficient environmental management practices on minesites.

The first objective was pursued through a series of experimental programs at 4 different scales: the laboratory flume, the field rainfall simulation plots, the field erosion plots and the field catchments. An erosion survey of existing rehabilitated sites was initiated during the latter part of the project, while a substantial effort was devoted into the integration of the results into computer models that are useful in the landscape design process at minesites.

There were 7 component projects within this program and details of these are contained in the main report. These components and the institutions responsible for each component are:

1. Laboratory erosion experiments using the tilting flume-rainfall simulation facility at the Erosion Processes Laboratory (EPL) of the University of Queensland, and the development of a methodology to predict potential erosion in the field from laboratory derived parameters (The University of Queensland);

2. Laboratory experiments on salt generation using the EPL and the development of a model to predict salt generation from eroding surfaces (The University of Queensland);

3. Field rainfall simulation and the development of a methodology to determine the optimal slope-slope length-vegetative cover combinations required for effective erosion control (Queensland Dept of Natural Resources Toowoomba & The University of Queensland);

4. Field erosion plots to determine the extent of erosion and salt generation for a limited set of treatments (bare spoil and soil, spoil and soil with grasses and native vegetation developed on 10, 20 and 30% slopes) under natural rainfall (Queensland Dept of Natural Resources, Emerald). Project C5006 was originally conceived as an extension of the main project, to monitor the water relations of these plots and derive the Plant Available Water Capacity (PAWC) of the soils and spoils in these field plots. However, approval was not received for an increase in the commitments required from our QDNR collaborators, and the steering committee decided to move this project to the University of Queensland and expand the determination of PAWC to all soils and spoils. Results of this work are reported as part of the material characteristics (Table 3.1);

5. Field catchments to determine the extent of erosion and salt generation from a series of small catchments, to be used for the adaptation and calibration of the Landscape

Evolution Model SIBERIA for use on the materials from the Bowen Basin (Queensland Dept of Natural Resources Emerald & The University of Newcastle);

6. Development of a computer package which links SIBERIA to existing landscape design packages such as ARGUS, MINCOM, VULCAN etc. This package is intended to predict the effect of erosion on future designed landscapes (The University of Newcastle & ACIRL);

7. Field erosion survey to determine the success of existing rehabilitation strategies for the prevention of erosion, and to examine the factors responsible for erosion on these sites (The University of Queensland).

Experimental Strategy:

The 7 components of the project represent the collective approach adopted by the research team and the relationship between them is shown diagrammatically in Figure 1-1.

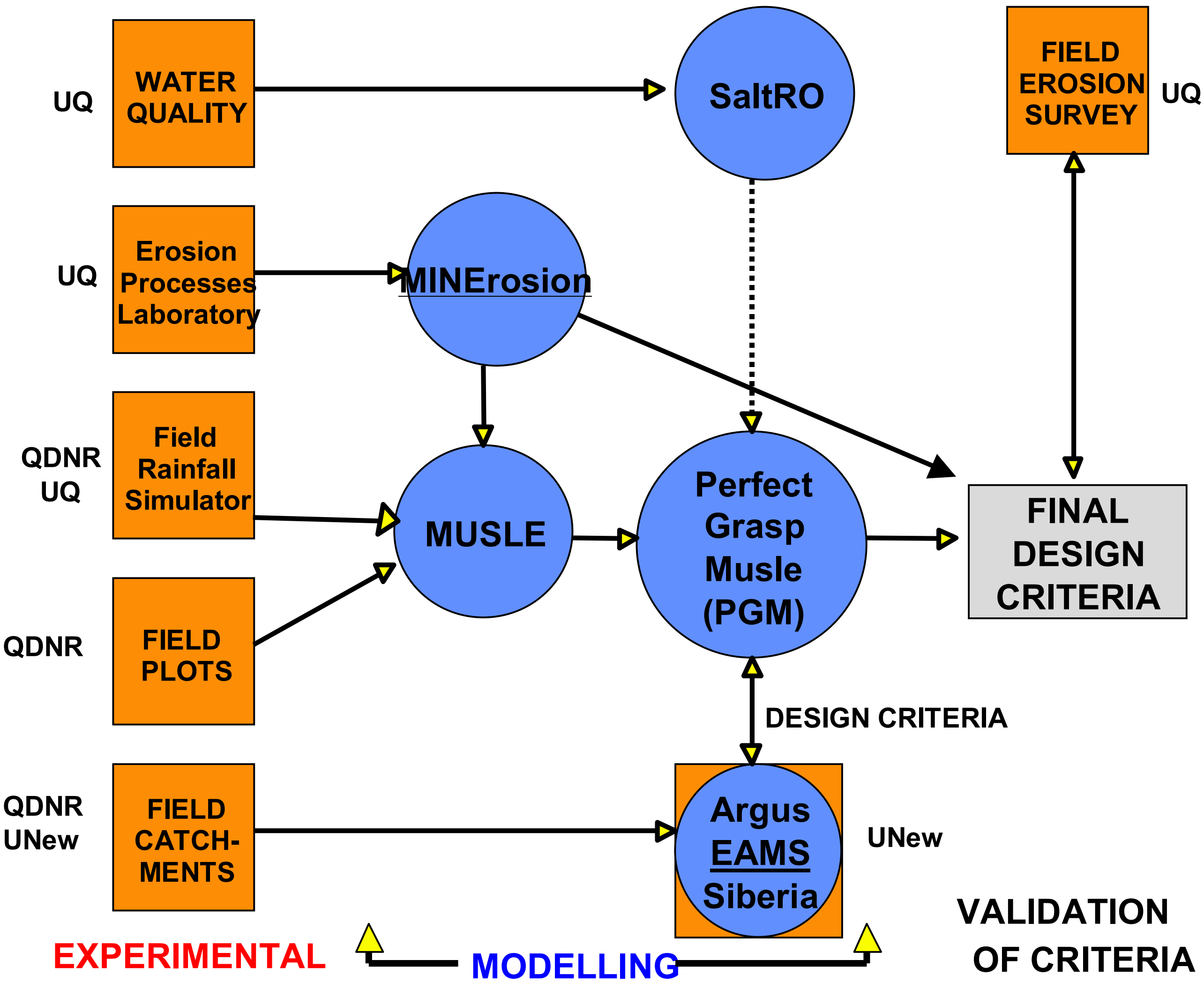

Figure 1-1 Key activities of the project

The essential elements of the experimental strategy adopted for this project are:

1. Hillslope field plots of 20 m x 5 m (100m^2) and catchments (up to 2.5 ha) under natural rainfall should provide the best representation of the physical system under study, and hence it should provide the most realistic data. They were designed to measure field parameters most relevant to the erosive events expected on these soils/spoils. These parameters are required for the prediction of potential soil loss that may occur on soil/spoil under a set of environmental conditions, which will be unique for each mine. However this type of research is very expensive to conduct, and it requires continuous monitoring over an extended period to cover a sufficiently representative range of climatic conditions. Investigations are therefore restricted to 3 representative mines covering the range of materials from the Bowen Basin, with a limited range of treatments;

2. Due to the large variability between materials, determinations of field parameters for all other materials were conducted with the portable field rainfall simulator on 12 m x 1.5 m (18 m^2) plots. Erosion parameters were determined under similar conditions with rainfall of 100 mm/h for 30 minutes considered to be representative of the intensity of rainstorms that can be expected in the Bowen Basin. Therefore, these erosion parameters represented valid comparisons between mine materials. An additional advantage of the simulator is that vegetated plots can be investigated to derive relevant vegetative cover functions. The Modified Universal Soil Loss Equation (MUSLE) was selected for extrapolation beyond the experimental conditions, due to its simplicity and robust nature;

3. Laboratory techniques, using a combination of tilting flume and rainfall simulator, were developed to explore whether potential erosion in the field could be predicted from laboratory measurements, as field rainfall simulations are expensive to conduct. An appropriate robust and rapid laboratory based methodology could significantly reduce future cost to the industry for the determination of the relevant erosion parameters. Furthermore planning postmining landscapes can be initiated prior to the mining operation. This facility was also used to develop the necessary parameters for a salt generation model;

4. In anticipation of the possible need to predict future landscapes after mining, the landscape evolution model SIBERIA was adapted and calibrated for the materials from the Bowen Basin. The University of Newcastle developed the landscape evolution model;

5. However, the ultimate test of the sustainability of rehabilitation strategies will be in the field itself. The materials used to derive the erosion parameters for the models could not represent the spatial, temporal and material variability in the field. Therefore, a field survey was initiated during the last two years of the project to determine potential site factors that affect erosion and the probability of erosion events on existing rehabilitated sites, and to provide data for the validation of model results. Furthermore, this survey may provide relevant information on the industries' best practice.

During the early years of the project, each individual project component operated independently. Contact was maintained between components to ensure that the results could be integrated. The first two years following installation of instruments in the field were drought years in central Queensland, and progress on the field plot and catchment components was very slow. Much of the work was concentrated in the laboratory and in the field with the rainfall simulator. Integration between the various components was conducted during the last two years through informal meetings and two formal workshops amongst the researchers. At the last workshop, industry members of the steering committee participated to put forward the industry viewpoints and to maintain an industry focus during the integration process.

The results showed good agreement in the values of erodibility and sediment delivery rates measured at the different levels. However a lack of representative data from field plots allowed only limited comparisons to be made between the field plots and the field/laboratory simulator plots. The comparison with field data is expected to be revisited at the end of the year 2000 when the current monitoring program of the field plots will be completed and data collection can be expected to cover a representative range of climatic conditions for Central Queensland. Currently, the most extensive and immediately useful data for the design of postmining landforms are derived from the field and laboratory rainfall simulator components of the project.

The results from the field rainfall simulation part of the project indicated that in general, the materials studied (topsoils and spoils) showed relatively low infiltration capacities. Therefore infiltration of rain will initially be poor, making establishment of vegetation difficult. Erodibilities (susceptibility to erosion) vary considerably, and effective erodibilities (with surface rock cover taken into account) will be low for some spoils in particular. However, the low water holding capacity of rocky materials is likely to impose limitations on the potential productivity and stability of rehabilitated areas based on those materials, unless the rock weathers to produce finer-grained minerals within a reasonably short period.

The potential impact of vegetation on erosion from rehabilitated soils is enormous. Under vegetation, infiltration capacities increase greatly, soil structure is improved and erosion can be greatly reduced. The type of vegetation established and its productivity can impact on the effectiveness of site stabilization. As a general rule, 30 to 40% vegetation covers will be required to reduce erosion to acceptable levels. For that reason, the *PGM* model, a combination of 3 existing public domain models *Perfect-Grasp-Musle*, was specifically designed to focus on impacts of vegetation on runoff and erosion, while giving information on slope gradients and length that would guide the design and management of rehabilitated sites. *Perfect* models the hydrology of the soil/spoil and determines the amount of plant available water, which is used by *Grasp* to determine the grass biomass and the vegetative cover. This vegetative cover is then used as the input into *Musle* to determine the slope gradient-length-vegetative cover that will result in acceptable erosion rates. The PGM modeling package represents the simplest and most relevant way for the extensive database (rainfall simulator data and physical-chemical data of all materials) from this study to be accessed by environmental officers at the participating minesites. Like all models, it will gradually become obsolete or in need of upgrade. However, in the short term it presents a powerful tool for assessing many aspects of mine rehabilitation.

The PGM module should be useful for deriving appropriate criteria for designing suitable post-mining landscapes specific to each minesite. However should the mine be interested in what the future landscape will look like, after it has been subjected to erosion, it can gain an appreciation of that future landscape through the *EAMS* (Environmental Assessment Management System) module. If the designed landscape is not likely to be sustainable, EAMS can be used to derive a more acceptable set of criteria as a feedback to the PGM module, which can produce a final acceptable design criteria for landscape design.

Extrapolation to other soil-climate combinations from the current field rainfall simulation and field plot data may not be appropriate and may require additional field measurements which are expensive and resource intensive. If potential field erosion can be predicted from laboratory based measurements, additional data collection necessary for future rehabilitation activities will be faster and less costly. Landscape design can be initiated and potential failures predicted prior to mine construction. The laboratory research demonstrated that potential soil losses from bare unconsolidated hillslope surfaces associated with the combined processes of rill and interill erosion could successfully be predicted from laboratory scale measurements of erodibility. This project has also shown that material erodibility parameters can be predicted from the physical and chemical properties of the media, which are readily available from routine soil analysis. Relevant analyses are texture (clay and fine sand contents), organic carbon contents, pH, bulk density, dispersed silt and clay contents, Exchangeable Sodium Percentage (ESP) and the electrical conductivity (EC) of the soil solution. A user-friendly Windows based application of the MINE*rosion* model should enable these research findings to be utilized by the mining industry as an aid towards the successful design of stable post-mining landforms.

The major potential offsite pollutant associated with erosion is salt generated by run-off from postmining landscapes. This project has developed the *SaltRO* model, which predicts potential salt generation associated with erosion from these landscapes. A library of the relevant parameters has been completed for 8 minesites. Work is continuing to complete this library for the other 7 minesites and results will be made available to all participating mines as soon as these become available.

Field experience at minesites indicated that successfully revegetated minesites might still erode at significant rates. Similarly, minesites designed using the methodology developed in this project may still be subject to erosion after successful revegetation. A simple methodology was developed towards the latter part of the project to estimate the degree of erosion that had occurred on rehabilitated minesites, to relate these erosion rates to relevant site factors, and to provide information on the potential best practice in rehabilitation of opencut coal mines. This information may also be useful for the validation of the model outcomes. This component of the project is continuing and results will be made available to all participating mines.

During the life of the project, all environmental officers of the participating mines and officers of the Department of Mines and Energy were briefed annually at workshops held for this purpose. Other interested parties also attended these workshops. A two-day workshop was held on 30 October-1 November 1997, as a training workshop for environmental officers in the use of the models developed in this project.

Outcomes from the project:

Overall the project has achieved its major objective of providing the industry with methodologies and design packages that will be useful for the prediction, prevention or minimization of erosion from postmining landscapes. Optimal landscape design can now be achieved using data derived from field plots, field catchments and field rainfall simulator plots. It can also be achieved using laboratory flume data and data derived from routine soil analysis, but is currently limited to bare, unconsolidated materials only. Similarly, salt generation can be predicted from data derived from the laboratory for bare, unconsolidated materials only.

Further work will be necessary if these results are to be extrapolated to other regions or soils, and to further develop the laboratory components of the project, if they are needed to cover a wider range of conditions in the field. The field erosion plots and catchments and the field erosion survey are currently incomplete and this part of the project is on-going with continued ACARP funding for the field plots and catchments.

The major outcomes from this project are:

1. An extensive database of physical and chemical properties for 34 materials from the Bowen Basin covering spoil and topsoil;
2. A user-friendly Windows - based PGM (PERFECT/GRASP/MUSLE) design package to determine the optimal combination of slope, slope length and vegetative cover that will limit erosion to acceptable levels. The PGM Module estimates the hydrology, grass production and erosion rates from mine overburdens and soils at the hillslope scale. The model is based on the integration of three different models, a grass growth model, a surface runoff model and a soil erosion model. The model is particularly suited to the investigation of the interaction between vegetation growth and erosion in the medium term. The effect of combinations of topsoil on overburden can also be investigated. The model can be applied to the soils and overburdens tested within this project. The model is accessible to users with little or no prior knowledge of erosion modeling;
3. A Windows-based EAMS (Environmental Assessment Management System) package that predicts future landscapes. The EAMS package allows the prediction of long term (up to 1000 years) three dimensional landscape evolutions resulting from erosion by runoff. The model brings together several existing models, including SIBERIA, a grid DTM based long-term erosion model and DISTFW, and a grid DTM based hydrology model. These sub-models have been linked together within a Windows based application. Landform designs can be inputted from conventional mine packages such as ARGUS, VULCAN, MINCOM etc for evaluation using the EAMS package. The outputs from the model can be used to determine long-term erosion rates and assess the possibility and potential location of gully development;
4. A user-friendly Windows-based MINE*rosion* model to predict the potential soil loss from laboratory rainfall simulator-tilting flume derived parameters. MINE*rosion* is a computer-based application that allows the estimation of erosion rates from design storms at the hillslope scale. The processes of rill and interill erosion are modeled separately, providing an improved ability to predict the relationship between slope gradient, slope length and erosion rates from bare unconsolidated media. If a soil or overburden has not been tested by this project, the model can predict its erodibility from the easily measured properties of the media and use this value to predict erosion rates. The model can be used by non-experts to answer questions such as "How much erosion can I expect from a design (eg 1 in 10 year) storm, given a particular combination of slope length, slope gradient and media type". The model will be useful to estimate the potential erosion from post-mining landscapes prior to mining operations;
5. A SaltRO model to predict potential salt generation from eroding surfaces. SaltRO is a windows based application that allows the prediction of salt accumulation, depletion and release with runoff water from the surface of reconstructed mining landscapes. The model is one-dimensional and confines itself to the surface layer. The model is currently being checked for problems and the necessary parameter libraries are nearly completed. This model will be supplied to all participating mines as soon as it is completed;
6. A simple field survey methodology to systematically evaluate and record the success of existing rehabilitation strategies with respect to surface erosion. Results from this

survey may provide a method for validating the erosion prediction from this project. The methodology has been used to evaluate rehabilitated landforms on eight minesites and results are being processed. This methodology will also be useful as a performance indicator for erosion control;

7. A 22 minute video report of the project, a database of soil/spoil properties and the models (PGM and MINE*rosion*) are included as a CD-ROM with this report.

1.1 Project personnel

Research Personnel:

The University of Queensland: Assoc. Prof. Hwat Bing So -Project Leader 1994/98
Professor L.C.Bell - Project Leader 1992-1993
Assoc. Prof. T Aspinall
Dr J Kuszmaul
Project Coordinator: Dr Bernie Kirsch, 1992-1995
Mr Andrew Grabski, 1995-1997
Mr Gary Sheridan, 1998
Post Graduate students: C M Walker, C Pocknee, G Sheridan, M Short, C Caroll and C Balisacan

Queensland Department of Natural Resources, Toowoomba and Landloch Pty:
Dr R J Loch

Queensland Department of Natural Resources, Emerald:
Mr C Carroll

The University of Newcastle, Department of Civil Engineering:
Dr G Willgoose
Dr Yeboah Agassi (Research Fellow)

Australian Coal Industry Research Laboratories (ACIRL):
Mr David Haneman

Industry Personnel:

Steering Committee members:
Mr Peter Roe, BHP Coal Pty Ltd and ACARP Monitor
Mr Frank Ford, Callide Coalfields Ltd and Shell Australia Ltd
Mr Mick O'Keefe, Callide Coalfields Ltd
Mr Rob McNamara, MIM Holdings Ltd
Mr Alex Armstrong, Arco Coal Aust Inc - Curragh Queensland Mining Ltd
Mr Peter Johnstone-Kevin Smith, Curragh Queensland Mining Ltd
Mr Bruce Foster, Randall Hinze & Peter Baker, Tarong Coal
Mr Nick Lefebre-Mark Garraghy, Oakey Creek Coal Pty Ltd
Mr Alex Campbell, BHP Coal Pty Ltd
Mr Tim Crossley–Ross Wilson, Goonyella-Riverside Mine, BHP Coal Pty Ltd
Mr John Merritt, Capricorn Coal Management Pty Ltd

2. Publications arising out of this project

1. Carroll, C., Loch, R., and Halpin, M. (1992). Post-mining landscape parameters for erosion and water quality control. Poster presentation. AMIC Environmental Conference. Yeppoon Qld. 5-9 October 1992.
2. L.C.Bell; R.J.Loch; D.Haneman and G.R. Willgoose (1993) A Post-mining landform research program for open-cut coal mines. AMIC Environmental Workshop, Burnie 1993.
3. R.J. Loch; C Pocknee and B. Kirsch (1993). Infiltration properties of spoil and topsoil on open cut coalmines in Qld. Proceedings Waste Rock Dump Symposium, Darwin 1993.
4. Kirsch, B.; So, H.B.; and Pocknee, C. (1994). Surface sealing, crusting and hardsetting on open-cut coal mining in Queensland. 2nd Intl Symp on Sealing, Crusting and Hardsetting Soils: Productivity and Conservation. Aust Soc Soil Sci Inc, Brisbane, 7-11 Feb 1994.
5. Sheridan, G.J.; Walker, C.M.; Kirsch, B. and So, H.B. (1994). The effect of wetting/drying cycles on run-off and erosion for a Queensland minesite soil and overburden. 2nd Intl Symp on Sealing, Crusting and Hardsetting Soils: Productivity and Conservation. Aust Soc Soil Sci Inc, Brisbane, 7-11 Feb 1994.
6. Walker, C.M.; Sheridan, G.J.; Kirsch, B.; So, H.B. and Loch, R.J. (1994). A laboratory rainfall simulator -tilting flume facility for the determination of soil erosion model parameters. 2nd Intl Symp on Sealing, Crusting and Hardsetting Soils: Productivity and Conservation. Aust Soc Soil Sci Inc, Brisbane, 7-11 Feb 1994.
7. So, H B, Kirsch, B; Loch, R J; Carroll, C and Wilgoose, G (1994). Postmining landscape parameters for erosion and water quality control. Aust Mining Industry Council annual conference, Dampier, Oct 10-13, 1994.
8. Walker, C.M.; Sheridan, G.J.; Kirsch, B.; So, H.B. and Loch, R.J. (1994). A laboratory rainfall simulator -tilting flume facility for the determination of soil erosion model parameters. Aust Mining Industry Council annual conference, Dampier, Oct 10-13, 1994.
9. Sheridan, G.J.; Walker, C.M.; Kirsch, B. and So, H.B. (1994). The effect of wetting/drying cycles on run-off and erosion for a Queensland minesite soil and overburden. Aust Mining Industry Council annual conference, Dampier, Oct 10-13, 1994.
10. Willgoose G R and Gyasi-Agyei Y. 1995. "New technology in hydrology and erosion modeling for mine rehabilitation", APCOM XXV Application of Computers and Operations Research in the Mineral Industries, Brisbane, 10-12 July
11. So, H B; Loch, RJ; Caroll, C; Willgoose, G and Kirsch, B H (1996). Postmining landscape Parameters for Erosion and Water Quality Control. Austr and New Zealand National Conference, Melbourne 1-4 July 1996, vol. 2, 265-266.
12. Sheridan, GJ; Walker, CM; Kirsch, B H and So, H B (1996). Predicting Infiltration under rainfall on open-cut coal mine overburden and soil from the physical and chemical characteristics of the media. 1996 Western Pacific Geophysics meeting of the American Geophysical Union, Brisbane, July 23-27, 1996. Eos Trans. AGU 77, 46.
13. Short, MP; Kirsch, B H, Sheridan, GJ and So, HB (1996). Importance of sediment mobilization for the release of soluble salts in water runoff from reclaimed open-cut coal mine landscapes in the Bowen Basin Queensland. 1996 Western Pacific Geophysics Meeting of the American Geophysical Union, Brisbane, July 23-27, 1996, Eos Trans AGU 77, 47.
14. Sheridan, GJ; Caroll, C; Kirsch, B H and So, HB (1996) Determination of the contribution of rill and interrill processes to the erosion of reclaimed open-cut coal

mining landscapes. 7th Meeting of the Aust & New Zealand Geomorphology Group, James Cook University, Cairns Qld.

15. Short, MF; Kirsch, BH; Sheridan, GJ and So, HB (1996). Depressional salt accumulations on rehabilitated open-cut coal landscapes in the Bowen Basin Queensland. 7th Meeting of the Aust & New Zealand Geomorphology Group, James Cook University, Cairns Qld.
16. Loch, RJ; So, HB; Aspinall, TO; Caroll, C; Willgoose, GR and Sheridan, GJ (1996). Postmining Landscape Parameters for Erosion and Water Quality Control. Proceedings Postmining Landform Stability and Design Workshop Sept 18-20, 1996, Brisbane, Qld.
17. Sheridan, G.J., Walker, C.M., So, H.B., & Kirsch, B.H. (1996) Predicting the erodibility of open-cut coal mine overburdens and soils from the physical and chemical characteristics of the media. In Proceedings of the Australian and New Zealand Soils Conference, 1st – 4th July, Melbourne
18. Willgoose, G; Gyasi-Agyei, Y; Loch, R J and So, B (1996). Plot hydrology and erosion experimental data: Scaling issues, land and mine rehabilitation. Inst. of Engineers Hydrology Conference, May 1996, Hobart, Tasmania.
19. So, HB; Grabski, A; Sheridan, GJ; Short, M; Caroll, C; Loch, RJ and Willgoose, G (1997). Postmining landscape parameters for erosion and water quality control. Poster to the Aust Minerals Council 22nd Env Workshop, Adelaide, 17-22 October 1997, pp 287-289.
20. Loch, RJ (1997). Landform design – better outcomes and reduced costs by applying science to above and below ground issues. Proceedings Aust Minerals Council 22nd Environmental Workshop, Adelaide, 17-22 October 1997, pp550-563.
21. Goh, E.K.H., Kuszmaul, J., and Sheridan, G.J. (1997) Computerized environmental management for erosion prediction of disturbed soils. In Bulletin, The Institute of Engineers Malaysia
22. Sheridan, GJ; So, HB; Loch, RJ; Pocknee, C and Walker, CM (1998). Predicting hillslope scale soil erosion on rehabilitated coal mines from laboratory scale measurements of rill and interrill erodibility. Proceedings National Soils Conference, Brisbane 27-29 April 1998, pp 318-326.
23. Carroll, C., Merton, L., and Burger, P. (1998). MUSLE erodibility parameters for soil and overburden material in central Queensland, Australia. 16th World Congress of Soil Science, Montpellier, France. Volume II: 575.

Technical reports to individual minesites:

1. Sheridan, G.J. (1993) Erosion Processes Laboratory - A Technical Report. Internal technical report for The University of Queensland, School of Land and Food and Center for Mined Land Rehabilitation.
2. Arkinstal M, Willgoose G R, Loch R and Pocknee C. 1994a. Calibration of DISTFW parameters for the QDPI rainfall simulator for Tarong, Research Report 095.04.1994, Department of Civil Engineering and Surveying, The University of Newcastle, Australia, Callaghan.
3. Arkinstal M, Willgoose G R, Loch R and Pocknee C. 1994b. Calibration of DISTFW parameters for the QDPI rainfall simulator for Wandoan, Research Report 094.04.1994, Department of Civil Engineering and Surveying, The University of Newcastle, Australia, Callaghan.
4. Arkinstal M, Willgoose G R, Loch R and Pocknee C. 1994c. Calibration of DISTFW parameters for the QDPI rainfall simulator for Oaky Creek, Research Report 093.04.1994, Department of Civil Engineering and Surveying, The University of Newcastle, Australia, Callaghan.

5. Gyasi-Agyei Y and Willgoose G R. 1995a. "Prediction of the evolution of post-mining landforms due to erosion", Annales Geophysicae Supplement II, 13, Hamburg, May 1995, p C454.
6. Gyasi-Agyei Y and Willgoose G R. 1997a. Calibration of SIBERIA parameters for 15 mine sites using runoff and erosion data obtained from the QDPI rainfall simulator, Research Report 146.05.1997, Department of Civil, Surveying and Environmental Engineering, The University of Newcastle, Callaghan, NSW.
7. Gyasi-Agyei Y and Willgoose G R. 1997b. "A hybrid model for point rainfall modeling", Water Resources Research, 33(7), pp 1699-1706.
8. Gyasi-Agyei Y and Willgoose G R. 1998a. "Generalization of a hybrid model for point processes: Rainfall example", Water Resources Research, in press.
9. Gyasi-Agyei Y and Willgoose G R. 1998b. Point rainfall modeling within Central Queensland, Research Report, Department of Civil, Surveying and Environmental Engineering, The University of Newcastle, Australia, Callaghan, in preparation.
10. Gyasi-Agyei Y and Willgoose G. R. 1996. "Evaluation of the use of contour banks as post-mining rehabilitation control option using a digital terrain based rainfall-runoff-erosion models", Holzmann H and Nachtnebel H P (Ed), Application of Geographic Information Systems in Hydrology and Water Resources Management, HydroGIS '96, Vienna, Austria, 16-19 April, 1996, pp 143-150.
11. Gyasi-Agyei Y, Willgoose G R, Pocknee C and Loch R. 1995b. Calibration of the DISTFW parameters for the QDPI simulator, Blackwater Mine, Research Report 124.11.1995, Department of Civil, Surveying and Environmental Engineering, The University of Newcastle, Australia, Callaghan.
12. Gyasi-Agyei Y, Willgoose G R, Pocknee C and Loch R. 1995c. Calibration of the DISTFW parameters for the QDPI simulator, Blair Athol Mine, Research Report 123.11.1995, Department of Civil, Surveying and Environmental Engineering, The University of Newcastle, Australia, Callaghan.
13. Gyasi-Agyei Y, Willgoose G R, Pocknee C and Loch R. 1995d. Calibration of the DISTFW parameters for the QDPI simulator, Callide Mine, Research Report 122.11.1995, Department of Civil, Surveying and Environmental Engineering, The University of Newcastle, Australia, Callaghan.
14. Gyasi-Agyei Y, Willgoose G R, Pocknee C and Loch R. 1995e. Calibration of the DISTFW parameters for the QDPI simulator, Curragh Mine, Research Report 121.11.1995, Department of Civil, Surveying and Environmental Engineering, The University of Newcastle, Australia, Callaghan.
15. Gyasi-Agyei Y, Willgoose G R, Pocknee C and Loch R. 1995f. Calibration of the DISTFW parameters for the QDPI simulator, German Creek Mine, Research Report 120.11.1995, Department of Civil, Surveying and Environmental Engineering, The University of Newcastle, Australia, Callaghan.
16. Gyasi-Agyei Y, Willgoose G R, Pocknee C and Loch R. 1995g. Calibration of the DISTFW parameters for the QDPI simulator, Gregory Mine, Research Report 119.11.1995, Department of Civil, Surveying and Environmental Engineering, The University of Newcastle, Australia, Callaghan.
17. Gyasi-Agyei Y, Willgoose G R, Pocknee C and Loch R. 1995h. Calibration of the DISTFW parameters for the QDPI simulator, Moura Mine, Research Report 118.11.1995, Department of Civil, Surveying and Environmental Engineering, The University of Newcastle, Australia, Callaghan.

18. Gyasi-Agyei Y, Willgoose G R, Pocknee C and Loch R. 1996a. Calibration of the DISTFW parameters for the QDPI simulator, Goonyella Mine, Research Report, Department of Civil, Surveying and Environmental Engineering, The University of Newcastle, Australia, Callaghan.
19. Gyasi-Agyei Y, Willgoose G R, Pocknee C and Loch R. 1996b. Calibration of the DISTFW parameters for the QDPI simulator, Peak Downs Mine, Research Report, Department of Civil, Surveying and Environmental Engineering, The University of Newcastle, Australia, Callaghan.
20. Gyasi-Agyei Y, Willgoose G R, Pocknee C and Loch R. 1996c. Calibration of the DISTFW parameters for the QDPI simulator, Saraji Mine, Research Report, Department of Civil, Surveying and Environmental Engineering, The University of Newcastle, Australia, Callaghan.
21. Carroll, C., Merton, L., Burger, P., and Halpin, M. (1998). Curragh Qld. Mining Ltd. Erosion and Water Quality Field Study (1993-97). Project Report.
22. Loch R.J.; Pocknee, C.; Bourke, J.; Kirsch, B.; Myers, K. and Sheridan, G. (1993-1995). Field Rainfall Simulator Studies. **Report to each of 15 mines**.

3. Laboratory Rainfall Simulation

G.J. Sheridan[ac], C.M. Walker[a], H.B. So[a] and B.H. Kirsch[b]

[a]Research Officer, Post-graduate student and Associate Professor of Soil Physics, School of Land and Food & Centre for Mined Land Rehabilitation, The University of Queensland, St Lucia, Q 4072
[b]Environmental Officer, Norwich Park Mine, Dysart, Qld. Previously Research Officer, The University of Queensland.
[c]Currently: Research Scientist, Australian Road Research Board, Victoria.

3.1 Aims

The aim of the laboratory erosion research was to:

1. Determine the erodibility of a broad range of soils and overburdens from 15 participating minesites;
2. Relate erodibility to the physical and chemical properties of the media;
3. Determine the effect of slope gradient and slope length on soil erosion processes and rates;
4. Predict hillslope scale erosion from laboratory measurements;
5. Produce a user friendly computer application for predicting the effect of slope gradient and length on soil erosion rates.

3.2 Introduction

Open-cut mining and associated activities disturb large areas of land which must be stabilized and rehabilitated following mining operations. In central Queensland, the area disturbed by open-cut coal operations exceeds 50,000 ha (Welsh *et al.* 1994). The first step during mine-site rehabilitation is the design of the post-mining landform. This is also the most expensive component of the rehabilitation process as it involves extensive earthworks requiring heavy plant and equipment. It was estimated that costs might range from $5,000 to $25,000 per hectare (Bell *et al.* 1993). The primary aim of the earthworks is to produce a post-mining landscape that is resistant to geo-technical failure and surface erosion processes due to rainfall and runoff. The extent and cost of earthworks may be minimised, and rehabilitation failures avoided, if soil erosion from design landforms can be predicted prior to construction.

Soil erosion prediction models have developed almost exclusively to solve erosion problems associated with agricultural land use. The use of erosion models on mined land is very limited (Evans 1992). The surface media, topography and management practices on mines are very different to those found in agricultural settings, so it is unclear whether agriculturally based models will work under these different conditions. Rubio-Montoya and Brown (1984) found that the USLE significantly over-predicted observed erosion rates from strip-mine areas along the Gulf Coast of the USA. However Wu *et al.* (1996) reported that the ANSWERS model performed on overburdens with about the same accuracy as it did on agricultural lands. Gilley *et al.* (1977) reported low rates of erosion from overburdens on North Dakota surface mine sites, and Mitchell *et al.* (1983) compared erosion rates on newly reclaimed topsoils to unmined areas and found the reclaimed sites to be less erodible.

Of all the factors affecting erosion, erodibility is the most difficult to quantify. The accurate quantification of the erodibility of soils is generally determined from field rainfall simulation or long-term field plots (Middleton, *et al.* 1934; Barnett and Rogers 1966; Wischmeier *et al.* 1969; Elliot *et al.* 1989). Data collection can be expensive and time consuming. In an effort to simplify this, some researchers have utilized laboratory rainfall simulation and tilting flumes to determine erodibility (Verhaegen 1987). The use of laboratory scale measurements for the prediction of hillslope scale erosion offers many technical advantages and considerable cost savings over traditional data collection methods for erosion prediction. However, there has been limited success in the parameterization of predictive hillslope scale models usually due to the inadequate representation and separation of the relevant erosion processes (Trieste and Gifford 1980; Foster *et al.* 1981).

A methodology and modeling approach is proposed and tested whereby data for the parameterization of hillslope scale, process based, erosion models can be collected at the laboratory scale. The prediction of erosion from laboratory scale research will enable post-mining landscapes to be designed more efficiently and effectively, while at the same time reducing research costs.

3.3 Methods & Materials

Sixteen soils and sixteen overburdens were collected by back-hoe from 15 open-cut coal mines in Queensland and shipped in 200 litre drums to the Erosion Processes Laboratory at the University of Queensland (Figure 3-1). Each media was uniformly mixed in a 6 m^3 cement mixer and sieved to remove rocks greater than 5 cm diameter. The texture of the soils and overburdens was then determined by the sedimentation and pipette technique described by Day (1965).

Figure 3-1 The erosion processes laboratory at The University of Queensland showing the tilting erosion flume and the rainfall simulator.

Soil erosion experiments were conducted at the Erosion Processes Laboratory at the University of Queensland. Rainfall was applied over a tilting flume at 100 mm/h for 30 min to bare, unconsolidated plots, 3 m long, 0.8 m wide, and 0.15 m deep at 20% slope. A rainfall simulator was set at the same slope, 2.2 m above the soil surface. The rainfall simulator, similar in design to that used in section 5 and constructed by the Queensland Department of Natural Resources, is supplied with de-ionized water. It produced rainfall from four fan-shaped nozzles (80100 Veejet®) swept intermittently across the plot. Meyer (1958) reported that the nozzles produce a median drop diameter of 2.1 mm, with 80% of the drops being between 1.0 and 3.2 mm and a kinetic energy of rainfall of 295 kJ/ha.mm.

Timed runoff samples were collected at eight intervals during the rainfall event, weighed, oven dried at 105^{o} C, and re-weighed to determine runoff rate, sediment concentration, and sediment yield. The mean of the last four runoff measurements was used to calculate the steady-state sediment delivery rate and runoff rate for a given replicate. The steady-state infiltration rate was calculated as the difference between the rainfall rate and the steady-state runoff rate.

Slope gradient was then set to 5, 10, 15 and 30%, respectively, with four runoff samples collected during 12 minutes of simulated rainfall at each slope. The mean of the last two measurements was used to calculate the erosion rate for a given slope. Following the last rainfall application, overland flow was added to the top of the plots at 20% slope at increasing rates ranging from 0.1 to 1.8 l/s. Rills were allowed to develop naturally over the plot surface. Each flow rate was held constant for three minutes and the sediment concentration of three runoff samples averaged to determine the sediment delivery at a given flow rate. Flow rates were increased until the maximum possible flow was attained, or until the flow-lines cut to the base of the flume. Where possible, three replicates of the above experiments were carried out for each media giving a total of 91 replicates. The rainfall simulation data from the 20% rainfall experiments was used to estimate interill erodibility, while the overland flow data from the 20% experiments was used to estimate rill erodibility coefficients.

3.3.1 Field measurements

Rainfall simulation experiments were carried out on 15 Queensland open-cut coal mines on the same soils and overburdens as were used for the laboratory research. Details of the field rainfall simulation experimentation are presented in Section 4. Briefly, rainfall was applied at 100 mm/h for 30 minutes, from a simulator of the same design as the laboratory simulator. Bare field plots measured 12 m long and 1.5 m wide, with the average slope gradient ranging from 5% to 30%. Plots were lightly tilled by hand raking prior to rainfall to produce a loose surface of low surface roughness and an approximately even slope gradient. The number of replicates on each media varied depending on the variability of the plot and availability of appropriate rainfall simulation sites, resulting in a total of 113 field simulation plots. Runoff rates were measured using computer-logged tipping buckets. Sediment concentrations were measured as described for the laboratory procedure. The texture of the media was determined to confirm that the field erosion events were carried out on the same media as the laboratory experiments.

3.3.2 Soil erosion equations

Two modeling approaches were tested to allow laboratory measurements of rill and interill soil erosion to be used for prediction of soil erosion rates observed at the hillslope scale. For both approaches, erosion is modeled as a time invariant steady-state process on a uniform, unconsolidated, bare slope of low surface roughness. Only rill and interill processes are potentially active. Rills are assumed to flow perpendicular to the contour with equal flow in each rill at a density of 1 rill/m (Gilley, 1990). The streampower required to detach sediment is assumed to be greater than the streampower required to transport that sediment. As a result of this, and the simple linear slope shapes being modeled, rill sediment loads are assumed to be detachment limited (less than transport capacity) and no sediment transport routines were used for either model. The two modeling approaches tested differ with respect to the way they model rill erosion. The relevant equations are presented below.

The steady-state runoff rate Q (m/s) may be calculated as the difference between the steady-state rainfall rate, I, (m/s) and the steady-state infiltration rate, I_r, (m/s);

$$Q = I - I_r \qquad [1]$$

where the steady-state infiltration rate is estimated from laboratory rainfall simulation data. The continuity equation (Foster *et al.* 1977) may be used to describe sediment movement down a slope profile;

$$\frac{\partial Et}{\partial L} = E_{rt} + E_i \qquad [2]$$

where Et (kg/m.s) is the sediment load, L (m) is the distance downslope, E_{rt} (kg/m^2.s) is the rill erosion rate and, E_i (kg/m^2.s) is the interill erosion rate. Sediment load is therefore given by;

$$E_t = \int_{L1}^{L2} (E_{rt} + E_i)dL + E_{tL1} \qquad [3]$$

where E_{tL1} is the sediment load at L =1. The interill erosion rate (E_i) may be calculated from (Kinnell, 1993a);

$$E_i = K_i * I * Q * S_f * C_f \qquad [4]$$

where K_i (kg.s/m^4) is an interill erodibility coefficient related to soil properties, and S_f and C_f are non-dimensional slope and cover adjustment factors respectively, and may be calculated from (NSERL, 1995);

$$S_f = 1.05 - 0.85\ exp^{(-4 \sin (S2))} \qquad [5]$$

$$C_f = e^{-2.5C} \qquad [6]$$

where $S2$ is the slope in radians, and C is assigned a value equal to the rock content, *Creek* (fraction by volume > 2mm) of the media.

The rill erosion rate (E_{rt}) per plot may be calculated from the erosion rate *per rill*, multiplied by the number of rills, and divided by the plot area. In this study, the erosion rate per rill is estimated using two contrasting approaches.

Firstly, the erosion rate *per rill* may be estimated using the critical-shear-based approach (as taken in the WEPP model). The WEPP model is fully described by Nearing *et al.* (1989), however under the simple conditions used for this study, the detachment capacity of the rill flow may be estimated by the critical shear based equation;

$$D_c = K_r(\tau - \tau_c) \qquad [7]$$

where D_c (kg/m^2.s) is the detachment capacity of the flow, K_r (s/m) is the rill erodibility of the soil, τ_c (Pa) is the critical shear stress below which there is no detachment and τ (Pa) is the hydraulic shear stress of the flowing water. Rill erodibility parameters K_r and τ_c are calculated from the measured erosion rates at a range of flow shear values. The rill erosion rate is plotted against the calculated shear for each of the flow rates. The slope of the regression line is the rill erodibility, K_r and the intercept with the horizontal axis is the critical shear, τ_c. Flow hydraulic shear is calculated as per the WEPP Technical Documentation (NSERL, 1995).

Alternative to Eq. 7, the sediment delivery rate *per rill*, E_r, (g/s) may be calculated as a power function of flow rate per rill, q_r (l/min), and rill slope S_3 (fraction);

$$E_r = K_{r2} * q_r^{\,a} * S_3^{\,1.5a} \qquad [8]$$

where K_{r2} and *a* are empirically determined non-linear regression coefficients representing soil properties, calculated (SAS Institute Inc. 1988) from the measured erosion rates at a range of flow rates (Kemper, 1985; Gilley *et al.,* 1992).

3.4 Results

3.4.1 Media properties

The physical and chemical properties of the soils and overburdens are listed in Table 3-1. The range of textures of the laboratory soils and overburdens is plotted on a texture triangle in Fig 3-2. Media (soil & overburden) texture ranged from a heavy clay soil (58% clay) at Curragh mine to a sandy loam soil (16% clay) at Norwich Park. Soils and overburden cover a similar range of textures, however soils were generally more erodible than overburdens, as many of the overburdens either contained considerable amounts of rock, or tended to form a strong surface seal.

3.4.2 Media properties and erodibility

indicates that the physical and chemical properties that are best correlated with interill erosion rates are different at different slopes, and for soils as compared to overburdens. Texture class was found to be an excellent predictor of interill erodibility for soils at 30% slope (r2 = 0.80), but a poor predictor for soils at 5% slope (r2 = 0.25). This may be due to the stripping of the soil seal as a result of the high soil loss rates at the 30% slope. For this to occur, the soil loss rate would need to be greater than the rate of seal development. As a result, the properties of the bulk media (ie texture) may influence erosion rates at the 30% slope, while the surface seal properties may control soil loss at lower slopes. Detachment rates are commonly related to cohesion, which is strongly related to texture.

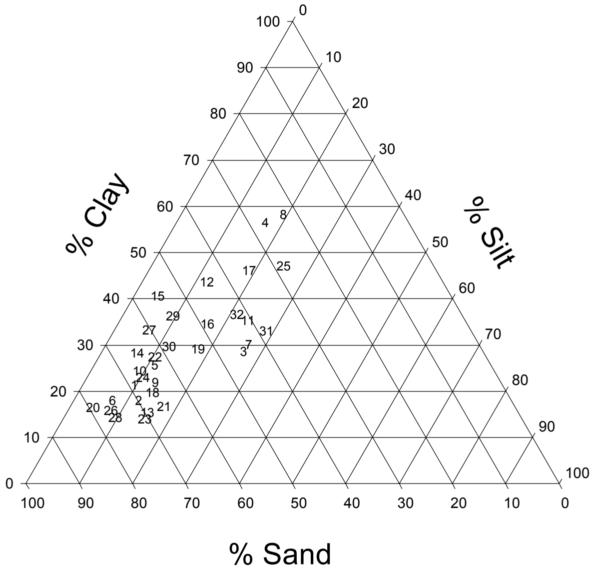

Figure 3-2 Texture triangle showing the texture of the less than 2mm portion of the soils and overburdens used in the laboratory research. Plotted numbers correspond to the media number listed in Table 3-1.

In general it appears that the factors which may affect surface seal development (dispersion indices, organic carbon content, aggregation index, EC, pH and ESP) are all better predictors at low slopes, while at high slopes the matrix properties ie texture are more important.

Increasing rock content was consistently correlated with decreasing erosion rates at all slopes and for both soils and overburdens. This reflects the major effect of rock on interill erosion, which is to protect the soil from raindrop impact. It should be noted that for all correlations, the soils from Blackwater and Curragh were excluded. These soils, from adjacent mines, have very high clay contents, are highly aggregated, and are dominated by expanding clay minerals. As a result, they behaved differently to most of the other soils, and when included in the analysis tended to mask relationships for all the other soils.

Interestingly, a strong negative correlation between clay content and erosion rate for the soils is completely reversed for the overburden. Thus, increasing clay is associated with reduced erosion for the soils, while being related to increased erosion for the overburdens. This result requires further analysis.

In general, the strongly aggregated high clay soils (eg. Blackwater, Curragh) tended to be the most erodible, followed by the lighter textured sandy loams and loamy sands (eg. Norwich Park and Peak Downs soils). Soils or overburdens with 20%-30% silt tended to form strong raindrop impact seals under rainfall and consequently had very low erodibilities (eg. Norwich Park overburden and Wandoan soil).

Table 3-1 The physical and chemical properties of the soils and spoils used in the laboratory research.

Mine name	#	Media [A]	EC[B] (DS/m)	pH[B]	CEC[C]	ESP[D] (%)	-1.5[E] (MPa)	-0.01[E] (MPa)	PAWC[F] (%)	DR_2 [G] (%)	DR_{20} [H] (%)	OC[J] (%).	WSA[K] (%)	%Clay[L] (g/g)	%Silt[L] (g/g)	%Sand[L] (g/g)	%Rock[M] (cm^3/cm^3)
Blair Athol	1	O	0.284	7.66	7.6	11.8	0.07	0.16	0.09	6.8	20.7	--	25.6	17.72	10.48	71.80	8.55
	2	S	0.106	7.06	8.6	4.0	0.06	0.15	0.09	2.6	20.5	1.33	32.2	23.69	15.31	61.00	6.04
Blackwater	3	O	0.471	8.62	23.0	15.9	0.10	0.23	0.13	8.7	24.4	--	21.5	20.65	29.26	50.08	8.28
	4	S	0.306	8.69	40.2	10.6	0.21	0.44	0.23	4.9	17.2	2.35	25.2	57.65	14.20	28.15	2.45
Calide	5	O	0.228	6.68	12.7	5.5	0.08	0.15	0.07	6.9	23.6	--	28.1	18.48	11.91	69.61	12.77
	6	S	0.040	5.19	1.4	22.8	0.05	0.13	0.08	1.2	6.2	2.30	18.9	19.02	4.31	76.68	3.59
Curragh	7	O	0.690	8.89	26.9	26.1	0.12	0.29	0.17	14.0	34.7	--	33.6	22.56	25.24	52.20	1.56
	8	S	0.750	7.67	60.2	6.5	0.17	0.37	0.20	9.4	37.0	1.60		57.13	17.26	25.62	0.90
German Creek	9	O	1.430	7.57	24.6	10.1	0.08	0.17	0.09	0.8	23.4	--	25.3	4.63	28.49	66.88	16.16
	10	S	0.710	7.57	13.2	13.9	0.06	0.17	0.11	4.0	16.3	0.79	21.4	22.58	7.92	69.50	4.25
Goonyella	11	O	1.373	8.82	36.5	39.8	0.16	0.31	0.15	21.8	41.9	--	30.6	26.85	22.17	50.98	1.31
	12	S	0.207	6.30	10.1	7.9	0.11	0.18	0.07	6.7	18.0	1.44		44.23	7.23	48.54	1.58
Gregory	13	O	1.051	7.80	16.2	6.5	0.07	0.15	0.08	0.6	17.7	--	25.1	9.76	18.16	72.08	6.66
	14	S	0.078	6.33	13.6	0.5	0.09	0.21	0.12	3.9	13.7	0.78	17.9	30.33	5.51	64.16	2.80
Moura1	15	O	0.439	7.88	25.1	19.2	0.14	0.29	0.15	10.8	28.6	--	14.0	24.13	25.38	50.49	28.01
	16	O	0.755	8.57	32.6	31.3	0.12	0.26	0.14	9.5	29.9	--	32.8	31.06	16.66	52.28	4.93
Moura2	17	S	0.269	7.81	34.6	9.0	0.20	0.47	0.27	6.9	18.8	1.67	18.6	48.85	15.73	35.42	4.37
Norwich Pk1	18	O	0.711	8.34	14.6	27.7	0.07	0.12	0.05	7.4	20.7	--	18.6	17.22	25.19	57.59	33.14
	19	O	0.485	7.29	15.4	35.4	0.11	0.20	0.09	12.4	30.0	--	43.8	31.91	13.04	55.05	4.47
Norwich Pk2	20	S	0.142	6.56	3.5	29.2	0.04	0.11	0.07	4.7	10.6	0.56	26.6	15.72	2.71	81.57	1.22
Newlands	21	O	0.303	8.16	14.8	3.1	0.07	0.14	0.07	4.7	17.0	--	37.9	13.82	18.30	67.88	9.93
	22	S	0.574	8.93	24.7	36.8	0.10	0.22	0.12	16.5	29.3	0.68	41.6	28.58	10.40	61.02	1.49
Oaky Creek	23	O	1.600	7.60	30.0	6.9	0.06	0.16	0.10	1.2	21.1	--	26.6	0.72	24.18	75.10	7.34
	24	S	0.257	7.10	10.2	9.8	0.07	0.17	0.10	4.4	17.6	1.39	49.1	22.88	8.47	68.65	0.97
Peak Downs	25	O	1.552	8.55	25.1	52.7	0.12	0.27	0.15	19.5	50.4	--	26.9	27.45	42.91	29.64	6.96
	26	S	0.227	7.53	9.5	17.1	0.05	0.14	0.09	6.6	15.5	0.80	53.2	20.17	7.03	72.80	2.63
Saraji	27	O	0.447	9.44	26.5	28.5	0.13	0.30	0.17	15.4	29.5	--	54.1	34.00	9.08	56.92	0.98
	28	S	0.144	8.67	5.8	5.5	0.04	0.13	0.09	3.3	14.7	1.04	44.7	14.01	9.00	76.99	1.26
Tarong	29	S	0.351	4.99	4.9	14.4	0.09	0.19	0.10	5.4	21.9	3.49	22.0	30.06	12.13	57.82	16.77
	30	S	0.096	4.75	2.7	3.3	0.13	0.22	0.09	3.3	10.1	2.63	16.9	37.84	6.92	55.24	8.86
Wandoan	31	O	0.856	8.17	25.9	31.3	0.13	0.30	0.17	17.0	48.4	--	50.2	26.57	36.62	36.81	6.05
	32	S	0.113	8.07	23.9	3.0	0.11	0.23	0.12	2.6	19.6	2.43	27.7	33.54	17.94	48.52	0.72

A. O = overburden, S = soil
B. 1:5 soil/water suspension
C. Cation Exchange Capacity ($cmol_c$/kg soil) (see text for method)
D. Exchangeable Sodium Percentage
E. Gravimetric water content at given potential
F. Plant Available Water Capacity
G. Dispersion Index – clay
H. Dispersion Index – silt and clay
J. Organic Carbon content
K Water Stable Aggregation Index % by weight particles and aggregates < 125µ on the soil surface following rainfall
L. Analysis of less than 2mm portion. Clay < 0.002mm, 0.002<Silt<0.020, 0.020<Sand<2.0mm
M.% by weigt > 2mm, converted to volumetric assuming the densities of rock and soil are 2.65 and 1.65.

Table 3-2 Correlations between interill erodibility and soil and overburden physical and chemical properties at a range of slopes.

Media Property	Soil					Overburden					Soil & overburden				
	Slope %					Slope %					Slope %				
	5	10	15	20	30	5	10	15	20	30	5	10	15	20	30
EC	0.45	0.33	0.08	-0.25	-0.20	-0.05	-0.04	-0.19	-0.35	-0.33	0.03	-0.17	-0.40	0.51**	-0.47**
PH	0.67**	0.47	0.47	0.16	0.06	0.51*	0.48*	0.40	0.19	0.26	0.44*	0.19	0.01	-0.22	-0.24
CEC	0.25	0.28	-0.18	-0.44	-0.48	0.44	0.45	0.30	0.07	0.08	0.29	0.12	-0.30	-0.52**	-0.53**
ESP	0.53*	0.25	0.52*	0.42	0.49	0.47	0.48*	0.39	0.31	0.21	0.45*	0.24	0.12	0.01	0.03
-1.5 (MPa)	-0.31	-0.22	-0.67**	-0.69**	-0.72**	0.62**	0.65**	0.54*	0.42	0.38	0.17	0.11	-0.33	-0.47**	-0.51**
-0.01 (MPa)	-0.18	-0.07	-0.50	-0.58*	-0.57*	0.62**	0.63**	0.51*	0.40	0.36	0.25	0.22	-0.19	-0.34	-0.36*
DR2	0.63*	0.26	0.16	-0.12	-0.19	0.54*	0.57	0.48	0.43	0.35	0.50**	0.28	-0.01	-0.19	-0.23
DR20	0.4	0.14	-0.15	-0.44	-0.57*	0.45	0.46	0.32	0.27	0.18	0.34	0.08	-0.27	-0.44*	-0.48**
OC	-0.75**	-0.77***	-0.76***	-0.54*	-0.46	--	--	--	--	--	--	--	--	--	--
WSA	0.50	0.09	0.57*	0.36	0.22	0.73***	0.81***	0.80***	0.71**	0.73***	0.61***	0.45*	0.50**	0.30	0.23
Clay	-0.23	-0.17	-0.65**	-0.67**	-0.70**	0.81***	0.81***	0.82***	0.78***	0.72***	0.31	0.41*	0.13	0.02	-0.03
Silt	-0.09	-0.21	-0.45	-0.57*	-0.62*	-0.06	-0.06	-0.23	-0.32	-0.36	-0.07	-0.25	-0.51	-0.57***	-0.58***
Sand	0.52*	0.48	0.90***	0.85***	0.84**	-0.08	0.09	0.08	0.07	0.12	0.25	0.24	0.46**	0.46**	0.48**
Rock	-0.53*	-0.64*	-0.62*	-0.50	-0.42	-0.66**	-0.67**	-0.66**	-0.64**	-0.63**	-0.59***	-0.68***	-0.63***	-0.53**	-0.49**
Bulk Density	0.49	0.55*	0.67**	0.66**	0.64**	-0.46	-0.41	-0.35	-0.36	-0.29	-0.07	-0.04	0.08	0.13	0.16
Liquid Limit	-0.19	-0.07	-0.53	-0.59*	-0.61*	0.42	0.56	0.28	-0.17	-0.20	0.08	0.06	-0.45	-0.57*	-0.58*
Plastic Limit	-0.49	-0.42	-0.73***	-0.72**	-0.76**	0.2	0.39	0.06	-0.37	-0.40	-0.16	-0.15	-0.52	-0.58*	-0.61**
Plastic Index	-0.03	0.11	-0.37	-0.47	-0.47	0.59	0.69	0.47	0.03	0.00	0.20	0.16	-0.36	-0.49*	-0.49*

3.4.3 Predictive equations

Based on the data presented in Section 3.4.2, stepwise regression procedures were carried out to develop predictive equations for rill and interill erodibility. The aim was to be able to achieve a coefficient of determination of 0.6 or better, using three or less soil properties to predict erodibility coefficients. Media properties with a high inter-correlation with other properties, or a low correlation with erodibility, were identified and removed from further analysis. Texture classes identified as having high correlations with erodibility were included in the analysis. Where a satisfactory r^2 value could not be achieved using the above properties, logarithms of the property values were calculated and included in the regression.

The following equations for the prediction of rill and interill erodibility values for use in equations 4 and 9 were developed using stepwise multiple regression procedures.

Soils[a]

Interill K = 3.72 – 0.8891 * OC [9]
$r^2 = 0.59$

Rill K = 63.96 + 0.00008797 * $(\%0.02\text{-}1mm)^3$ – 3.20 * pH – 30.47 * BD [10]
$r^2 = 0.71$

Overburdens

Interill K = -2.8307 + 0.11089 * CLAY + 4.13 * D20 [11]
$r^2 = 0.82$

Rill K = 25.02 – 30.55 * D20 – 0.18 * ESP + 4.80 * EC [12]
$r^2 = 0.61$

[a] soils from Blackwater and Curragh not included in analysis
OC = organic carbon content as a percent
(%0.02-1mm) = % by weight in this particle size class
CLAY = % by weigh<2μm
BD = Bulk Density (g/cm^3)
ESP = Exchangeable Sodium Percentage
EC = Electrical conductivity (dS/m)

Thus, for the soils, interill erodibility was negatively related to the level of organic carbon while rill erodibility was positively related to the proportion of fine sand particles in the 0.02 to 1.0 mm range and negatively related to the pH and bulk density. These factors are related to the macro-structure of the soil with OC as the main stabilizing influence against raindrop impact. Rill development in soils is a result of shear forces from overland flow, and the state of soil consolidation (BD) is an important factor in the resistance of soils to rilling. Increasing fine sand content, associated with increasing structural instability increases rilling in soils. For overburdens, interrill erodibility is positively correlated with clay content and silt and clay dispersion ratio was found for interill erodibility. However, overburden rill erodibility is negatively correlated with dispersion as indicated by the silt & clay dispersion ratio and ESP. It is positively correlated with EC, which is consistent with the suppressive effect of increasing EC on dispersion.

Figure 3-3 plots the predicted rill and interill erodibility values from equations 9 to 12 against the observed values used to develop the above multiple regression equations. The results indicate that the multiple regression equations developed from this research are appropriate for the prediction of erodibility for the range of media types investigated in this study. Equations 9 to 12 have been incorporated into the MINE*rosion* application (Section 3.5) allowing erosion predictions to be made from inputs of a few simple media properties.

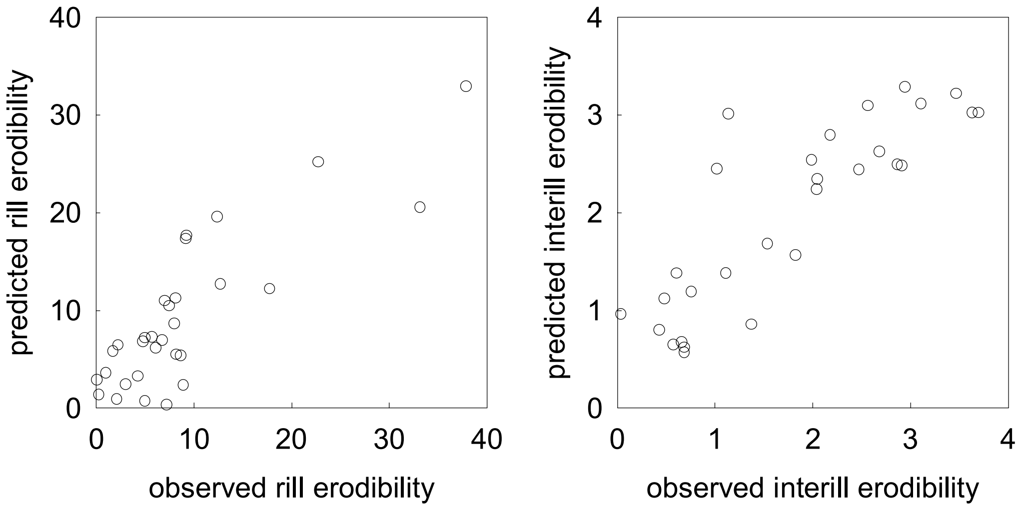

Figure 3-3 Observed rill and interill erodibility values plotted against predicted values from equations 9 to 12.

3.4.4 The effect of slope gradient on sediment delivery rates.

One of the most significant findings of this study was the enormous diversity of responses to slope gradient shown by different media types. The measured sediment delivery rate at each slope gradient is listed in Table 3-3. The effect of increasing slope gradient from 5% to 30% varied from a 2.5 fold increase for an overburden from Peak Downs, to a 49.5 fold increase for a soil from Callide mine. On average, the soils showed greater increases than the overburdens, probably due to the initiation of rills at higher slopes on many of the soils.

The implications of a “soil dependent” slope is significant. All media are arranged in ascending order from left to right based on the measured soil loss rate at 5% slope. The corresponding soil loss at 30% slope is shown by the paired bar. The relative rankings of the media are strongly affected by slope gradient, indicating a significant interaction between slope gradient and media properties. A correlation of the sediment delivery rates measured at 5% slope against those measured at 30% slope for all media yields a coefficient of determination of only 0.14. When the same correlation is carried out for soils and overburdens separately, the r^2 values are 0.22 for soils & 0.87 for overburdens. Given that rilling was observed on many of the soil plots (Table 3-3) it is possible that the change in erosive process from interill to rill may be responsible for the highly variable responses to slope gradient shown in Table 3-3.

3.4.5 Critical-shear based model

The values for interill erodibility (K_i), rill erodibility (K_r), critical shear (τ_c) and steady state infiltration rate (I_r), estimated from laboratory flume and rainfall simulator experiments, are shown in Table 3-4. The standard error is shown to the right of each estimated parameter value. The r^2 value represents the fit of the regression of soil loss against shear for the estimation of the K_r and τ_c parameters.

Interill erodibility was found to vary by approximately an order of magnitude from 0.54 x 10^6 kg.s/m^4 for an overburden from Blackwater to 6.01 x 10^6 kg.s/m^4 for a soil from Curragh. The tertiary overburden from Norwich Park (no. 18) recorded an interill erodibility of only 0.09 x 10^6 kg.s/m^4, however this is due to the extremely high infiltration rate on this media (71 mm/h). Only one replicate of this media produced runoff during the rainfall event. Consequently the value does not reflect the physical nature of the erodibility parameter, which should primarily represent the detachability and transportability of the soil particles and aggregates. There was a clear trend for the soils and particularly the well-aggregated clay soils (eg. Blackwater) to be the most susceptible to interill erosion. Rocky overburdens tended to have very low interill erodibilities, even though the effect of rocks >2mm was accounted for in the cover factor (Eq. 6) of the interill equation (Eq. 4).

The range of interill erodibility values recorded during this study are similar to the range of values reported in the 1989 WEPP Compendium (0.87 x 10^6 kg.s/m^4 for a Bonifay soil to 4.32 x 10^6 kg.s/m^4 for a Palouse soil), although these do not approach the lower range of expected rangeland values (0.01 x 10^6 kg.s/m^4) as reported in the WEPP 1994 User Summary (NSERL, 1989, 1994). Thus, the degree of variability in the interill erodibility parameter found in this study is similar to that found by other researchers working with agricultural soils.

Rill erodibility could not be determined for five of the overburdens, as these media formed strong surface seals which resisted rill initiation even at the highest overland flow rate possible (2.5 l/s) with the laboratory equipment. A further 9 media produced results where the r^2 for the estimation of K_r and τ_c was not significant or was low ($r^2 < 0.60$). For the remaining 18 media, rill erodibility was found to vary by approximately a factor of 8, from 10.7 x 10^{-3} s/m for a soil from Newlands, to 85.4 x 10^{-3} s/m for a soil from Norwich Park. However, the Norwich Park soil was a highly erodible outlier, with the next lowest K_r value being 46.5 x 10^{-3} s/m for a soil from Curragh. The Norwich soil aside, these values are similar in range to those reported in the WEPP compendium (1.18 x 10^{-3} s/m to 45.30 x 10^{-3} s/m), though the mean value for K_r from this study is somewhat higher, suggesting that, on average, the mine site media are more susceptible to rill erosion than the soils recorded in the WEPP compendium (NSERL, 1989).

Measured critical shear (τ_c) values for rill detachment varied from 4.7 Pa for a soil from Saraji to 28.9 Pa for an overburden from Peak Downs. Detachment could not be initiated on 5 media at shear values of 40 Pa. WEPP compendium values range from 0.7 Pa to 6.6 Pa. The critical shear values for the media studied are very high compared to the WEPP compendium (NSERL, 1989) values, reflecting the sealing and hardsetting nature of the media.

Table 3-3 The effect of slope gradient on sediment delivery rates (g/m^{2}s).

Mine name and media type	Slope gradient %					Rills at 20% (Y/N)[b]	ratio 30% to 5%
	5	10	15	20[a]	30		
Overburdens							
Blair Athol	0.24	0.32	0.77	1.38	1.53	N	6.4
Blackwater – Rocky	0.10	0.15	0.28	0.33	0.49	N	5.0
Callide -	0.19	0.25	0.63	1.09	1.40	N	7.5
Curragh	0.33	0.59	0.89	1.09	1.12	N	3.4
German Ck – Rocky	0.12	0.18	0.35	0.28	0.57	N	4.6
Goonyella – Permian	0.47	0.96	1.22	1.18	1.32	N	2.8
Gregory – Rocky	0.24	0.44	0.55	0.70	0.92	N	3.8
Moura – Rocky	0.09	0.15	0.21	0.37	0.30	N	3.3
Moura Permian	0.63	1.00	1.57	1.80	1.83	N	2.9
Norwich Pk rocky	0.00	0.00	0.00	0.03	0.04	N	NA
Norwich Pk Tertiary	0.34	0.83	1.38	1.64	1.51	N	4.4
Newlands – Rocky	0.13	0.23	0.42	0.57	0.68	N	5.4
Oaky Ck – Rocky	0.11	0.22	0.30	0.31	0.40	N	3.8
Peak Downs – Sodic	0.24	0.31	0.42	0.59	0.61	N	2.5
Saraji – Sodic	0.71	1.32	2.11	1.86	2.68	N	3.8
Wandoan – Shale	0.44	0.92	1.08	1.18	1.30	N	3.0
Mean value for overburdens	0.27	0.49	0.76	0.90	1.04	--	4.2
Soils							
Blair Athol Sandy Loam	0.20	0.61	1.47	2.47	2.41	Y	12.1
Blackwater Heavy Clay	0.79	1.84	2.37	3.69	3.73	Y	4.7
Callide Sandy Clay Loam	0.13	0.53	1.71	3.66	6.46	Y	49.5
Curragh Medium Heavy Clay	0.88	2`.19	2.31	2.85	3.38	Y	3.8
German Ck Clay Loam	0.36	1.16	2.06	2.07	3.45	N	9.7
Goonyella Light Clay	0.18	0.80	1.06	1.93	1.47	N	8.1
Gregory Clay Loam	0.37	1.20	1.64	2.25	2.63	Y	7.0
Moura Medium Clay	0.18	0.67	0.93	1.12	1.30	Y	7.0
Norwich Pk Sandy Clay Loam	0.44	1.17	3.79	7.00	8.27	Y	18.8
Newlands Sandy Clay Loam	0.59	1.01	2.35	2.36	2.68	N	4.5
Oaky Ck Clay Loam	0.39	1.03	2.48	3.40	3.43	Y	8.8
Peak downs Loamy Sand	0.26	0.37	2.29	3.15	4.05	Y	15.3
Saraji Sandy Loam	0.36	0.70	2.74	4.51	5.51	Y	15.2
Tarong Lithosol	0.12	0.21	0.42	0.68	0.73	N	5.9
Tarong Krasnozem	0.11	0.19	0.73	1.49	1.75	Y	15.5
Wandoan Light Clay	0.22	0.62	1.15	1.49	1.36	N	6.1
Mean value for soils	0.35	0.89	1.84	2.76	3.29	--	12.0

a. 20% slope data comes form initially dry plots and may have a positive error relative to the data at other slopes
b. presence of absence of rills during rainfall at 20% slope, Y = yes, N = no
c. texture is based on the less than 2 mm fraction of the soil

Table 3-4 Critical-shear based erosion model parameters determined from laboratory rainfall simulation experiments

Mine site	Media no.	Media#	Infiltration (mm/h)	s.e.	10^{-6} x K_i (kg.s/m^4)	s.e.	10^3 x K_r (s/m)	s.e.	τ_c (Pa)	s.e.	r^2
Blair Athol	1	O	4.5	1.52	1.38	0.20	21.1	3.0	12.5	0.82	0.61*
	2	S	2.72	1.10	2.31	1.10	16.3	2.2	11.3	0.92	0.65*
Blackwater	3	O	8.86	1.69	0.54	0.05	4.7	2.5	16.7	1.15	0.12^{n}
	4	S	7.58	1.33	5.78	0.35	34.8	3.0	9.7	0.55	0.83*
Calide	5	O	8.94	1.86	1.04	0.07	17.9	2.3	14.6	1.08	0.77*
	6	S	14.24	4.04	1.68	0.55	30.6	2.2	14.0	0.44	0.88*
Curragh	7	O	22.61	5.66	2.13	0.31	--	--	--	--	--
	8	S	16.84	3.34	6.01	0.33	46.5	6.5	19.3	1.16	0.76*
German	9	O	21.98	2.73	0.87	0.24	7.2	3.4	1.6	1.43	0.11*
	10	S	20.41	1.03	4.04	0.80	5.1	4.6	18.0	1.82	0.05^{n}
Goonyella	11	O	15.64	4.06	3.05	0.06	--	--	--	--	--
	12	S	19.36	3.15	2.57	0.23	25.1	6.4	13.6	1.39	0.79*
Gregory	13	O	18.21	1.67	1.63	0.20	4.6	3.2	9.4	2.08	0.09^{n}
	14	S	20.05	0.76	3.97	0.24	44.3	8.8	13.8	0.60	0.57*
Moura1	15	O	5.46	4.20	0.98	0.21	8.6	3.1	20.9	1.74	0.28*
	16	O	0.14	1.03	3.30	0.33	28.3	4.1	23.0	0.66	0.65*
Moura2	17	S	8.03	1.74	2.28	0.20	19.2	3.6	13.6	1.06	0.66*
Norwich	18	O	70.97	8.38	0.09	--	--	--	--	--	--
	19	O	14.10	0.30	2.87	0.22	--	--	--	--	--
Norwich	20	S	12.03	2.45	3.58	0.98	85.4	15.3	11.7	0.64	0.76*
Newlands	21	O	13.01	1.99	0.88	0.13	39.5	5.7	21.1	0.81	0.67*
	22	S	4.66	2.75	3.23	0.39	10.7	1.3	20.1	1.04	0.77*
Oaky	23	O	21.03	2.71	0.80	0.09	17.1	4.9	10.6	1.29	0.33*
	24	S	10.06	0.64	2.94	0.94	20.9	2.5	12.0	0.55	0.77*
Peak	25	O	6.22	3.18	1.22	0.05	11.5	2.8	28.9	1.07	0.63*
	26	S	6.86	2.88	1.22	0.10	45.9	3.9	9.6	0.60	0.81*
Saraji	27	O	12.74	1.82	4.20	0.40	14.2	4.2	23.1	1.27	0.36*
	28	S	5.84	1.63	2.25	0.21	12.9	1.4	4.7	0.97	0.70*
Tarong	29	S	8.51	0.33	0.76	0.04	14.4	2.0	8.9	0.92	0.71*
	30	S	7.06	2.48	1.05	0.21	21.3	2.5	14.4	0.94	0.74*
Wandoan	31	O	8.15	3.73	3.12	0.32	--	--	--	--	--
	32	S	8.38	4.28	1.86	0.40	1.3	0.6	7.1	1.88	0.15^{n}

S=soil, O=overburden. Ns = not significant at 0.05 level, significant at 0.05 (*), 0.01 (**) and 0.001 (***) level. -- not determined

Sediment delivery rates based on laboratory determinations of erodibility and the critical shear based erosion equations were tested against field data from a total of 113 rainfall simulation events carried out on 15 mine-sites. The relationship between predicted and measured sediment delivery rates is shown in Figure 3-4a-b. Regression analysis demonstrated a reasonable relationship (r^2=0.64) and a slope of 0.6 between predicted and measured sediment delivery rates. Hence the critical shear based model generally under-predicted erosion rates under these experimental conditions.

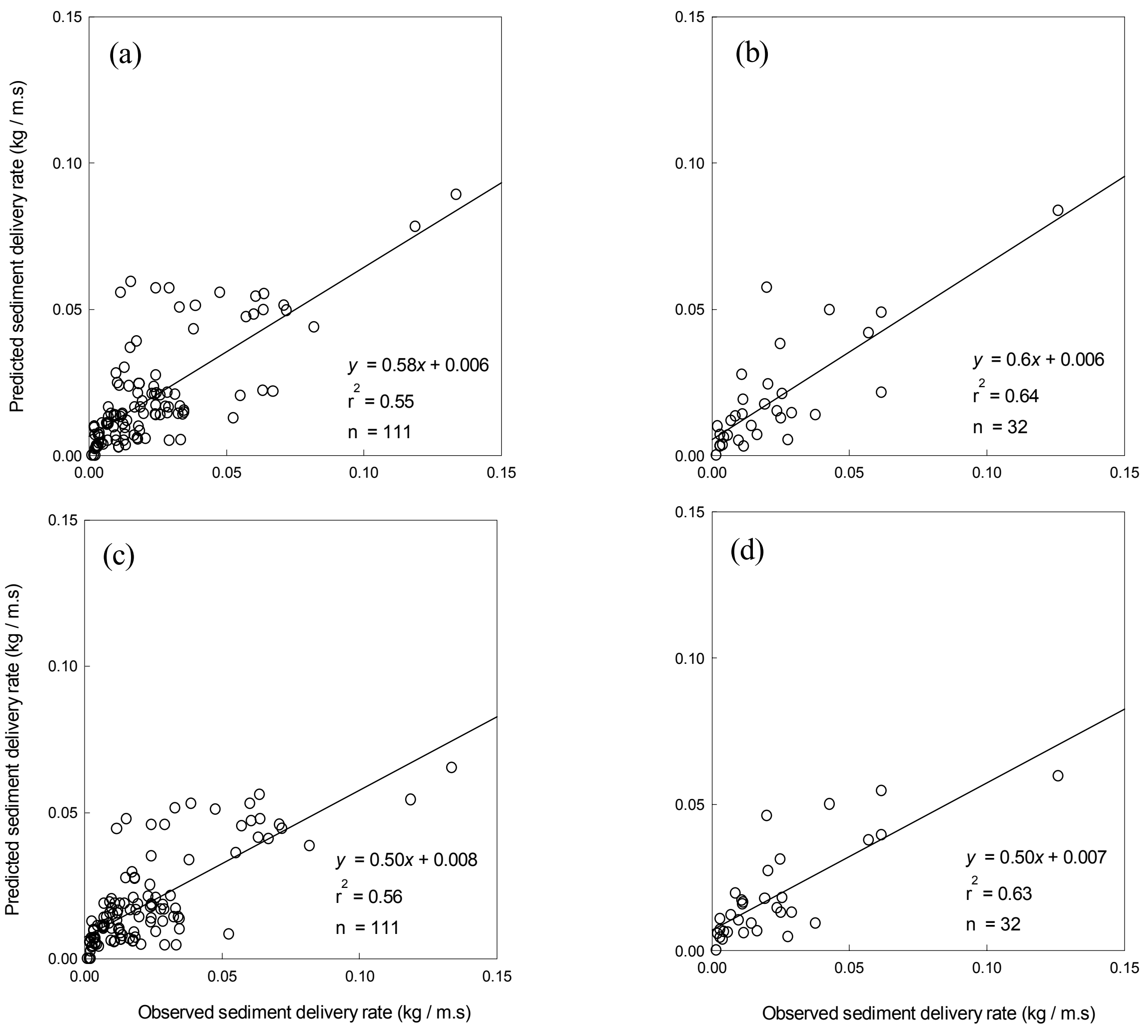

Figure 3-4 Plots of observed and predicted field sediment delivery rates for the critical shear based rill model (a-b) and the flow-rate based rill model (c-d). Plots on the right (b-d) have been averaged by media type.

3.4.6 Flow rate based model

Laboratory and field results were also compared using a flow-rate based power function to model rill detachment (Eq. 8) instead of the shear-based approach (Eq. 7). All other model parameters were calculated as described previously. The coefficients *a* and K_{r2} in Eq. 8 were calculated for each media from laboratory overland flow data at 20% slope (Table 3-4).

Equation 8 shows that rill erodibility is determined by two parameters, K_{r2} and *a*. However, if a is kept constant, erodibility can be represented by a single coefficient K_{r3} which can be calculated from equation 13. Results are shown in Table 3-5. The simplification using equation 13 did not affect the reliability of the prediction (numerical reduction in R^2), except for Oaky Creek overburden and Saraji soil.

Table 3-5 Rill erodibility parameters for the non-linear flowrate based rill model (Eq 8 and 9).

Mine site	Media #	K_{r2}	a	r^2	K_{r3} (a =1.6)	r^2	*Reduction in* r^2
Blair Athol	O	8.76	1.67	0.73	8.69	0.73	0.00
	S	8.71	1.55	0.82	7.09	0.81	0.00
Blackwater	O	0.88	1.68	0.21	0.88	0.21	0.00
	S	27.12	1.48	0.89	21.90	0.89	0.01
Calide	O	1.60	2.27	0.94	5.04	0.91	0.02
	S	32.12	1.33	0.94	22.76	0.90	0.04
Curragh	O	0.53	0.41	0.12	0.05	-	-
	S	6.71	1.94	0.85	11.07	0.84	0.01
German	O	12.96	1.21	0.57	5.76	0.54	0.04
	S	34.60	0.57	0.29	8.19	-	-
Goonyella	O	0.59	0.12	0.02	0.07	-	-
	S	1.85	2.59	0.90	7.24	0.85	0.05
Gregory	O	28.26	0.50	0.23	3.75	-	-
	S	6.28	2.27	0.61	12.72	0.58	0.03
Moura1	O	0.13	2.88	0.56	1.74	0.52	0.04
	O	0.32	3.22	0.77	4.82	0.68	0.09
Moura2	S	8.87	1.62	0.74	8.24	0.74	0.00
Norwich Pk1	O	0.06	1.48	0.61	0.04	0.60	0.00
	O	2.10	0.10	0.00	0.21	-	-
Norwich Pk2	S	26.67	2.07	0.88	37.92	0.85	0.03
Newlands	O	2.61	2.25	0.79	7.53	0.75	0.03
	S	1.12	2.04	0.90	2.26	0.89	0.01
Oaky Creek	O	19.76	0.98	0.41	6.14	0.30	0.10
	S	8.97	1.71	0.82	9.24	0.82	0.00
Peak Downs	O	0.05	3.10	0.83	1.02	0.78	0.06
	S	51.54	1.27	0.84	33.15	0.81	0.04
Saraji	O	0.82	2.12	0.55	2.12	0.54	0.01
	S	30.18	0.84	0.79	12.43	0.46	0.33
Tarong	S	6.23	1.73	0.83	6.81	0.83	0.00
	S	16.17	1.23	0.83	9.30	0.77	0.06
Wandoan	O	0.48	1.09	0.35	0.18	0.31	0.04
	S	0.48	1.62	0.60	0.43	0.60	0.00

S = soil, O = overburden. $^{\alpha}$ r^2 value may be negative as non-linear model is not necessarily nested within data

An average value for a of 1.60 (SD = 0.78) was determined and rill erodibility (K_{r3}) was subsequently calculated from;

$$K_{r3} = \frac{E_r}{Q_s^{1.60} S^{2.40}} \qquad [13]$$

The simplification of Eq. 8 to Eq. 13 allows rill erodibility to be represented by a single coefficient, K_{r3}.

Flow-rate based rill erodibility values varied by approximately 3 orders of magnitude, from 0.04 for the overburden from Norwich Park mine to 37.92 for a soil, also from Norwich Park. These findings compare with analysis by Gilley (1992) of the WEPP data set using a value of 1.18 for a giving a range of the K_{r2} parameter from 6.9 to 220. The higher K_{r2} values found by Gilley partially reflect the compensating effect of the lower exponents used on flow and slope in that study.

Predicted sediment delivery rates based on laboratory determinations of erodibility and the flow-rate based erosion equations were tested against the field data described previously. The relationship between predicted and measured sediment delivery rates is shown in

Regression analysis demonstrated a similar relationship (r^2 = 0.63 and a slope of 0.50) to that found using the shear based model, resulting in an under-prediction of field erosion rates.

3.4.7 Interill slope adjustment function

Analysis of the data from the interill experiments at 5, 10, 15, 20, and 30% showed an interaction between the erodibility of the media and the slope gradient. Most existing erosion models assume these components to be independent. Figure 3-5 shows that the relative ranking of the soil loss rate for all the media at 5% slope and at 30% slope is very different. Clearly, interill erodibility is not independent of slope gradient. Correlation of the soil loss rates measured at 5% slope against those measured at 30% slope for all media yields a coefficient of determination of only 0.14 (0.22 for soils & 0.87 for overburdens).

These results may be explained in terms of the changing processes as slope gradient increases. At 5% slope the erosive system may be transport limited due to the low velocity of surface flow. As slope gradient increases, and flow transport increases, the system approaches detachment limiting conditions. For a very cohesive media, for example Moura soil, erosion rates may be detachment limited at both 5 and 30%, and so display little response to slope gradient. In contrast, sandy soils with low cohesion, such as Norwich Park soil, may be strongly transport limited at 5% slope, and thus display dramatic increases in soil loss as slope gradient, and hence transport capacity, is increased. Clearly, there exists an interaction between erodibility and slope gradient.

To address this interaction, the interill slope adjustment factor S_f (Eq. 4) used for the calculation of interill erodibility for both models, was replaced with a sigmoid interill slope adjustment function S_{f2}; fitted to laboratory data;

$$S_{f2} = c_1+(c_2/(1+exp(-(S_2-c_3)/c_4))) \qquad [14]$$

where c_1,c_2,c_3 and c_4 are empirically derived coefficients fitted to the laboratory data from the 5, 10, 15, 20 & 30% slope experiments.

Thus, interill sediment delivery rate was predicted from

$$E_i = K_i*I*Q*S_{f2}*C_f \qquad [15]$$

Figure 3-6a compares observed and predicted erosion rates as a result of the replacement of Eq. 4 with Eq. 15 for both models. r^2 increases to 0.74 and the slope of the regression line is not significantly different from 1, and the intercept is not significantly different from zero, at the 0.05 level of significance.

Figure 3-6c,d compares the observed and predicted rates when the fitted slope function is used *and Q* in Eq. 1 is replaced with measured field runoff rates. Regression analysis demonstrated a slight improvement in prediction over the use of laboratory estimates of run-off from infiltration rate.

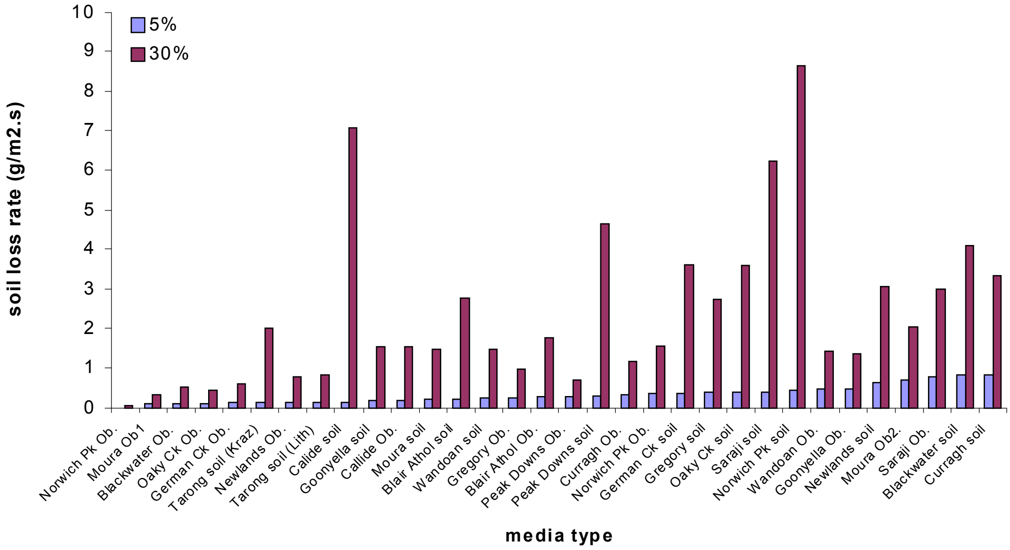

Figure 3-5 A comparison of the relative soil loss rankings of all the media types at 5% slope and 30% slope. This data demonstrates an interaction between slope gradient and erodibility.

The results show the critical shear based model and the non-linear flow based model produced similar predictions of sediment delivery rates from field rainfall simulation plots. This result suggests that rill erosion can effectively be modeled as either a linear (with a non-zero intercept) or a non-linear process. Rill erosion is commonly modeled as a linear function of shear stress (Nearing *et al.* 1989), though empirical evidence (Gilley *et al.* 1992) and theoretical investigations (Kemper 1985) suggest this relationship is often non-linear. Nearing, (1994) stresses that the parameters τ_c and K_r (Eq. 7) are mathematical entities resulting from a linearization of the commonly non-linear relationship between detachment and shear stress, and warns against a physical linear interpretation. A comparison of the r^2 values for the estimation of the rill erodibility parameters from the laboratory overland flow data (Table 3-4 and Table 3-5) reveals the non-linear equation fits better for 30 of the 32 media tested. However, this did not result in better field predictions from the non-linear model.

A significant improvement in the predictive ability of both models was achieved by the replacement of the standard interill slope adjustment function (Eq. 5) with an alternative function (Eq. 14) calibrated with data from the 5, 10, 15, 20, and 30% slope experiments (Figures 3-6c,d). The extremely variable and media dependent effect of slope gradient on the interill erosion rate found in this study has also been reported by Kinnell & Cummings (1993b). These authors concluded that a common relationship between interill erosion and slope gradient does not exist. Consequently, a range of functions containing coefficients to represent individual media responses were fitted to the slope data, and a sigmoid function (Eq. 14) was selected and incorporated into the interill prediction equation (Eq 15). The improved predictive ability of the models using this function must be weighed against the additional data required for estimation of the media-dependent coefficients within the sigmoid function. Fortunately, this data can easily be collected using the laboratory flume and rainfall simulator.

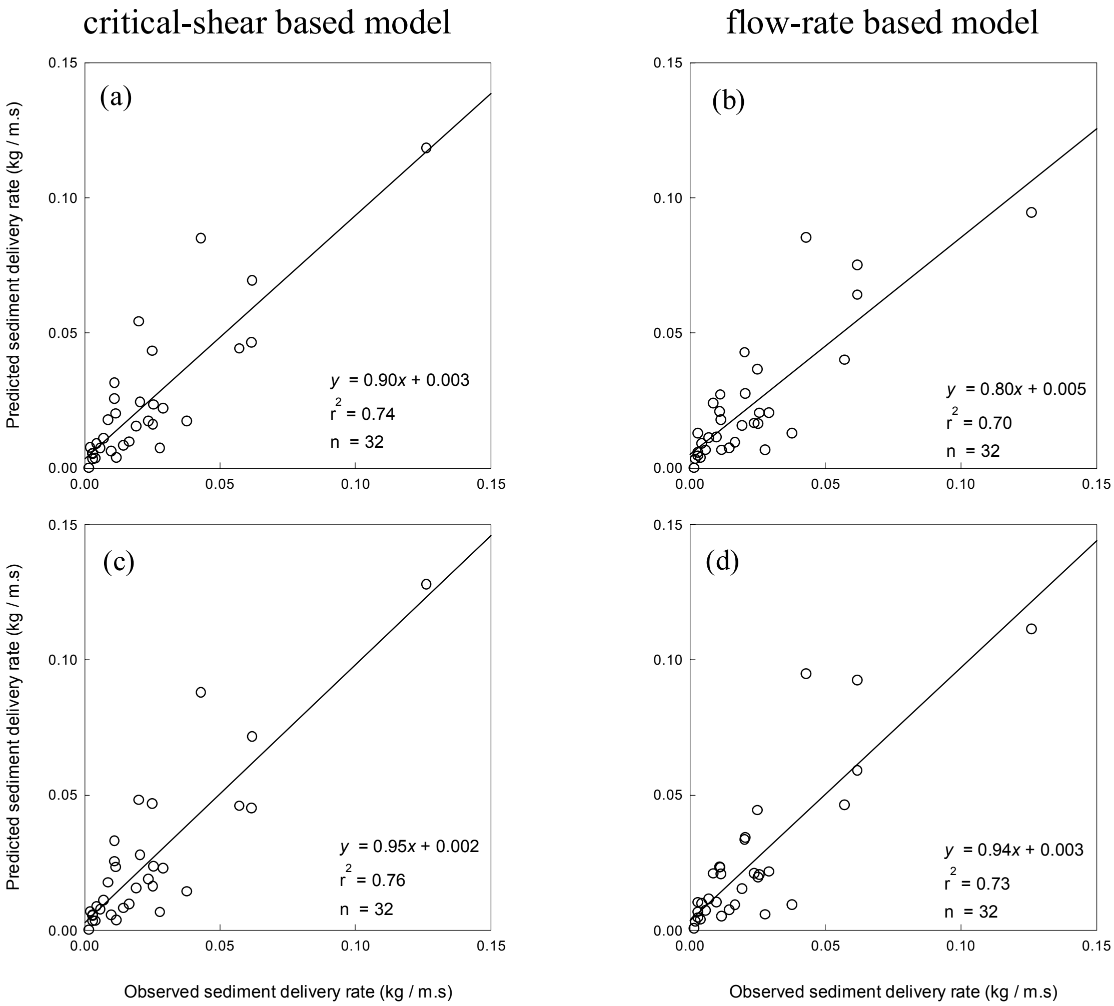

Figure 3-6 Plot of the predicted and observed field sediment delivery rates for the critical-shear based (a-c) and flow-rate based (b-d) erosion models. Predicted values plotted in a-b incorporated a sigmoid interill slope adjustment function, and in c-d, laboratory estimates of runoff have been replaced with field runoff rates.

The use of laboratory estimates of infiltration rate (Table 3-4) in both erosion models produced similar improvement in the predictions of field erosion to when runoff rates measured in the field were used (Figure 3-6). The results suggest that the runoff rates predicted from laboratory rainfall simulation provide suitable estimates of field runoff rates. Some authors (Mutchler *et al.* 1994) have reported laboratory simulations to be unsuitable in this regard as plots either become saturated due to lack of drainage or fail to replicate field matric potential when perforated flume floors are used. In this study, however, most of the overburdens and many of the soils developed surface seals and infiltration was limited to the top few centimetres. As a result, the effects of the shallow flume plot on surface hydrology were negligible.

In summary, this research demonstrates that soil losses due to the combined processes of rill and interill erosion at the hillslope scale can successfully be predicted from laboratory scale measurements of erodibility, provided a suitable methodology and modeling approach is adopted. The success of this approach greatly reduces the cost and effort required for the prediction of hillslope scale soil erosion.

3.5 The MINE*rosion* application

From a practical perspective, the results of this research are to be applied by environmental officers on mines to predict potential erosion rates from a range of landform design options. To maximize the usage of the data collected in the laboratory, and the modeling approaches developed, a user friendly computer application was developed called MINE*rosion* (Figure 3-7). The key objective of the MINE*rosion* application was to make the results of this research accessible to landform design decision-makers. The MINE*rosion* for Windows95 application provides a simple method for the rapid assessment of potential erosion from unconsolidated, unvegetated, post-mining landscapes. Landforms are particularly vulnerable to erosion in the period immediately following earthworks and prior to the establishment of vegetation cover. In tropical environments, most of the erosion is due to a limited number of high intensity storms (Wockner and Freebairn 1991). The MINE*rosion* model is an event-based model and can be used to assess worst case scenarios in this window of risk. The model can best be used to answer the question, "How much erosion can I expect from a 1 in *x* year storm, given a particular combination of media type, slope gradient and slope length?"

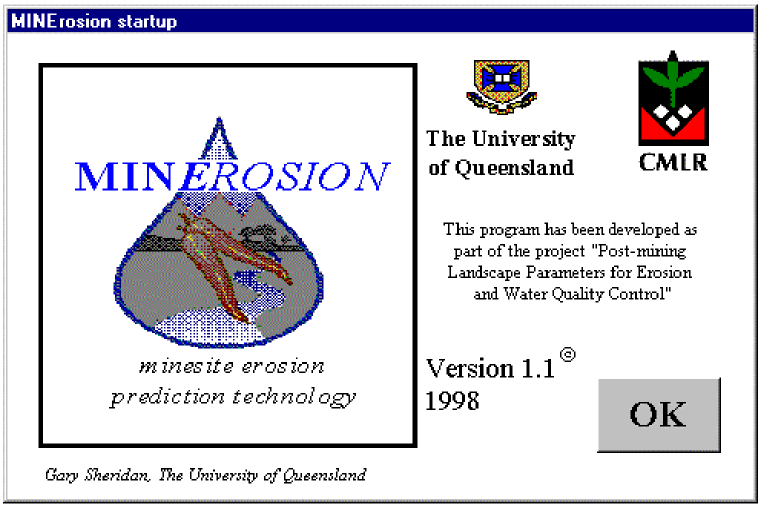

Figure 3-7 Startup screen for the MINE*rosion* computer model.

The application contains a database of erodibility parameters for 16 open-cut coal minesites and 32 different soil and overburden types. These media types can be selected from a drop down list to allow calculation of erosion rates. If the erodibility of a soil or overburden is not known, the MINE*rosion* program can calculate this from the easily measured properties of the media. Two types of output are produced. The first is a plot showing the predicted erosion rates for a range of slope length and gradient combinations. This output can be used to determine an optimal combination of slope length and gradient for a particular media type. The second output is a plot of the individual contributions of rill and interill processes to the total erosion rate. This output can be used to determine which erosive process is dominant for a particular combination of media type, slope length and slope gradient. Different erosive processes can be controlled in different ways, so this output can be used to guide the selection of the most appropriate management practices for erosion control.

The equations listed in this section were used to develop algorithms for the prediction of erosion from a set of input parameters. The application was written in Visual Basic 5.0 using the native controls shipped with Visual Basic program. The application has been structured so that future researchers can easily add to the database of media types and erodibility values within the program.

3.5.1 Inputs to the MINE*rosion program*

The inputs to the MINE*rosion* program are rainfall intensity, rainfall duration, rill erodibility, interill erodibility, infiltration rate and rill spacing. The inputs can be selected in three ways, depending on the level of information available to the user about the soil or overburden of interest.

If the erodibility of the soil or overburden of interest has been determined by this research, it will appear in the drop down list on the front-page of the MINE*rosion* application shown in Figure 3-8. The user makes a selection from this list and the program retrieves the appropriate erodibility values for this media type from a database and carries out the necessary calculations to determine erosion rates. The physical and chemical properties of the media selected should be checked to ensure the appropriate selection has been made.

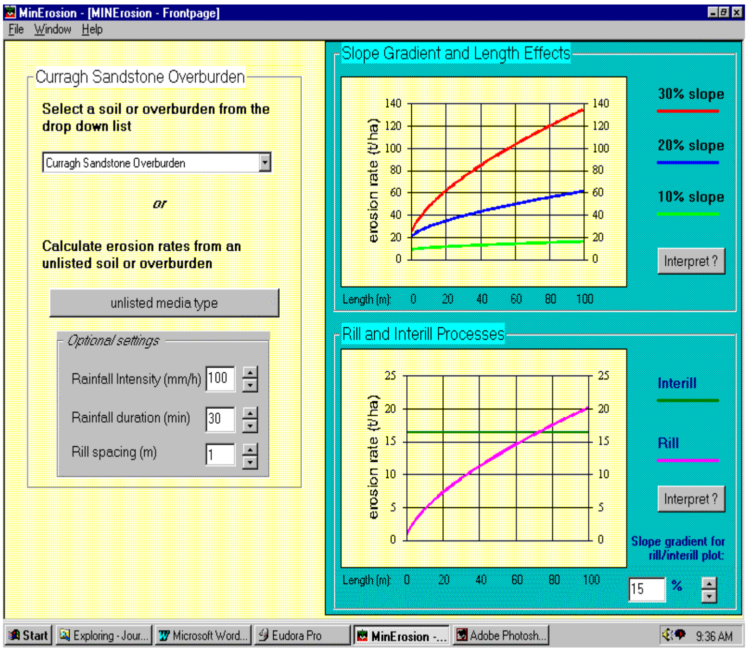

Figure 3-8 The graphical user interface for the MINE*rosion* model, showing the drop down list for selection of minesite and media type.

To do this, select “window” from the menu bar and click on “soil/overburden properties”. This window (Figure 3-9) allows the user to browse a database of the physical and chemical properties of all the media tested as part of this research.

If the soil or overburden of interest does not appear in the drop down list on the MINE*rosion* front-page, then the erodibility of your media has not been determined as part of this research. However, the erodibility can be *estimated* from media properties based on predictive equations developed from laboratory research and reported in this section. To access the erodibility calculation page, select “window” from the menu bar and click on “estimating erodibility”. This window (Figure 3-9) allows the user to input values for selected media properties for the prediction of erodibility. The user must first select whether the media is a soil or an overburden. The range of the values, which can be entered, is restricted to the values displayed in the ‘tool tip’ when the mouse is positioned over the value box. When the *plot soil* or *plot overburden* button is pressed, the program estimates erodibility and carries out the necessary calculations to determine erosion rates.

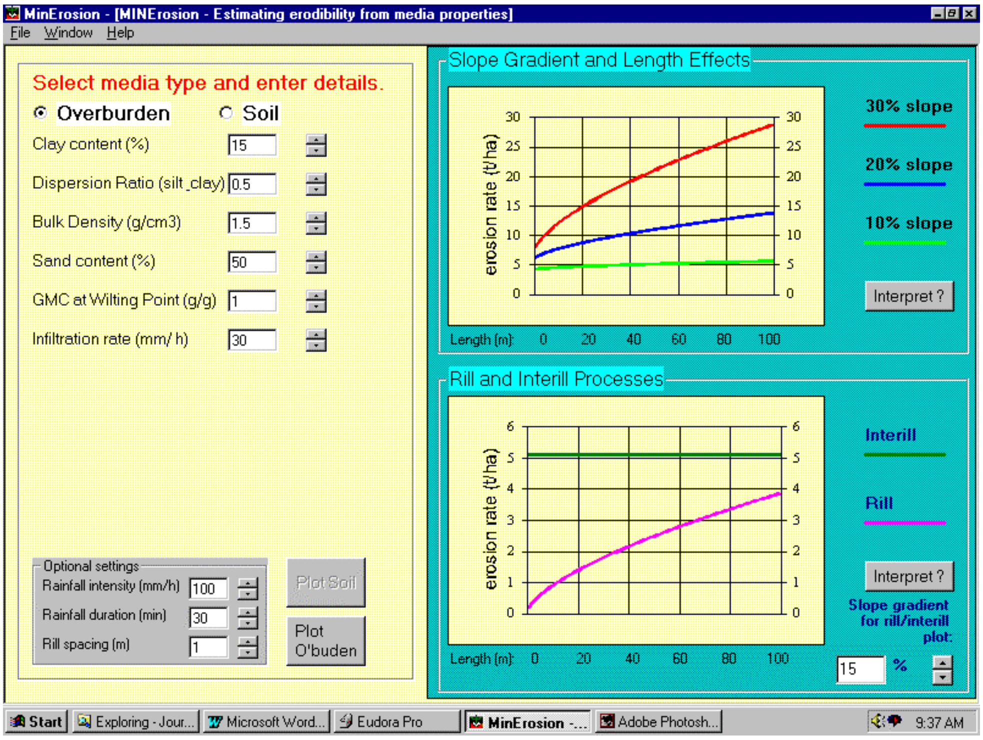

Figure 3-9 The graphical user interface for the MINE*rosion* model, showing the section for the estimation of erodibility from media properties.

If your soil or overburden does not appear in the drop down list on the MINE*rosion* front-page, and you don't have the measurements of media properties needed to calculate erodibility, then you may be able to match your media to one of the media types listed in the media properties database window (Figure 3-10). The user can peruse the list of known media types in the drop down list, and view the physical and chemical properties of each media to find one similar to the media of interest. The matching media can then be used as a "surrogate type" by selecting it in the dropdown list on the MINE*rosion* front-pages.

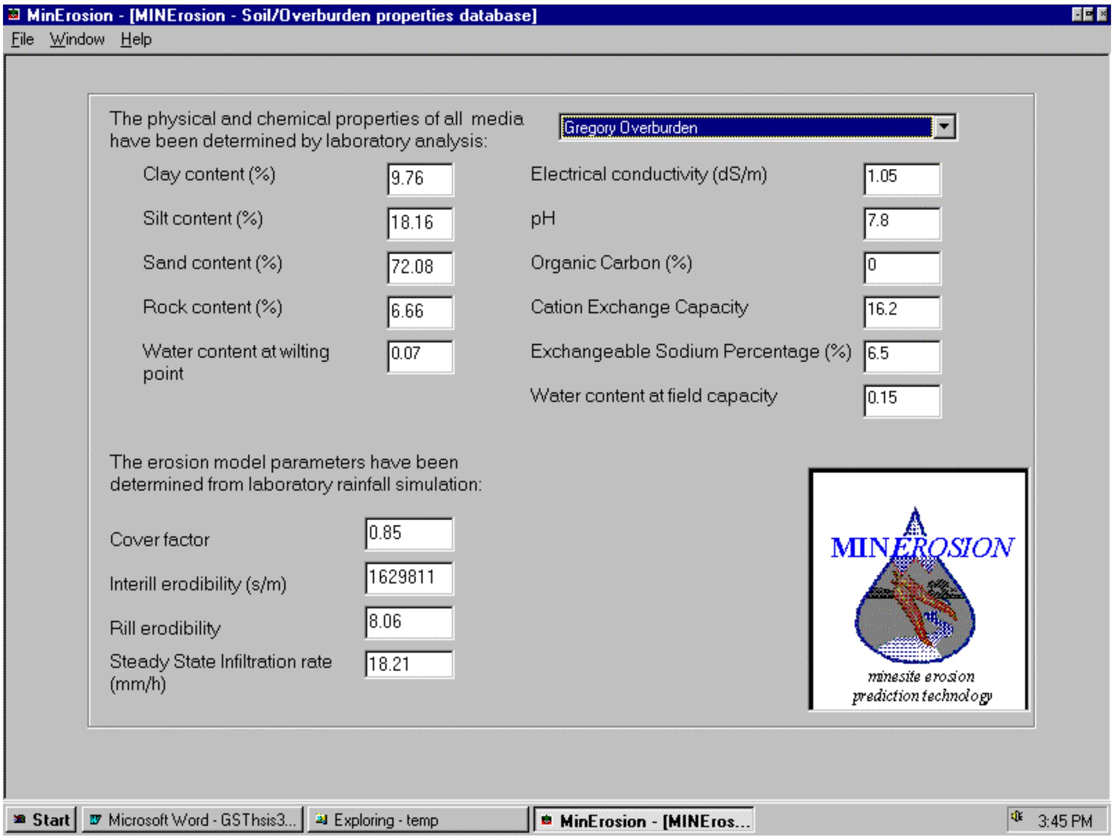

Figure 3-10 The media properties database window for the MINE*rosion* application.

Regardless of which of the three input methods described above is used, the user must also select the rainfall intensity and duration, and the rill density. The input for these variables is made in the "optional settings" box shown in the bottom left of Figure 3-7 and Figure 3-8. The rill density value is the number of metres between each rill on the hillslope. The rill density will alter the predicted rill detachment rate. The default value is 1, based on analysis of rill density data by Gilley *et al.* (1990). If the media of interest tends to develop fewer, more concentrated flow lines, then this value should be increased. This may occur when the slope varies laterally, or when cross ripping across the contour has tended to channel overland flow to low points across the slope.

The rainfall intensity and duration settings allow the erosion from a design storm to be predicted. The return period for a storm of a particular intensity and duration can be determined for a particular region from standard civil engineering charts and tables. The rainfall intensity in the model can be set between 40mm/h and 100 mm/h. The duration can be varied between 10 minutes and 120 minutes. The default values are 100mm/h for 30 minutes.

3.5.2 **MINE***rosion program outputs*

The MINE*rosion* model is a single event based model. The erosion rates predicted by the model are in tons per hectare per rainfall event. This is not the same as an annual average tons/ha value computed by models such as the Universal Soil Loss Equation. The USLE is useful for estimating long term annual average erosion rates for a particular set of conditions. The MINE*rosion* model is useful for predicting erosion from a single, high intensity storm.

In regions exposed to tropical rainstorms (i.e. the central Queensland coalfields), most of the soil erosion is associated with a small number of high intensity rainfall events. Given information on the return period for a particular storm (1 in 5 years for example), the model can be used to estimate erosion rates for a 1 in 5 year storm. Return periods for storms are published for use by civil engineers and hydrologists to adequately design drainage structures.

The plot titled "Slope gradient and length effects" show the effect of slope gradient and slope length on erosion rates. The relative contributions of rill and interill processes to total erosion are shown by the plot titled “Rill and interill processes”.

The most functional aspect of the MINE*rosion* model is the ability to compare and contrast different slope length and gradient combinations in terms of the effects on erosion rates. The plot “ Slope length and gradient effects” should be inspected carefully to obtain as much information as possible for the media of interest. Firstly, look at the absolute values erosion on the Y – axis and compare your media to some of the others in the database. This will give you a feel for whether or not your media is highly erodible, or relatively stable, relative to others in the region. Next, look at the steepness of the curves. The steeper the curves, the more susceptible the media is to increases in slope length. Finally, look at how closely the curves plot to one another. If the curves are nested closely together, it means the media is not strongly affected by increases in slope gradient.

An example of the style of output from the MINE*rosion* application is shown in Figure 3-11. The interaction between slope length, slope gradient, and soil erosion is shown for two contrasting media types. The example on the left is a clay soil from Wandoan. The example on the right represents a sandy soil from Norwich Park mine. Note the strong response to slope gradient and length by the Norwich Park soil, compared to the limited response on the Wandoan soil.

Knowledge of the relative rates of rill and interill erosion can be obtained by carefully inspecting the plot “Rill and interill processes". If the curve for rill erosion is steep, and above the interill line for most of the slope length, then this media is strongly susceptible to rill erosion (at the selected slope gradient). Figure 3-12 shows an example of the style of the rill and interill graphical output from the MINE*rosion* application. The example on the left shows a soil strongly susceptible to interill erosion. The example on the right is a soil dominated by rill erosion.

Rill erosion is caused by the accumulation of overland flow, so managing a slope that is susceptible to this process should involve a) reducing the amount of water running over the slope, or b) controlling the flow so that it is not eroding the media.

The amount of water running over the slope can be reduced by either increasing the infiltration rate, or by reducing the catchment area. Vegetation is the best method for increasing infiltration. Surface mulches, and even surface rock can also be beneficial. The catchment area can be reduced by ensuring there is no run-on coming onto the slope from the catchment above. The surface storage (for water) of the surface can also be increased by cross ripping, or ponding. The flow running over the media can be controlled using vegetation, contour banks, and rock lined waterways.

If the curve for interill erosion is above the curve for rill erosion, then this media is more susceptible to interill than rill erosion. Interill erosion results form raindrop impact, so any management technique which results increased surface cover will be beneficial. Vegetation, mulches, litter or rock cover all have the potential to reduce this form of erosion to a negligible level.

For online assistance with the output produced by the MINE*rosion* model, see the help section titled "How do I interpret the results".

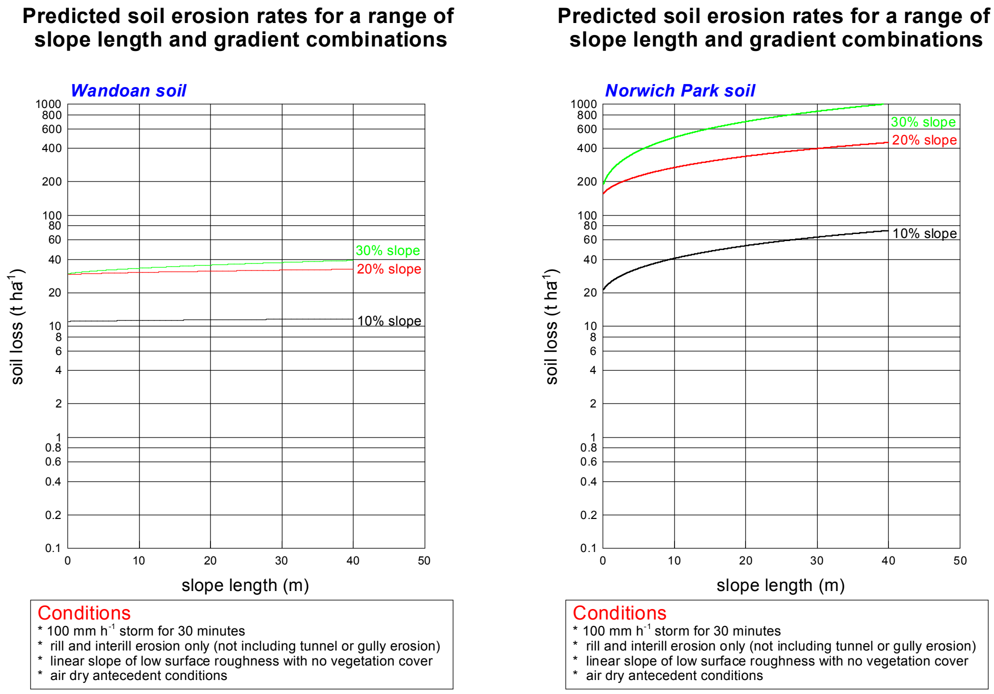

Figure 3-11 An example of the graphical output from the MINE*rosion* application showing the effect of slope length and slope gradient on soil erosion rates.

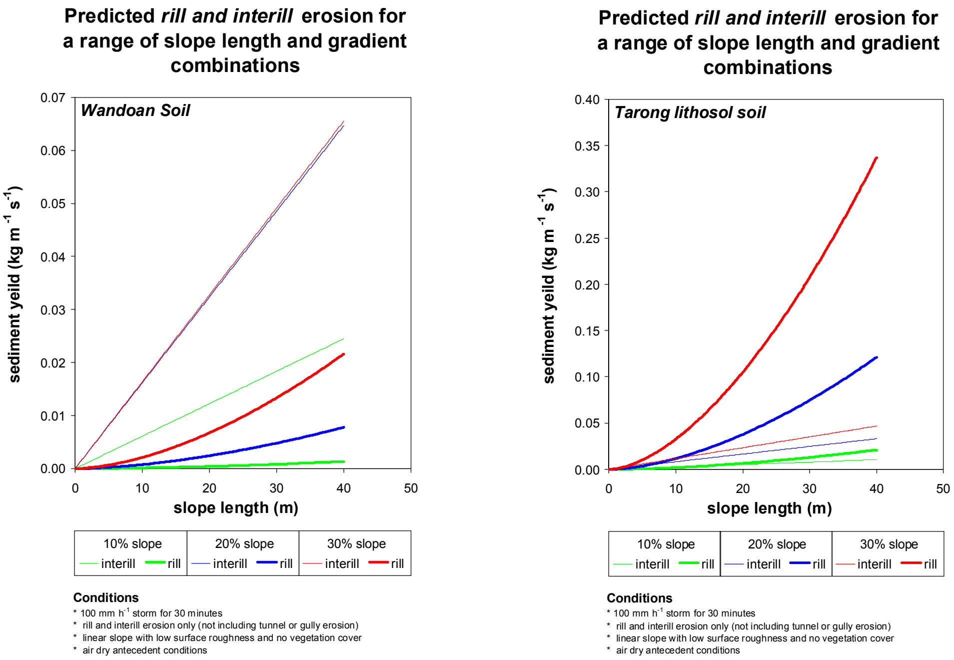

Figure 3-12 An example of the graphical output from the MINE*rosion* application showing the relative significance of rill and interill processes.

3.5.3 Limitations of the **MINE***rosion application*

The MINE*rosion* model should not be used to predict annual average erosion rates. Annual average and event based models are fundamentally different, and the results from each type of model can not be directly compared. The MINE*rosion* model should only be used for predictions on bare, unvegetated slopes. There is no facility within the model to account for the effects of vegetation on erosion rates. Further work is needed before it can be used with vegetation and consolidation of the material.

The MINE*rosion* model predicts erosion due to rill and interill processes only. In cases where other erosive processes are significant (such as gullying, mass movement and tunnel erosion) the model will significantly under-predict erosion rates. The MINE*rosion* model should not be used for concave slopes, or for slopes where the gradient decreases and allows deposition of sediment to occur. In these cases the model will over-predict erosion rates. Where there is significant surface storage of runoff water, such as in ponds and cross rips, the model will probably overestimate the interill component, and underestimate the rill component.

As the predictions from any model are extrapolated beyond the limits of the data used to parameterize them, the confidence in the predictions decreases. Extrapolations beyond the range of slope lengths used in the model may be in error, for example in cases where other processes such as gullying and mass movement become significant at longer slopes.

The MINE*rosion* model has been developed from data collected on Queensland open-cut coalmines, however it can potentially be used in other areas where land disturbance has resulted in erosion problems. The model has been designed so that new media types can be added to the database following determination of the erodibility values using the laboratory methodology and modeling approach described in this paper. The model would be particularly suited to base and precious metal mines in the north of Australia where rainfall intensities are high, and erosion is often caused by large single storms.

The good agreement between sediment delivery rates predicted by MINE*rosion* with observed values from the field rainfall simulator plots indicates that it should be possible to derive an appropriate MUSLE erodibility value from laboratory measurement. This will then link MINE*rosion* to the Perfect-Grasp-Musle module in section 5, which derives appropriate landscape design criteria for each mine. This development will be undertaken and made available at a later date to all participating mines and ACARP.

3.6 Summary

In summary, this research demonstrates that potential soil losses from bare unconsolidated surfaces, due to the combined processes of rill and interill erosion at the hillslope scale, can successfully be predicted from laboratory scale measurements of erodibility. This project has provided a suitable methodology and modeling approach for that purpose.

Material erodibility parameters can also be predicted from the physical and chemical properties of the media, which are readily available from routine soil analysis. The necessary analysie are texture (clay and fine sand contents), organic carbon contents, pH, bulk density, dispersed silt and clay contents, ESP and the electrical conductivity of the soil solution.

The development of the MINE*rosion* model and its user-friendly Windows based application enables these research findings to be utilized by the mining industry as a tool towards the successful design of stable post-mining landforms. This approach can greatly reduce the cost and effort required for the estimation of potential hillslope scale soil erosion.

References:

Balisacan, C.M. (1996). The effect of salinity and rain intensity on the erodibility of overburden spoils from central Queensland open-cut coal mines. Masters Thesis. University of Queensland, Australia.

Barnett, A.P., and Dooley, A.E. (1972). Erosion potential of natural and simulated rainfall compared. *Trans. Am. Soc. Agric. Eng*. 15: 1112-14.

Barnett, A.P. and Rogers, J.S. (1966). Soil physical properties related to runoff and erosion from artificial rainfall. *Trans. Am. Soc. Agric. Eng*. 9: 123-28.

Bell, L.C., Loch, R.J., Haneman, D., and Willgoose, G.R. (1993). A post-mining landform research program for open-cut coal mines. In Proceedings of the Eighteenth Annual Environmental Workshop, Burnie, October 1993. pp 143-155. Australian Mining Industry Council.

Bubenzer, G.D. (1979). Inventory of rainfall simulators. In Proceedings of the rainfall simulator workshop, Tucson, Arizona, March 1979. pp 120-30. (USDA Agricultural Research (Western region), Science and Education Administration, Agricultural Reviews and Manuals)

Bubenzer, G.D. and Meyer, L.D. (1965). Simulation of rainfall and soils for laboratory research. *Trans. Am. Soc. Agric. Eng*. 8: 73, 75.

Day, P.R. (1965). Particle fractionation and particle size analysis. In 'Methods of Soil Analysis Part I' (Eds C.A. Black and D.D. Evans) pp.545-67. (Amer. Soc. Agron.: Madison, Wis.).

Duncan, M.J. (1972). The performance of a rainfall simulator and an investigation of plot hydrology. M.Agr. Sc. Thesis, Lincoln College, Univ. Canterbury, New Zealand.

Elliot, W.J., Laflen, J.M., and Kohl, K.D. (1989). Effect of soil properties on soil erodibility. Paper No 892150 at the International Summer Meeting of the American Society of Agricultural Engineers and the Canadian Society of Agricultural Engineering. June 25-28, Quebec, Canada.

Evans, K.G. (1992). Determination of interill erodibility parameters for selected overburden spoil types from central Queensland open-cut coal mines. Masters Thesis, University of Queensland, Brisbane, Australia.

Fentie, B., Rose, C.W., Coughlan, K.J., and Ciesiolka, C.A.A. (1997). The role of the geometry and frequency of rectangular rills in the ralationship between sediment concentration and stream power. *Aust. J. Soil Res*. 35: 1359-77.

Foster, G.R., Huggins, L.F., and Meyer, L.D. (1984). A laboratory study of rill hydraulics: II Shear stress relationships. *Trans. Am. Soc. Agric. Eng.* 29: 797-804.

Foster, G.R., Meyer, L.D., and Onstad, C.A. (1977). An erosion equation derived from basic erosion principles. *Trans. Am. Soc. Agric. Eng*. 20: 678-82.

Foster, G.R., Simanton, J.R., Renard, K.G., Lane, L.J., and Osborn, H.B. (1981). Discussion of "Application of the universal soil loss equation to rangelands on a per-storm basis" by Trieste and Gifford. *J. Range Manage*. 34: 161-64.

Gilley, J.E., Gee, G.W., Bauer, A., Willis, W.O., and Young, R.A. (1977). Runoff and erosion characteristics on surface mined sites in Western North Dakota. *Trans. Am. Soc. Agric. Eng.* 20: 697-700.

Gilley, J.E., Kincaid, D.C., Elliot, W.J., and Laflen, J.M. (1992). Sediment delivery on rill and interill areas. *J. Hydrology*. 140: 313-41.

Gilley, J.E., Kottwitz, E.R., and Simanton, J.R. (1990). Hydraulic characteristics of rills. *Trans. Am. Soc. Agric. Eng*. 33: 1900-06.

Hairsine, P.B. (1988). A physically based model of the erosion of cohesive soils. PhD Thesis, Griffith University, Brisbane, Australia.

Hairsine, P.B., and Lemin, H. (Unpublished) C.S.I.R.O. Field rainfall simulator and raintower module drop velocity and drop size measurements. C.S.I.R.O Division of Soils report, Canberra.

Kemper, W.D., Trout, T.J., Brown, M.J., and Rosenau, R.C. (1985). Furrow erosion and water and soil management. *Trans. Am. Soc. Agric. Eng.*

Kinnell, P.I.A. (1992). Sediment transport induced by raindrops impacting shallow flows. PhD Thesis. University of New England, New South Wales, Australia.

Kinnell, P.I.A., (1993) Sediment transport by shallow flows impacted by pulsed artificial rainfall. *Aust. J. Soil Res*. 31: 199-207.

Kinnell, P.I.A. (1993a). Interill erodibilities based on the rainfall intensity-flow discharge erosivity factor. *Aust. J Soil. Res*. 31: 319-32.

Kinnell, P.I.A. and Cummings, D. (1993). Soil/slope gradient interactions in erosion by rain-impacted flow. *Trans. Am. Soc. Agric. Eng*. 36: 381-87.

Kinnell, P.I.A., and McLachlan, C. (1988). An injection barrel for the top entry sedimentation tube. CSIRO Division of Soils Technical Memorandum No. 43.

Loch, R. J. (1989). Aggregate breakdown under rain: its measurement and interpretation. PhD Thesis, University of New England, Armidale, N.S.W. 139pp.

Loch, R.J. and Foley, J.L. (1994). Measurement of aggregate breakdown under rain: comparison with tests of water stability and relationships with field measurements of infiltration. *Aust. J. Soil Res*. 32: 701-720.

Meyer, L.D. (1958). An investigation of methods for simulating rainfall on standard runoff plots and a study of the drop size, velocity, and kinetic energy of selected spray nozzles. Special report no. 81, Soil Water Conserv. Res. Div., Agric. Res. Service, US Dept. Agric.

Meyer, L.D. and McCune, D.L. (1958). Rainfall simulator for runoff plots. *Agric. Eng*. 39: 644-48.

Meyer, R.D. and Harmon, W.C. (1977). Rainfall simulator for evaluating erosion rates and sediment sizes from row side slopes. ASAE paper no. 77-2025.

Meyer, R.D. and Harmon, W.C. (1979). Multiple intensity rainfall simulator for erosion research on row side slopes. *Trans. Am. Soc. Agric. Eng*. 22: 100-3.

Middleton, H.E., Slater, C.S., and Byers, H.G. (1934). Physical and chemical characteristics of the soils from the erosion experiment stations. USDA technical bulletin no 430.

Mitchell, J.K., Moldenhauer, W.C., and Gustavson, D.D. (1983). Erodibility of selected reclaimed surface mined soils. *Trans. Am. Soc. Agric. Eng*. 26: 1413-17.

Mulligan, D.R., Grigg, A.H., Madsen, P.A., Pearce, A.B., and Roe, P.A. (1996). Research initiatives for the remediation of land following open-cut coal mining in central Queensland. In Procedings of the International Conference on the Remediation and Management of Degraded Lands, Hong Kong, 3-6 December, 1996.

Mutchler, C.K., Murphree, C.E., and McGregor, K.C. (1994). Laboratory and field plots for erosion research. In 'Soil Erosion Research Methods. Second edition.' (Ed R.Lal.) pp 127-56. (Soil and Water Conservation Society: USA).

Nearing, M.A., Foster, G.R., Lane, L.J., and Finkner, S.C. (1989). A process-based soil erosion model for USDA-Water Erosion Prediction Project technology. *Trans. Am. Soc. Agric. Eng*. 32: 1587-93.

Nearing, M.A., Lane, L.J., and Lopes, V.L. (1994). Modeling soil erosion. In 'Soil Erosion Research Methods. Second edition.' (Ed R.Lal.) pp 127-56. (Soil and Water Conservation Society: USA).

NSERL (1989). A compendium of soil erodibility data from WEPP cropland soil field erodibility experiments 1987 & 88. National Soil Erosion Research Laboratory (NSERL) Report no 3. West Lafayette.

NSERL (1994). USDA-Water Erosion Prediction Project Erosion Prediction Model, Version 94.7 User Summary. National Soil Erosion Research Laboratory (NSERL) Report no 9. West Lafayette.

NSERL (1995). USDA-Water Erosion Prediction Project (WEPP) Technical Documentation. National Soil Erosion Reseat Laboratory (NSERL) Report no 10. West Lafayette.

Onstad, C.A., and Foster, G.R. (1975). Erosion modeling on a watershed. *Trans. Am. Soc. Agric. Eng*. 26: 1102-4, 1108.

Poesen, J., Ingelmo-Sanchez, F., and Mucher, H. (1990). The hydrological response of soil surfaces to rainfall as affected by cover and position of rock fragments in the top layer. *Earth Surface Processes.* 15: 653-71.

Poesen, J.W., Torri, D., and Bunte, K. (1994). Effects of rock fragments on soil erosion by water at different spatial scales: a review. *Catena* 23: 141-66.

Rubio-Montoya, D. and Brown, K.W. (1984). Erodibility of strip-mine spoils. *Soil Science* 138: 365-73.

SAS Institute Inc (1988). 'SAS/STAT™ users guide, release 6.03 edition.' (SAS Institute Inc:Cary, NC, USA).

Schmidt, J. (1991). A mathematical model to simulate rainfall erosion. *Catena Supp*. 19: 101-9.

Sheridan, G.J., Walker, C.M., Kirsch, B.H., and So, H.B. (1994). The effect of rainfall wetting/drying cycles on runoff and erosion for a Queensland mine site soil and overburden. In Proceedings of the symposium Sealing, crusting, hardsetting soils: Productivity and Conservation, Brisbane, Australia, 1994.

Sheridan, G.J., Walker, C.M., So, H.B., and Kirsch, B.H. (1996a). Predicting infiltration under rainfall on open-cut coal mine overburdens and soils from the physical and chemical characteristics of the media. *Eos Trans AGU* 77 (22):46.

Sheridan, G.J., Walker, C.M., So, H.B., and Kirsch, B.H. (1996b). Predicting the erodibility of open-cut coal mine overburdens and soils from the physical and chemical characteristics of the media. Australian and New Zealand Soils Conference; 1996; Melbourne. 1996; 241p.

Sheridan, G.J., So, H.B., Loch, R.J., Pocknee, C. and Walker, C.M. (1998). Predicting hillslope scale soil erosion on rehabilitated coal mines from laboratory scale measurements of rill and interill erodibility. In Procedings of National Soils Conference – Environmental Benefits of soil Management, Brisbane, Australia, April 27-29.

Short, M.F., Kirsch, B.H., Sheridan, G.J., So, H.B.. (1996). Importance of sediment mobilisation for the release of soluble salts in water runoff from reclaimed open-cut coal landscapes in the Bowen Basin Queensland. *Eos Trans AGU* 77 (22):47.

Trieste, D.J. and Gifford, G.F. (1980). Application of the universal soil loss equation to rangelands on a per-storm basis. *J. Range Manage.* 33: 66-70.

Verhaegen, T. (1987). The use of small flumes for the determination of soil erodibility. *Earth Surface Processes*. 12: 195-204.

Welsh, D., Hinz, R., Garlipp, D., and Gillespie, N. (1994). Coal mines on target with environmental planning. Queensland Government Mining Journal. February 1994.

Williams, J.R. (1975). Sediment yield prediction with universal equation using runoff energy factor. In 'Present and prospective technology for predicting sediment yields and sources.'. USDA, ARS-S-40, pp244-252.

Wischmeier, W.H. and Mannering, J.V. (1969). Relation of soil properties to its erodibility. *Soil. Sci. Soc. Am. Proc*. 33: 131-37.

Wischmeier, W.H., and Smith, D.D. (1978). Predicting rainfall-erosion losses - a guide to conservation planning. U.S. Dept Agric. Handbook no. 537.

Wischmeir, W.H. (1976). Use and misuse of the universal soil loss equation. *J. Soil Water Con*. :5-9.

Woolhiser, D.A. and Brakensiek, D.L. (1982). Hydrologic system synthesis. In Hydrologic modeling of small watersheds. *Am. Soc. Agric. Eng. Monograph* 5: 3-16.

Wu, T.H., Stadler, A.T., and Low, C. (1996). Erosion and stability of a mine soil. *Journal of Geotechnical Engineering*. 122: 445-53.

4. Field Rainfall Simulation

R.J. Loch[a] and C. Pocknee[b]
[a] Principal Research Scientist, Queensland Department of Natural Resources, Toowoomba, Q 4350; Currently Director, Landloch Pty Ltd.
[b] Postgraduate student, School of Land and Food, The University of Queensland, St Lucia, Q 4072. Currently Environmental Officer, Newlands Coal Mine, Central Qld.

4.1 Introduction

4.1.1.Role of field rainfall simulation within the project

Within the Post-Mining Landscape Parameters project, field rainfall simulation was used for two separate purposes:

(a) To provide an assessment of infiltration and erodibility characteristics of topsoil and spoil across all participating mines; and to

(b) Assess effects of vegetation on infiltration and erosion for a limited number of mines where suitable study sites could be identified.

The assessment of soil and spoil across all mines provided a means of extending results from the three detailed study sites to all participating mines. This approach took advantage of the mobility of the rainfall simulator, and its ability to apply relatively constant test conditions to a range of sites.

Studies of vegetation effects were planned to give more detailed data than would be available from the field plot and catchment studies, and that would enable parameterization of water balance/plant growth/erosion models. These studies took advantage of the ability of rainfall simulator studies to achieve both precise control of experimental conditions and to make relatively detailed measurements. The use of field plots also enabled study of changes in soil properties through time, and measurement of effects of features such as soil macropores and changes in salinity profiles that could not be duplicated in the laboratory.

4.1.2 Use of rainfall simulation for measuring soil properties

Runoff and erosion from a plot under a simulated storm are not a measure of the long-term runoff and erosion from a paddock or catchment. However, rainfall simulation can be used to study the properties of the particular soil and to derive a range of parameters describing soil behavior. It has also been widely used to assess impacts of particular management practices, and to increase our understanding of various processes of infiltration, runoff, and erosion.

A range of studies have shown that it is possible to use parameters derived from rainfall simulation as a basis for modeling the behavior of landscapes, sometimes under quite long periods of natural rain. Provided the parameters derived are appropriate, this can be quite successful. Examples of this (for runoff) include use of Green-Ampt parameters from rainfall simulation by Silburn and Connolly (1995), Connolly and Silburn (1995), Connolly *et al.* (1997 and 1998), and derivation and use of curve numbers by Littleboy *et al.* (1996, a,b) and Cogle *et al.* (1996). Examples of successful use of parameters from rainfall simulation to predict field-scale erosion include Loch *et al.* (1989) and Silburn and Loch (1990).

Therefore, studies of the infiltration and erosion properties of the wide range of spoils and soils within the Post Mining Landscape Parameters project focussed on deriving parameters that could be incorporated in runoff/erosion models such as the Modified Universal Soil Loss Equation (MUSLE) (Onstad and Foster 1975) and WEPP (Water Erosion Prediction Program) (Laflen *et al*. 1991). Because these models deal with single events rather than with long-term averages, model parameters can be derived from the single-event rainfall simulator data generated within this project.

4.2 Methods

4.2.1 Rainfall simulator design

The simulator used (Figure 4-1) was designed and built at the Department of Primary Industries, Toowoomba, and is a refinement of two previous versions used at that location. It is based on an original design of Bubenzer and Meyer (1965), and is similar to, though more streamlined than, a simulator design developed at the US National Soil Erosion Research Laboratory and presently used in studies across the United States.

Figure 4-1: The rainfall simulator in use at the Curragh Mine

Simulated rain is produced by flat fan Veejet 80100 nozzles mounted on an oscillating manifold. Kinetic energy produced by the nozzles is approximately 29.5 J/m^2/mm (Duncan 1972), which is consistent with natural rain at intensities above 40 mm/h (Rosewell 1986). The nozzles sweep to and fro across the plot, and achieve good spatial uniformity of intensity, with a coefficient of variation for intensity less than 10%.

The intensity used was standardized at 100 mm/h. Intensities of that order for 15 minutes duration would be encountered in the central Queensland area approximately every second year.

The rainfall simulator has an aluminium A frame structure, and is modular in design (Figure 4-1). The modular design keeps manifold lengths short and minimises variations in pressure head on the steep slopes studied. The simulator applies rain to plots 1.5 m wide, with plot length being a function of the number of simulator modules used. Up to six modules are used, covering a maximum plot length of 12 metres. For a runoff rate of 100 mm/h, the 12 m long plot produces a discharge of 0.5 litres/sec, equivalent to flows known to have established rills on gradients as low as 4%.

Runoff rate is measured using a set of three tipping buckets. The buckets are of differing sizes and interchangeable, ensuring that tip rates (and hence, accuracy of measurement) are maintained at optimum levels across a wide range of flow rates. During the second year of the study, a sediment trap was included in the runoff measurement system to avoid any effects of sediment load on bucket calibration and accuracy, though only one material in either year of the study produced sediment concentrations high enough to be of concern. Samples of runoff and sediment are taken prior to runoff passing through the sediment trap and tipping buckets. Techniques associated with the use of the simulator and recording of data are described by Loch *et al*. (1998).

4.2.2 Standard procedures for studies on bare soils (for parameter derivation)

The standard procedure had three components:

- Rain at *approximately* 100 mm/h applied to a plot 12m long and 1.5m wide for 30 minutes. Runoff rates were measured through time, and samples of sediment in runoff were taken for measurement of total sediment loads, sediment size and settling velocity distributions, and proportions of silt and clay sized particles in runoff. When rain ceased, the runoff recession curve was measured to enable estimates of surface roughness parameters.

- Within minutes of the first "run" being completed, rain at the same intensity was applied for approximately 10 minutes to the downslope 2.7m of the 12m long plot. Samples were taken of sediment in runoff to measure inter-rill erosion.

- At the conclusion of the inter-rill study, a series of overland flow rates was applied to the top of the 12m long plot, with each rate being maintained for 5 minutes. Samples of sediment in runoff were taken (and runoff rate measured) to gain information on the susceptibility of the material studied to rill erosion.

For each of the three "runs", a laptop computer functioned as a field notebook, recording plot descriptions, tipping bucket (and hence, runoff) rates through time, and recording the sediment sample bottles used together with the times at which they were taken. The runoff data were transferred directly to spreadsheet, and the sediment sampling information was transferred to the laboratory, where a range of DPI software programs ensured that laboratory procedures were accurate and efficient.

Associated measurements made include soil bulk densities, soil water contents pre- and post-rain, soil moisture characteristics, and a range of soil physical and chemical properties.

The basis for these procedures and interpretations of typical results are detailed in Loch (1996).

4.2.3 Procedures used for vegetation studies

Vegetation studies used procedures very similar to those applied to bare soil. In some instances (eg, heavy vegetation cover), low runoff and erosion rates made it impossible to measure inter-rill erosion, but generally the same pattern of measurements were made. In some instances, the higher infiltration rates found under vegetation made it necessary to use higher rainfall rates than normal to ensure that runoff occurred.

Associated measurements included projected vegetation cover and dry matter weight, as well as the usual measurements of soil water contents and bulk density.

4.2.4 Laboratory measurements

A temporary laboratory was established at each mine site visited to enable measurements during the field studies. For studies of runoff and erosion, typical laboratory measurements included concentrations of total sediment in runoff, size and settling velocity distributions of material both in runoff and at the soil surface available for erosion.

Sediment concentrations were measured gravimetrically. Sediment size was measured using wet sieving for particles >0.125 mm and sedimentation for particles <0.02 and <0.002 mm. Settling velocities was measured using an automated top entry tube (described by Loch and Rosewell 1992), with the automation being specifically developed for the laboratory studies in this project. Staff of the Agricultural Engineering Section, DPI Toowoomba, designed and constructed the necessary mechanical and electronic components of the settling columns.

A procedure of comparison of equivalent sand sizes and of size distributions from wet sieving can be used to estimate wet sediment densities, which are important information for some erosion models.

4.3 Results

4.3.1 Soil/spoil properties

Some chemical and physical properties of the materials studied are shown in Table 4-1.

4.3.2 Soil infiltration and erodibility parameters across all mines

Curve Numbers were derived for use in runoff prediction with the USDA curve Number approach (widely used in runoff and water balance modeling) (Table 4-2). In general, curve numbers derived were high (between 90 and 100), indicating that most of the materials studied were relatively impermeable. These data were incorporated in the PGM model, which was developed as a means of enabling data from this project to be used in site planning, as described by Loch (1997).

Soil erodibility (K) factors for the Modified Universal Soil Loss Equation (MUSLE) (Onstad and Foster 1975) were derived by solving the MUSLE equation for K, with all other factors being known.

The equation is:

$$A = (0.5\ EI_{30} + 0.349\ Q\ q_p^{0.333})\ K\ LS\ CP \quad [1]$$

Where A = event soil loss, EI_{30} is event rainfall erosivity, Q is total runoff for the event (mm), q_p is peak runoff rate (mm/h), K is erodibility, and L, S, C, and P are factors describing slope length, steepness, surface cover, and practices to minimise erosion respectively. An important point is that the MUSLE is an event-based equation, so that it is reasonable to derive MUSLE parameters from individual rainfall simulator events. The Universal Soil Loss Equation (Wischmeier and Smith 1978), being based on an annual time step, is much less appropriate to single rainfall/runoff events.

As the plots were bare, with minimal disturbance, the P factor could be set at 1. However, C factors were calculated on the basis of measured rock cover, so that rock cover (measured post-rain) was treated as cover rather than as an intrinsic property of the soil/spoil. This was done because there is potential for rock cover to be varied in field practice, and also for rock cover to change through time due to preferential removal of fines from the surface. Consequently, K values reported from this work would be higher than those reported by other components of the project, which did not separate effects of rock cover from erodibility. Effectively, the field rainfall simulator data reports a K value, whereas the other work reports a CK value. There is a degree of validity for each approach, with the decision to treat rock cover separately being taken simply for convenience in applying the data within the PGM model.

Overland flow studies were used to determine which LS relationship to adopt for each material (high, medium, or low response of erosion to slope length), and then LS factors were calculated for each plot on the basis of measured gradients and known plot length.

An overview of MUSLE K factor estimates is given in the Appendix. In general, there is quite good agreement between replications on each material. Exceptions are sites (Curragh and Goonyella) where a range of slopes were studied, for which it appears that the LS factors have not adequately accounted for the effects of gradient on rates of erosion.

At Curragh, it appears that the effect of gradient on erosion is underestimated for the spoil, whereas at Goonyella, the effect of gradient on erosion of the topsoil is overestimated. The problem is largely due to erosion process/gradient interactions that are more complex than can be described using the relatively simple LS factor approach of USLE-based models.

The data also show a large effect of water quality at one site (Blackwater), where erosion of the topsoil was approximately halved when saline water was used instead of deionised water. However, there was little effect of water salinity on erosion of spoils – possibly due to both a lack of clay to be affected by electrolyte concentration, and because many spoils are already quite saline.

Table 4-1 Chemical and physical properties of the materials studied.

Mine	Material	Texture (%) Clay (<0.002 mm)	silt (0.002-0.02mm)	sand (0.02-2.0mm)	Gravel (%) 2-20mm	Dispersion ratios (%) clay	silt&clay	Bulk density (g/cc)	pH	E.C. 1:5 (ms/cm)	15 bar Grav. (%)	Rock Cover %
BW	Spoil	13	22	65	14	32	59	1.5	9.0	0.16	0.06	30.00
	Soil	41	15	44	4	10	31	1.3	8.1	0.30	0.21	10.00
	M/S spoil	24	33	43	0	20	35	1.5	8.8	0.13	0.21	50.00
CAL	Spoil	17	11	72	6	34	71	1.5	6.5	0.29	0.08	63.00
	Soil	15	5	80	0	13	35	1.5	4.8	0.08	0.05	37.00
CUR	Spoil	20	27	53	3	34	62	1.6	8.7	1.01	0.12	45.00
	Soil	47	21	32	0	12	32	1.2	8.1	0.45	0.17	15.00
GC	Spoil	16	15	69	25	22	60	1.4	7.5	0.53	0.08	68.00
	Soil	17	8	74	1	22	68	1.5	7.4	0.28	0.06	35.00
	Sand	4	2	94	0	37	89	1.5	6.6	0.04		2.00
GYA	Spoil	53	13	33	0	24	72	1.4	7.8	1.95	0.16	27.00
	Soil	50	11	39	6	10	34	1.4	7.4	0.71	0.10	37.00
	Reject	14	13	72	41	0	0	1.3	3.3	1.96		
OC	Spoil	13	17	70	64	15	67	1.6	7.9	2.44	0.06	75.00
	Soil	22	9	69	0	8	55	1.5	6.9	2.37	0.07	18.00
TAR	S/S spoil	12	16	72	10	4	9	1.5	7.7	0.25	0.04	67.00
	Mud spoil	23	33	44	40	5	61	NA	8.1	1.17		
	Sodic spoil	30	14	55	3	17	46	NA	6.1	0.13		
	Lithosol	8	26	66	0	49	44	1.3	4.8	0.12	0.09	0.00
	Krasnozem	31	31	37	3	7	16	1.3	8.0	0.23	0.13	0.00
WAN	Spoil	16	37	46	12	102	99	1.5	7.6	0.26	0.13	40.00
	Soil	39	20	41	0	19	52	1.3	7.9	0.24	0.11	27.00
BA	S/stone spoil	20	15	65	23	24	66	1.8	7.5	0.36	0.07	43.00
BA	Soil	11	6	84	27	23	76	1.9	6.1	0.16	0.06	40.00
BA	Clay soil	39	13	48	12	4	53	1.4	7.4	0.50		27.00
GRE	Permian spoil	18	19	62	73	3	63	1.6	7.4	1.35	0.07	55.00
GRE	Soil	35	15	49	0	11	36	1.4	7.9	0.14	0.09	6.00
MOU	Rocky spoil	28	19	53	43	30	72	1.6	9.3	0.43	0.12	77.00
MOU	Black earth	45	23	32	12	13	42	1.3	8.5	0.30	0.20	17.00
MOU	Yellow spoil	33	20	47	5	18	69	1.4	9.4	0.34	0.14	33.00
NEW	Sand	24	10	66	1	65	83	1.6	9.6	0.61		33.00
NEW	Clay soil	57	17	26	19	17	45	1.2	8.2	0.26	0.10	17.00
NEW	Grey mudstone	16	18	65	0	1	55	1.9	8.5	0.39	0.07	73.00
NP	Tertiary spoil	32	18	50	10	84	89	1.6	5.4	0.33	0.11	68.00
NP	Permian spoil	22	18	60	44	52	65	1.7	8.1	0.65	0.07	82.00
NP	Sandy soil	12	4	83	0	64	80	1.4	6.2	0.14	0.04	9.00
PD	Tertiary spoil	31	33	35	10	51	75	1.6	9.0	0.87	0.15	78.00
PD	Permian spoil	26	42	32	25	52	66	1.5	9.1	0.75	0.12	64.00
PD	Soil	17	7	76	4	18	60	1.6	8.0	0.16	0.05	13.00
SAR	Tertiary spoil	34	10	55	0	24	79	1.5	8.4	0.54	0.13	27.00
SAR	Soil	14	10	77	0	19	66	1.5	7.5	0.11	0.04	13.00

Table 4-2 Curve Number (1) derived from rainfall simulator plots.

Mine	Material	CN (Rep 1)	CN (Rep 2)	CN (Rep 3)	***Mean CN***
BW	Spoil	89.1	91.0	NA	**90.1**
BW TW[a]	Soil	89.4	89.9	NA	**89.7**
BW	Soil	87.3	87.6	NA	**87.5**
BW TW	M/s spoil	93.7	92.4	NA	**93.1**
BW	M/s spoil	0.0	0.0	NA	**0.0**
CAL	Spoil	98.1	98.1	96.9	**97.7**
CAL	Soil	0.0	0.0	0.0	**0.0**
CUR	Spoil, 10%	97.7	97.7	NA	**97.7**
CUR TW	Spoil, 20%	97.3	98.4	NA	**97.9**
CUR	Spoil, 20%	96.2	96.9	NA	**96.6**
CUR TW	Spoil, 30%	95.8	98.1	NA	**97.0**
CUR TW	Soil 10%	92.7	87.0	NA	**89.9**
CUR TW	Soil 20%	92.7	92.7	NA	**92.7**
CUR	Soil 20%	93.7	91.7	NA	**92.7**
CUR TW	Soil 30%	93.0	92.4	NA	**92.7**
GC	Spoil	93.7	96.9	99.2	**96.6**
GC	Soil	98.8	95.8	NA	**97.3**
GC	Sand	90.4	88.5	95.1	**91.3**
GYA	Spoil, 10%	92.0	NA	NA	**92.0**
GYA	Spoil, 20%	90.0	84.8	NA	**87.4**
GYA	Spoil, 30%	85.2	92.3	NA	**88.8**
GYA	Soil 10%	NA	NA	NA	**NA**
GYA	Soil 20%	94.8	95.1	NA	**95.0**
GYA	Soil 30%	95.8	91.4	NA	**93.6**
OC TW	Spoil	93.0	92.4	95.5	**93.6**
OC	Spoil	94.1	NA	NA	**94.1**
OC TW	Soil	97.7	97.3	98.8	**97.9**
TAR	S/s spoil	97.3	90.7	92.4	**93.5**
TAR	Mud spoil	57.1	NA	NA	**57.1**
TAR	Sodic spoil	84.1	NA	NA	**84.1**
TAR	Lithosol	94.4	90.1	87.6	**90.7**
TAR	Krasnozem	84.7	87.3	83.6	**85.2**
WAN	Spoil	96.6	94.4	97.3	**96.1**
WAN	Soil	92.7	92.0	89.4	**91.4**
BA	S/stone spoil	96.8	98.1	97.1	**97.3**
BA	Soil	96.0	97.1	96.3	**96.5**
BA	Clay soil	89.5	89.4	91.3	**90.1**
GRE	Permian spoil	92.1	91.4	96.2	**93.2**
GRE	Soil	91.0	92.5	94.5	**92.7**
MOU	Rocky spoil	92.5	92.3	94.4	**93.1**
MOU	Black earth	92.5	90.7	93.7	**92.3**
MOU	Yellow spoil	96.0	96.2	94.5	**95.6**
NEW	Sand	91.9	96.4	93.7	**94.0**
NEW	Clay soil	66.9	69.6	70.4	**69.0**
NEW	Grey mudstone	85.5	91.2	91.4	**89.4**
NP	Tertiary spoil	95.7	91.5	93.8	**93.7**
NP	Permian spoil	95.9	94.1	95.1	**95.0**
NP	Sandy soil	97.8	96.7	NA	**97.3**
PD	Tertiary spoil	93.9	82.2	85.7	**87.3**
PD	Permian spoil	97.2	94.1	97.6	**96.3**
PD	Soil	96.3	99.1	97.5	**97.6**
SAR	Tertiary spoil	96.3	96.1	96.9	**96.4**
SAR	Soil	91.6	92.5	94.4	**92.8**

[a] TW = treated water. For mine sites where the available water was of high salinity, a deionising unit was used to treat the water used, and to allow comparison of runoff and erosion under water of low and high salinity.

4.3.3 Derivation of parameters for other erosion models

Spreadsheets were developed for estimation of the WEPP parameters:

- Critical shear for rilling (τ_c),
- rill erodibility (K_R), and
- inter-rill erodibility (K_i).

Rill parameters could be derived from the overland flow studies, and inter-rill erodibility from the inter-rill plots. However, this analysis was not carried out for all sites because there is currently no demand for these parameters.

The full data set from rainfall simulator studies on bare soils and spoils was supplied to Dr G. Willgoose, University of Newcastle, to enable derivation of parameters for the SIBERIA model. A series of reports have been issued detailing the parameter derivation process and the results obtained.

4.3.4 Effects of vegetation on infiltration

Although all sites studied showed large increases in infiltration under vegetation, the magnitude and form of the responses found varied between sites. This is attributed to differences in the age and form of the vegetation studied.

At the Meandu Mine, Tarong, the site studied had been under heavy Rhodes grass cover for two years, and there was a large effect of vegetation on Curve Number (Figure 4-2). Visual observations of wetting patterns indicated that water entry was closely associated with root channels (Figure 4-3). Other soil measurements at this site (Loch and Orange 1997) indicated that increases in soil hydraulic conductivity could be expected to continue over the first four years under vegetation, due to gradual increases in aggregation (Figure 4-4) and development of stable macropores (probably associated with root channels) (Figure 4-5).

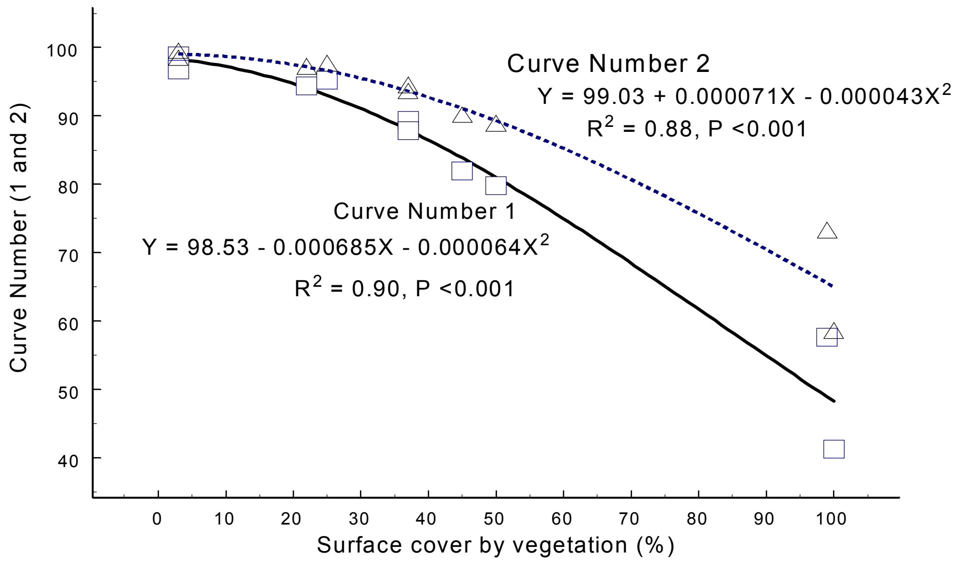

Figure 4-2 Effects of surface vegetation cover on Curve Number (2), Meandu Mine, Tarong.

Figure 4-3 Deep wetting front under a grass tussock compared with shallow wetting depths where soil was bare, Meandu Mine, Tarong.

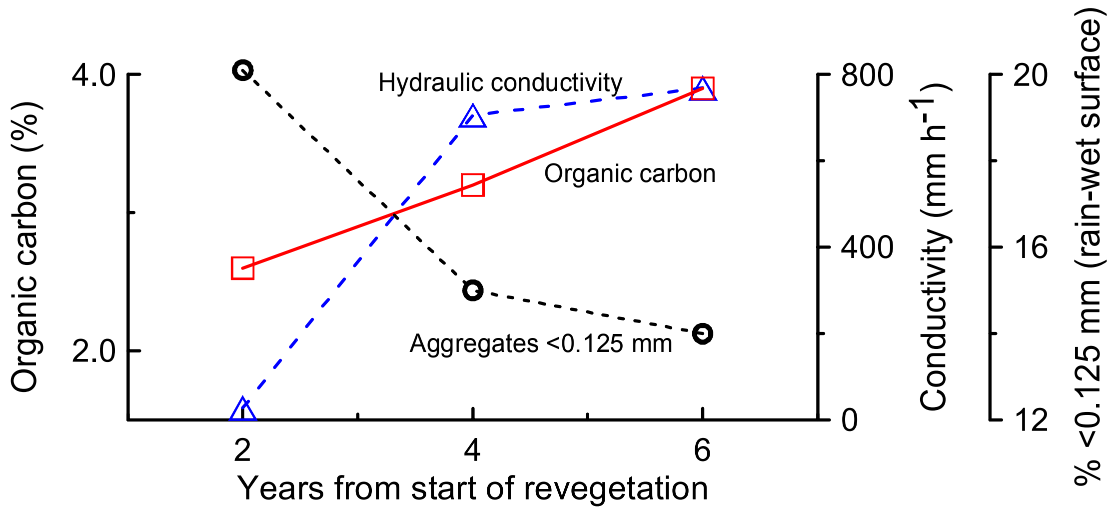

Figure 4-4 Changes through time in hydraulic conductivity and other properties of topsoil at Meandu Mine, Tarong, for sites from which macropores have been removed by disturbance.

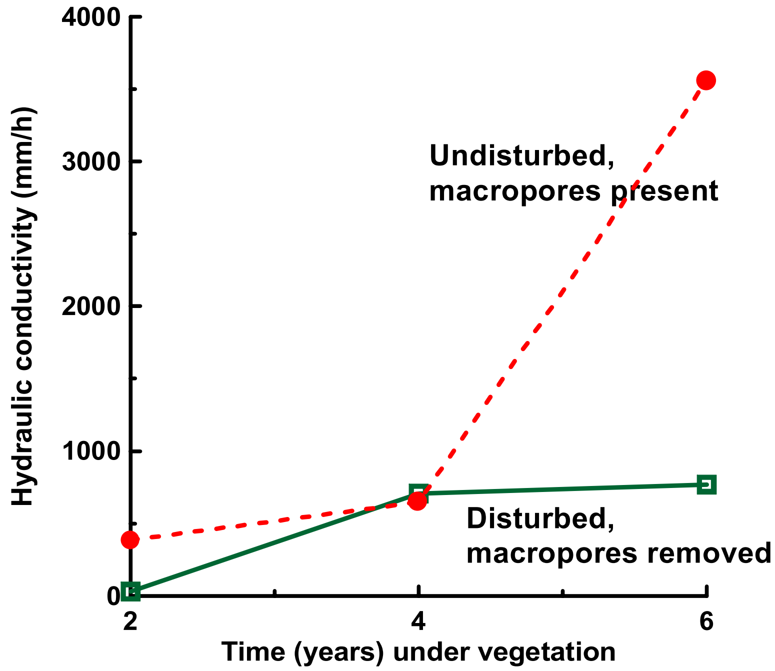

Figure 4-5 Importance and development of macropores in topsoil at Meandu Mine, Tarong.

At the Curragh Mine, Curve Number (2) also showed little decrease due to lower levels of surface cover, and a greater decrease at higher cover levels (Figure 4-6). However, overall the observed effects of cover on infiltration were lower than at Tarong. This was probably because the vegetation at Curragh had only been established for one year, and (particularly at the lower levels of cover) was predominantly single-stemmed weed seedlings that would have been less effective at protecting the surface from being sealed by fine particles in raindrop splash.

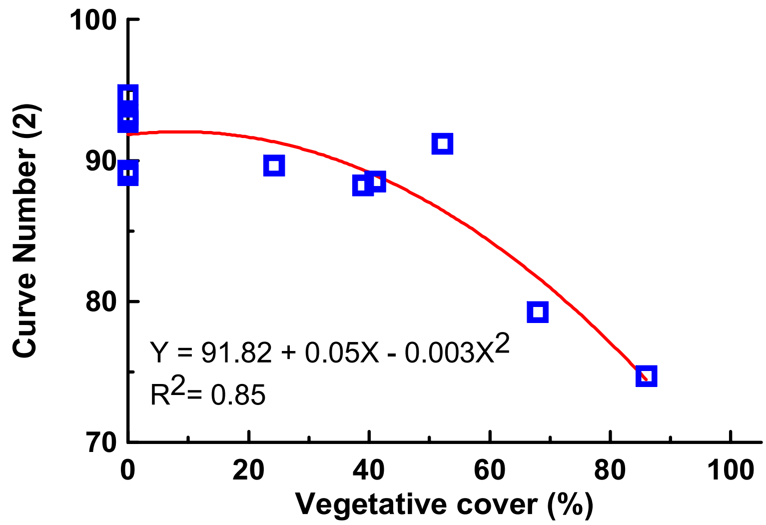

Figure 4-6 Effects of surface cover on Curve Number 2, topsoil at Curragh Mine.

At the Goonyella Riverside Mine, topsoil under vegetation showed an even smaller effect of vegetation on Curve Number (2) (Figure 4-7). The smaller response of curve number to vegetative cover at Goonyella may be due to several factors, including:

- the shorter period of grass growth (one growing season at Goonyella compared to two growing seasons at Meandu Mine) allowing less time for creation of macropores by plant roots

- the way in which vegetation was established (using sub-surface irrigation tape) compared to vegetation establishment under natural rain at Meandu Mine, so that there was less wetting of the bare areas between the vegetation, and hence, less re-aggregation

- the hardsetting nature of the Goonyella topsoil, and/or its high clay content relative to the topsoil at the Meandu Mine.

However, a decrease in CN 2 of 11 units (indicated for 100% cover relative to bare soil by the cover relationship developed for the Goonyella Riverside data) would still have dramatic effects on runoff from the topsoil. The potential impact of that reduction in CN 2 was assessed by comparing predictions of runoff from the PERFECT (Littleboy *et al.* 1992) water balance/infiltration model when it was run for 40 years of rainfall data from the region. Model predictions indicate that annual runoff would be reduced from 247 mm to 105 mm due to an 11 unit decrease in CN 2, in a simulation where water use by vegetation was ignored. That difference in annual runoff would have considerable impact on plant growth as well as on erosion.

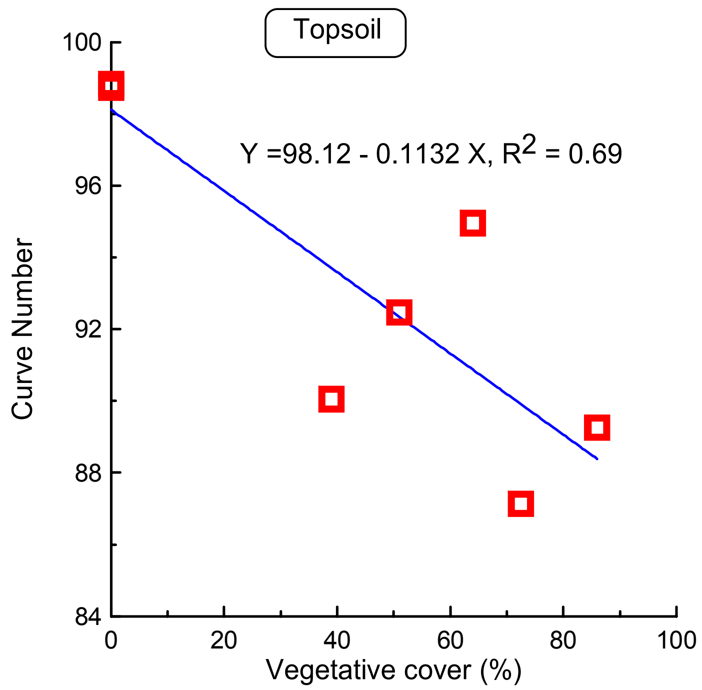

Figure 4-7 Effects of surface cover on Curve Number 2, topsoil at Goonyella Riverside Mine.

One site, a slope where a 30 cm deep layer of weathered basalt had been placed over spoil at the Callide Mine, showed considerable spatial variability. Plots showed obvious development of a perched water table in the surface layers during rain, evidence that an impeding layer had developed at relatively shallow depths in the soil. Final infiltration rates on plots in low, mid, and upper slope positions showed responses to vegetative cover as well as to their position on the slope (Figure 4-8). The effect of vegetation was probably associated with the density of plant roots (which may have created channels through the impeding layer) rather than with any impacts on permeability of the soil surface, which was obviously not a limiting factor for infiltration.

Overall, the data show that establishment of vegetation causes large improvements in infiltration capacity, with the magnitude of the improvement depending on the length of time under vegetation, soil properties, and the type of vegetation. In the longer term, there will be a need for infiltration measurements to be made on areas of older rehabilitation so that infiltration parameters can be derived to describe the long-term infiltration behavior of rehabilitated areas. However, at this stage, areas of older rehabilitation are relatively rare.

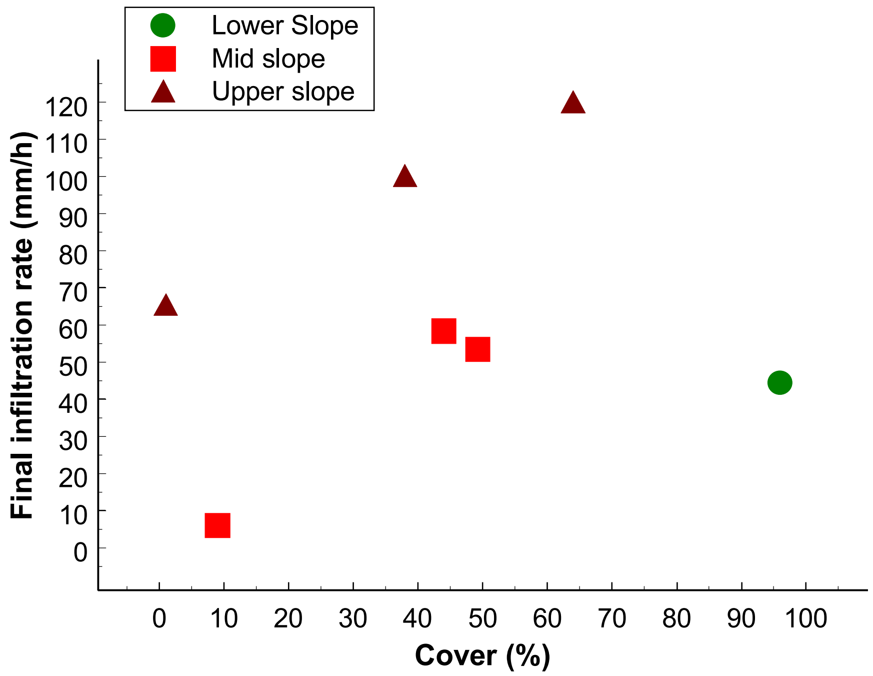

Figure 4-8 Effects of vegetative cover and slope position on final infiltration rates of simulated rain, Callide Mine.

4.3.5 Effects of vegetation on erosion

Vegetation has a range of effects on erosion, including:

- reducing runoff (so that there is less overland flow to transport sediment);
- protecting the soil surface from drop impact, thus reducing splash detachment and rates of inter-rill transport;
- increasing soil cohesion, thus increasing resistance to rill development;
- impeding overland flows, which both delays rill development and reduces the efficiency of sediment transport in overland flow.

There can also be interactions with sediment properties, with slope gradient, and with vegetation form, so that there is considerable potential for variation in effects of cover on erosion, both at the field and experimental scale.

The role of vegetation in reducing runoff has been reported in the previous section.

Effects of vegetation on inter-rill erosion often show a linear relationship between surface cover and sediment concentrations in inter-rill flow (Figure 4-9), because of the strong correlation between inter-rill transport and raindrop impacts. Interactions between drop impact, detachment of finer (suspended) particles, and transport capacity of shallow overland flows mean that on coarser soils such relationships can be expected to tend to zero at cover levels <100% (Figure 4-9), whereas on finer soils, cover will have less effect (Figure 4-10).

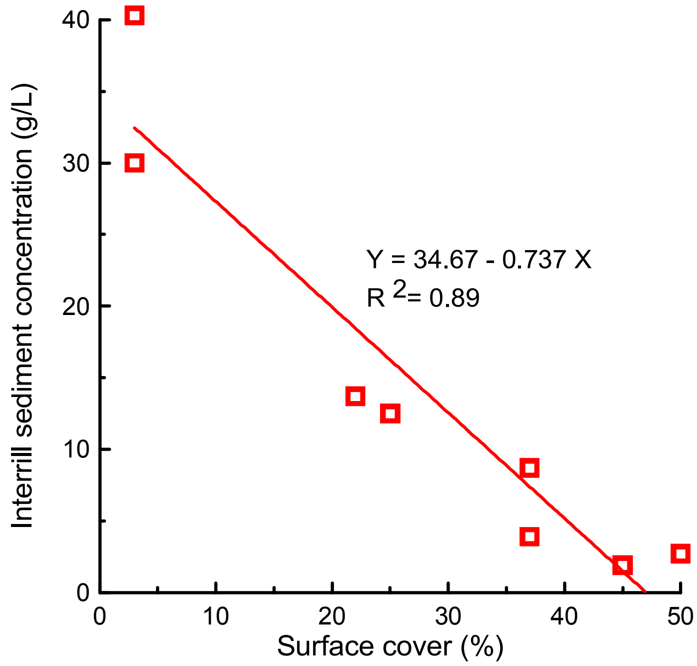

Figure 4-9: Effects of vegetative cover on inter-rill sediment concentrations for a coarse topsoil, Meandu Mine, Tarring.

The role of vegetation in preventing rill development is shown in Figure 4-11, which, for a study at the Meandu Mine, shows that erosion from 12 m long plots under simulated rain was predominantly inter-rill for all plots except those that were bare and disturbed. The concentrations shown for the bare plots are higher than those generated by inter-rill transport, indicating that rill development on the bare plots was contributing additional sediment.

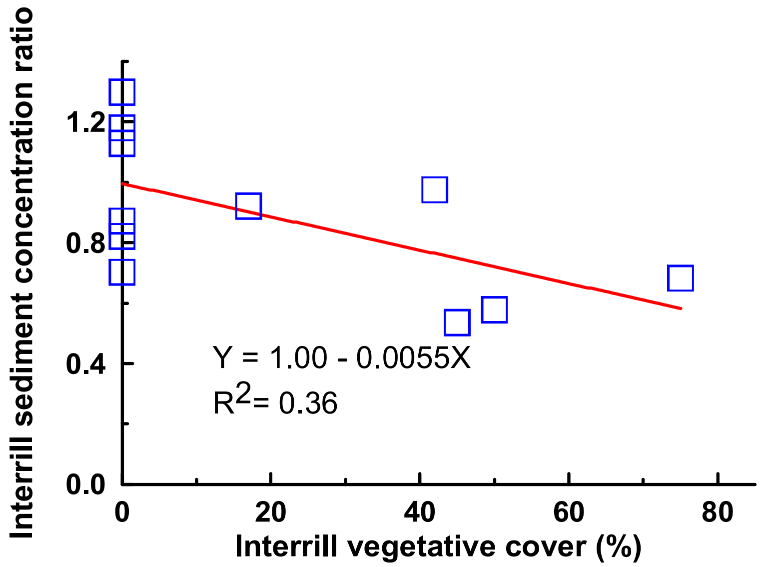

Figure 4-10 Effects of cover on inter-rill sediment concentrations for a clay topsoil, Curragh Mine. Combined data for three gradients, with concentrations expressed relative to inter-rill concentrations from bare soil at each gradient (10, 20, and 30%).

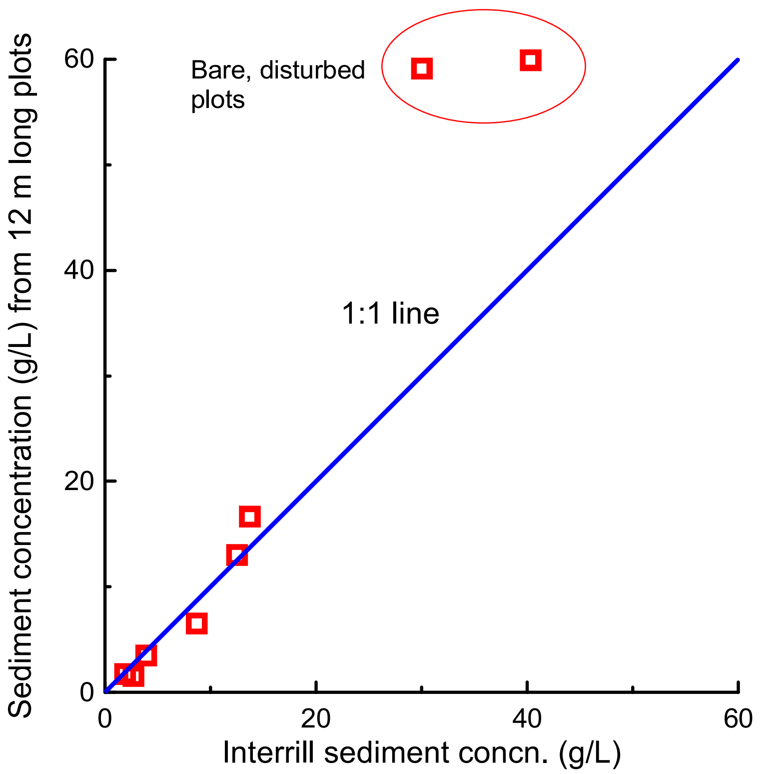

Figure 4-11 Comparison of sediment concentrations in runoff for two plots sizes to assess effects of vegetation on erosion processes, Meandu Mine, Tarong.

One consequence of the combination of factors and processes determining effects of cover on erosion is that observed responses tend to be curvilinear, as illustrated by the cover factors used in the Universal Soil Loss Equation (USLE) (Wischmeier and Smith, 1978) shown in Figure 4-12.

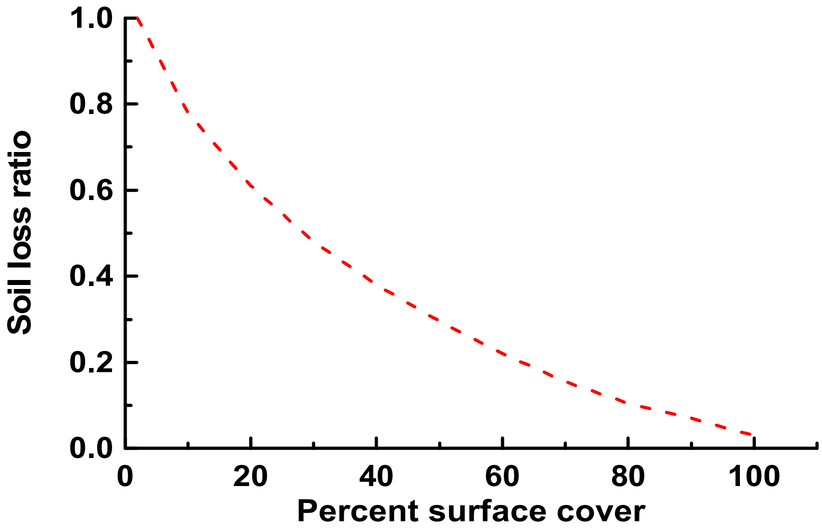

Figure 4-12 Variation in the C-factor of the USLE (referred to as soil loss ratio) with surface (contact) cover.

Studies on vegetation (both within this project and in other work) have indicated that the response curve shown in Figure 4-12 varies with the type and form of surface cover. It can be concluded that larger cover elements are more effective at reducing erosion, probably because they cause greater diversion of overland flow paths. The range of responses found is shown in Figure 4-13.

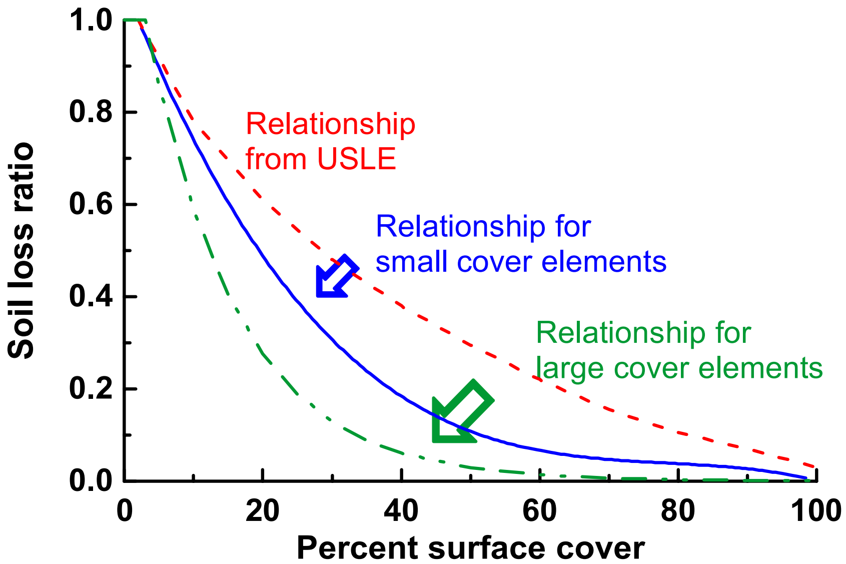

Figure 4-13 Effects of size of cover elements on Soil Loss Ratios.

If vegetative cover occurs as large clumps, eg. 0.3-0.6 m diameter, the clumps cause considerable diversion of overland flow and are very effective at reducing erosion. However, if the clumps are small, eg. <0.1 m in diameter, they appear to be less effective in diverting overland flow and in reducing erosion. A rill erosion study at the Callide Mine showed that especially for grasses that develop as small tussocks, the amount of surface litter is very important. A sward dominated by a grass forming small tussocks functions like a sward of larger clumps if there is considerable litter on the soil surface. However, if the sward is grazed or burnt, it will have little surface litter and will instead behave like a sward of small cover elements.

These differences between vegetation types can have large impacts on potential rates of erosion from a rehabilitated landform. Variations between the lines shown in Figure 4-13 are greatest in the range 30-50% surface cover, which is consistent with the levels of cover likely to be achieved on some central Queensland mine sites. In the 30-50% cover range, there may be up to six-fold variation in potential erosion, depending on the form of vegetation present. All else aside, it is clear that the type of plant cover grown and the way it is managed can be extremely important decisions.

Plant species that form large clumps include stoloniferous/rhizomatous grasses and some broad-leaved species that sucker or tend to root down from any nodes in contact with the soil surface. Plants forming small cover elements include single-stemmed weeds, some clovers and grasses.

The theory underlying the Soil Loss Ratio approach of the USLE implies that responses to cover should be independent of any variation in other factors affecting erosion (such as slope length, gradient, soil erodibility, and rainfall erosivity). The data available provide some support for that assumption. For example, very similar sediment concentration ratio curves were obtained for two sites that varied not only in soil erodibility (associated with higher rock cover) but also in gradient (Figure 4-14). One site (at Callide Mine) was quite rocky and on 25% gradient, whereas the other site studied (at the Tarong Mine) was on only 15% gradient and had little surface rock.

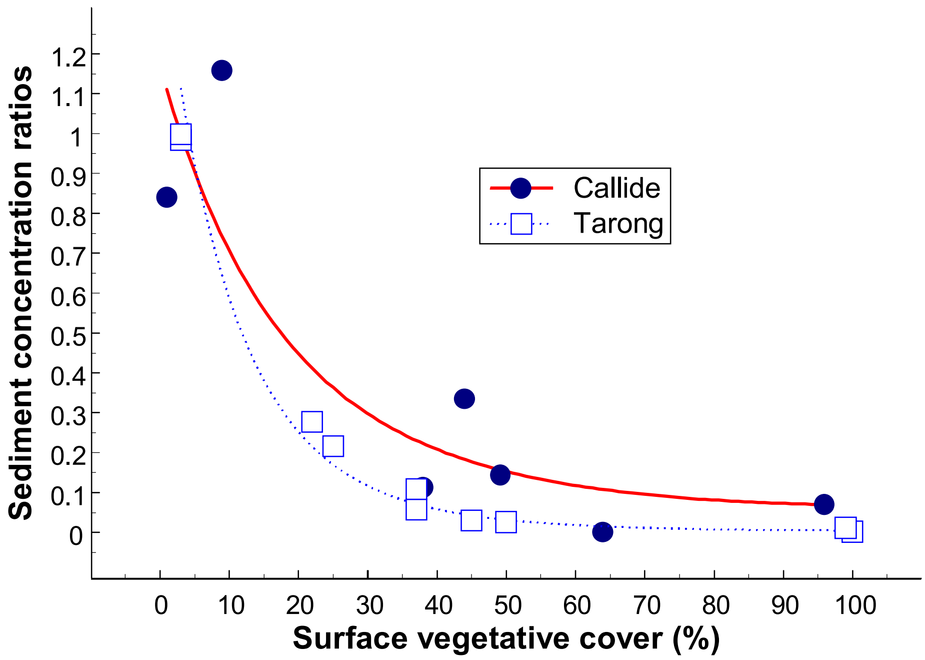

Figure 4-14 Comparison of effects of vegetative cover on sediment concentration ratios for Tarong and Callide Mines. Sediment concentration ratios were calculated as the ratio of sediment concentrations for a plot with cover relative to sediment concentrations from bare plots.

There are reasons why the relationship found experimentally for vegetated plots was different to that used in the USLE. They include:

- the initial USLE studies dealt with tilled soils, rather than rangeland sites, and hence, did not include an element of soil consolidation in their assessment of the effectiveness of the plant cover
- the initial USLE studies considered plots tilled up and down the slope, so that cover tended to be arranged in ways that made it less effective at intercepting overland flows
- effects of vegetation cover on infiltration would have been greater in this study, as the initial US studies tended to use fallow plots that would have been relatively wet, with less potential for cover to affect infiltration rate than the dry plots considered in this study.

4.3.6 Effects of vegetation on erosion by overland flows

Plots studied under the rainfall simulator were subjected to a series of increasing overland flows to simulate slope lengths longer than the 12 m plot that could be covered by the simulator.

For a number of sites, there was little apparent effect of flow rate over the range of flows tested. This is illustrated by Figures 4-15, 4-16 and 4-17.

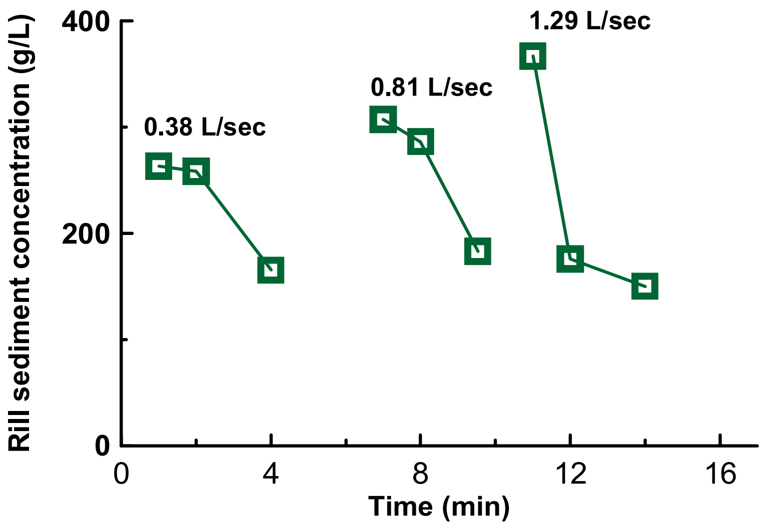

Figure 4-15 Changes through time in sediment concentrations in rill flow on a vegetated plot (plot 2) on 30% slope, Curragh Mine.

For 30% slope, Figures 4-15 and 4-16 indicate that 20% vegetation cover is not sufficient to greatly impact on erosion by overland flow. They also illustrate the typical changes through time in sediment concentrations in rill flow.

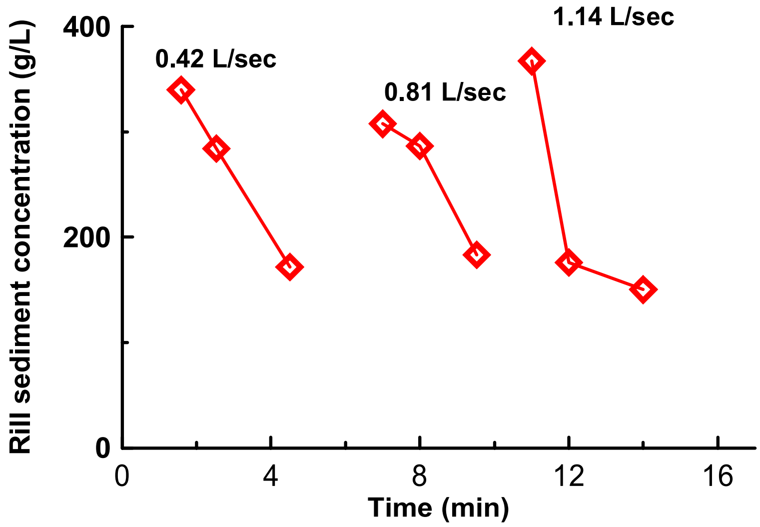

Figure 4-16 Changes through time in sediment concentrations in rill flow on a bare plot (plot 3) on 30% slope, Curragh Mine.

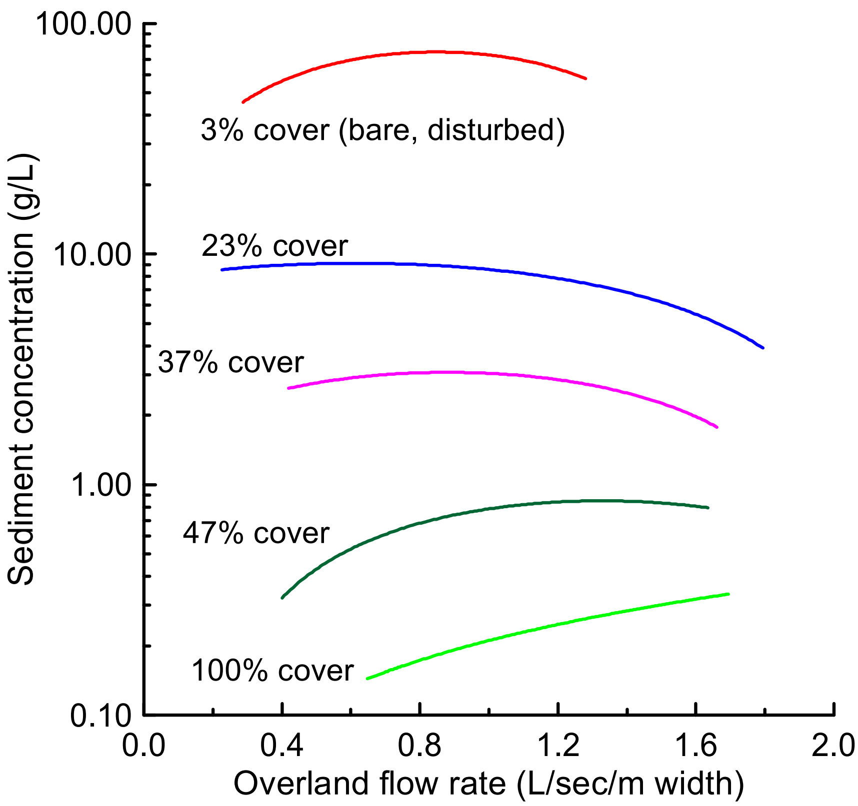

Figure 4-17 Effects of cover on average sediment concentrations carried by various rates of overland flow, Meandu Mine, Tarong.

For a site on 15% gradient at the Meandu Mine, Figure 4-17 illustrates the much greater effectiveness of lower cover levels when on sites of lower gradient.

The interaction of cover and gradient is shown by Figures 4-18 and 4-19, which indicate that steeper slopes require higher cover levels to control erosion by overland flow than do the lower gradients. Figure 4-18 shows 64% cover being only moderately effective on a 30% gradient, whereas Figure 4-19 shows effective control of erosion by 51% cover on a 20% gradient.

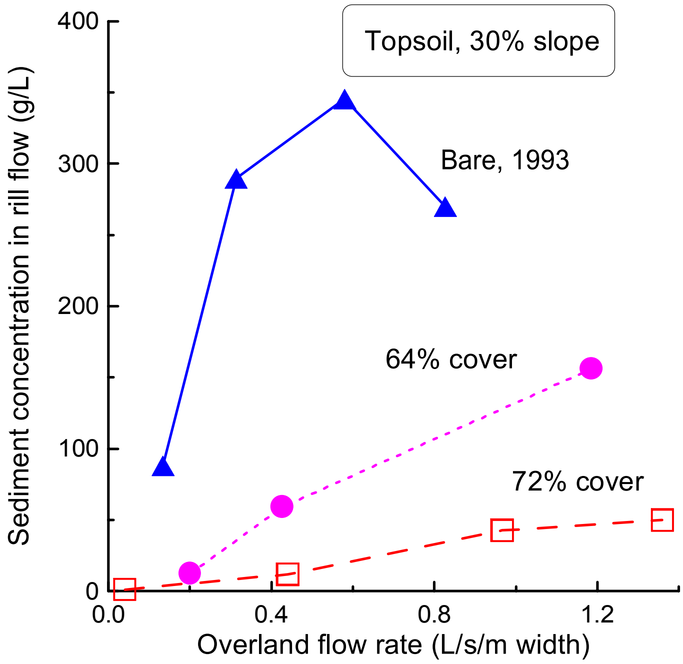

Figure 4-18 Effects of surface cover and increasing rates of overland flow on sediment concentrations in runoff, 30% slope, Goonyella Riverside Mine.

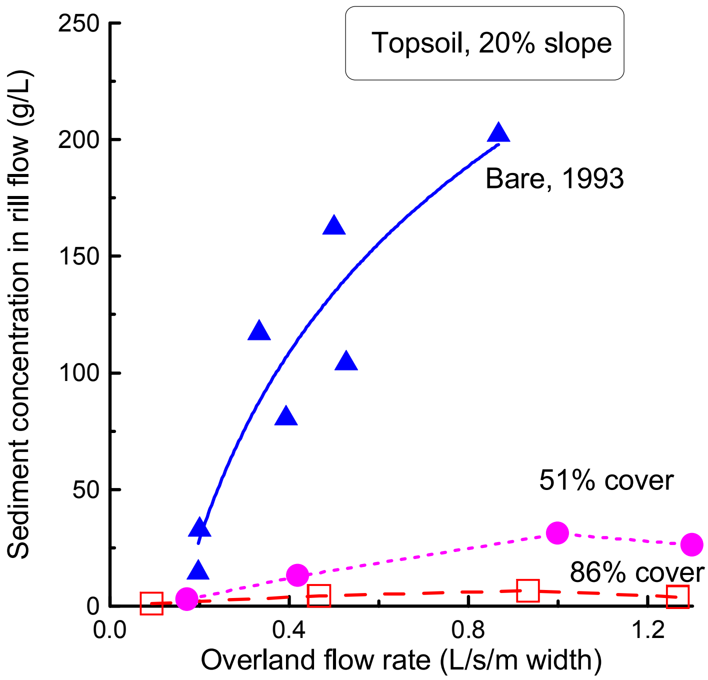

Figure 4-19 Effects of surface cover and increasing rates of overland flow on sediment concentrations in runoff, 20% slope, Goonyella Riverside Mine.

4.4 Development of the PGM model

From the field rainfall simulator research, two major issues became apparent:

1. The volume of data generated was enormous, and some way was needed to make the data easily accessible; and
2. Vegetation had an extremely important role in stabilizing rehabilitated sites, so that it was essential to be able to assess both effects of vegetation on runoff and erosion, and also to assess site design factors affecting vegetation growth. Poor growth could be expected to equate to poor site stabilization in virtually all cases.

It was apparent that vegetation needed to be considered in a relatively dynamic way, and that there was great benefit in considering climatic variability and its impact on both vegetation and erosion. This indicated that some form of computer modeling using a daily time-step would be particularly useful.

Therefore, a computer package was prepared. It combined components of three readily available models that had already been extensively validated under Queensland conditions. The models/components are:

- the Curve Number model of infiltration used in the PERFECT model (Littleboy *et al.* 1992);
- the GRASP model of pasture growth (McKeon *et al.* 1993); and
- the Modified USLE (MUSLE) (Onstad and Foster 1975) for estimation of soil loss from individual events.

The package was designed to be easy to use, and contains all rainfall simulator data in a database that is automatically accessed when the package is used (Figure 4-20). The database also contains specially prepared climate files for each of the participating mines, with information on daily rain, rainfall erosivity, evaporation, and temperature.

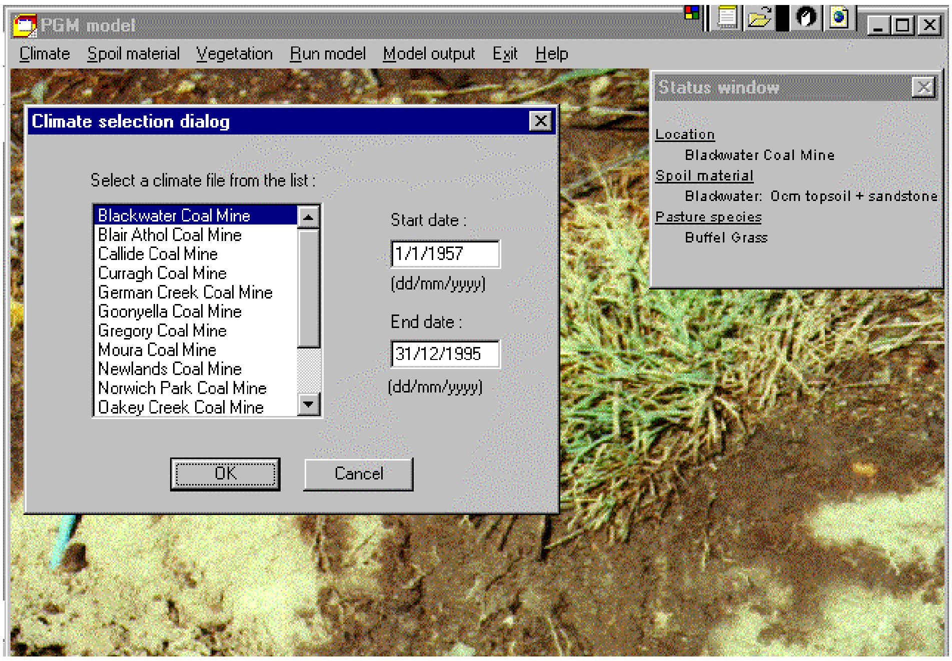

Figure 4-20 Screen from PGM model demonstrating selection of climate files and indication of other selections made.

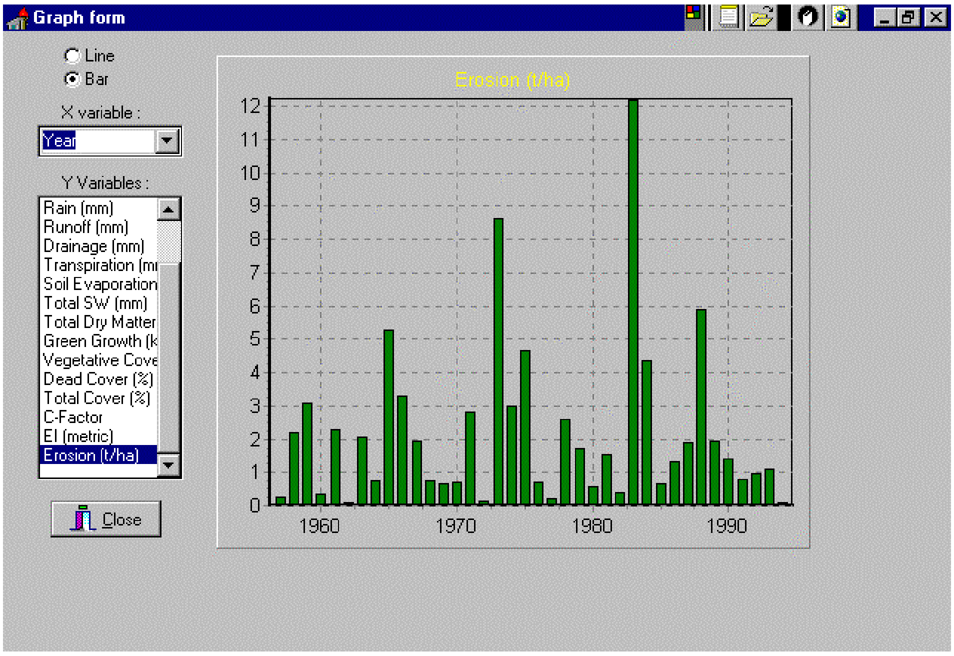

Figure 4-21 Output screen from PGM showing variation in predicted annual erosion (for LS equal to 1.0) and showing the range of outputs available.

Because the package is management oriented, it considers the broad range of site variables that ultimately affect erosion, such as plant growth, surface cover, runoff, deep drainage, and erosion (Figure 4-21). It also gives comparisons of a range of slope/slope length combinations. PGM can be used to consider effects of variation in topsoil depths on plant growth, water balances, and erosion (Figure 4-22).

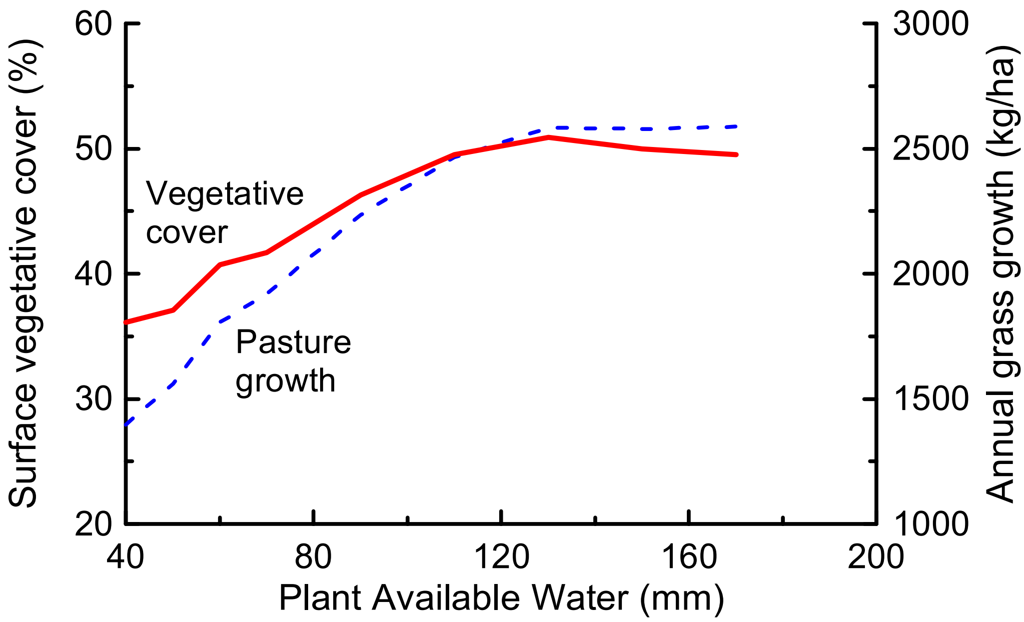

Figure 4-22 Predicted effects of Plant Available Water on annual grass growth and average surface vegetative cover, central Queensland (PGM output).

PGM allows for three plant growth options – bare soil, Buffel grass, and Rhodes grass. Possible enhancements that could be considered if any future work on the model is initiated include functions to adjust plant growth for soil fertility and salinity.

Areas where the model would benefit from greater (or more detailed/accurate) information include:

1. Plant Available Water Capacity and its variation with weathering
2. Considerations of soil/spoil rock contents, especially with respect to their impact on Plant Available Water Capacity
3. A better function to describe peak runoff rates from storms – fortunately, erosion predictions from the MUSLE are not highly sensitive to peak runoff
4. A model of vegetation establishment

Although the need for model improvement/enhancement may become apparent with time, the current version of the model represents a powerful tool for considering issues in design and management of minesite rehabilitation.

4.5 Overview

Although there are exceptions, the materials studied (topsoils and spoils) generally show relatively low infiltration capacities. From this it can be inferred that infiltration of rain will initially be poor, making establishment of vegetation difficult.

Erodibilities vary considerably, and effective erodibilities (with surface rock cover taken into account) will be low for some spoils in particular. However, the low water holding capacity of some rocky materials is likely to strongly limit the potential productivity and stability of rehabilitated areas based on those materials unless the rock weathers to produce finer-grained minerals.

Vegetation impacts on rehabilitated soils are enormous. Under vegetation, infiltration capacities increase greatly, soil structure is improved, and erosion can be greatly reduced. The type of vegetation established and its productivity can impact on the effectiveness of site stabilization. For that reason, the PGM model was designed to focus on impacts of vegetation on runoff and erosion, while giving information that would guide design and management of rehabilitated sites.

The PGM modeling package represents the easiest and most relevant way for the rainfall simulator data from this study to be accessed and applied. Like all models, it will gradually become obsolete or in need of upgrade. However, in the short term it presents a powerful tool for assessing many aspects of mine rehabilitation.

References

Bubenzer, G.D., and Meyer, L.D. (1965). Simulation of rainfall and soils for laboratory research. *Trans. ASAE.* 8: 73, 75.

Cogle, A.L., Littleboy, M., Rao, K.P.C., Smith, G.D., and Yule, D.F. (1996). Soil management and production of Alfisols in the semi-arid tropics. III. Long-term effects on water conservation and production. *Aust. J. Soil Res.* 34:113-125.

Connolly, R.D. and Silburn, D.M. (1995). Distributed parameter hydrology model (ANSWERS) applied to a range of catchment scales using rainfall simulator data. II Application to spatially uniform catchments. *J. Hydrol.* 172: 105-125.

Connolly, R.D., Silburn, D.M. and Ciesolka, C.A.A. (1997). Distributed parameter hydrology model (ANSWERS) applied to a range of catchment scales using rainfall simulator data. III Application to a spatially complex catchment. *J. Hydrol.* 193: 183-203.

Connolly, R.D., Ciesolka, C.A.A., Silburn, D.M. and Carroll, C. (1998). Distributed parameter hydrology model (ANSWERS) applied to a range of catchment scales using rainfall simulator data. IV. Evaluating pasture catchment hydrology. *J. Hydrol.* 201: 311-328.

Duncan, M.J. (1972). The performance of a rainfall simulator and an investigation of plot hydrology. M. Agr. Sc. Thesis, Lincoln college, University of Canterbury, New Zealand.

Littleboy, M., Silburn D.M., Freebairn, D.M., Woodruff, D.R., Hammer, G.L., and Leslie, J.K. (1992). The impact of soil erosion on sustainability of production in cropping systems. I. Development and validation of a simulation model. *Aust. J. Soil Res.* 30: 757-774.

Littleboy, M., Cogle, A.L., Smith, G.D., Yule, D.F., and Rao, K.P.C. (1996). Soil management and production of Alfisols in the semi-arid tropics. I. Modelling the effects of soil management on runoff and erosion. *Aust. J. Soil Res.* 34:91-102.

Littleboy, M., Sachan, R.C., Smith, G.D., and Cogle, A.L. (1996). Soil management and production of Alfisols in the semi-arid tropics. II. Deriving USDA curve numbers from rainfall simulator data. *Aust. J. Soil Res.* 34:103-111.

Laflen, J.M., Lane, L.J., and Foster. G.R. (1991). WEPP. A new generation of erosion prediction technology. *J. Soil Water Cons.* 46: 34-38.

Loch, R.J. (1996). Using rill/interrill comparisons to infer likely responses of erosion to slope length. Implications for land management. *Aust. J. Soil Res.* 34: 489-502.

Loch, R.J. (1997). Landform design – better outcomes and reduced costs by applying science to above- and below-ground issues. In "Demonstrating Environmental Excellence 97, 22nd Annual Environmental Workshop, 12-17 October 1997, Adelaide South Australia", pp 550-563. Minerals Council of Australia.

Loch, R.J. and Orange, D.N. (1997). Changes in some properties of topsoil at Tarong Coal – Meandu Mine coalmine with time since rehabilitation *Aust. J. Soil Res.* 35: 777-784.

Loch, R.J. and Rosewell, C.J. (1992). Laboratory methods for measurement of soil erodibilities (K factors) for the Universal Soil Loss Equation. *Aust. J. Soil Res.* 30: 233-248.

Loch, R.J., Silburn, D.M. and Freebairn, D.M. (1989). Evaluation of the CREAMS model. II. Use of rainulator data to derive soil erodibility parameters and prediction of field soil losses using derived parameters. *Aust. J. Soil Res.* 27: 563-576.

Loch, R.J., Bourke, J.J, Glanville, S.F., and Zeller, L. (1998). Software and equipment for increased efficiency of field rainfall simulation and associated laboratory analyses. *Soil & Tillage Res.* 45: 341-348.

McKeon, G.M., Littleboy, M., Carter, J., and Flood, N. (1993). *GRASP: Grass Production Model.* Draft Report, Queensland Department of Primary Industries, Brisbane.

Onstad, C.A., and Foster, G.R. (1975). Erosion modeling on a watershed. *Trans. ASAE.* 18: 288-292.

Rosewell, C.J. (1986). Rainfall kinetic energy in eastern Australia. *J. Climate & Appl. Met.* 25: 1695-1701.

Silburn, D.M., and Connolly, R.D. (1995). Distributed parameter model (ANSWERS) applied to a range of catchment scales using rainfall simulator data I. Infiltration modelling and parameter measurement. *J. Hydrol*. 172: 87-104.

Silburn, D.M., and Loch, R.J. (1990). Present capabilities and constraints in modelling soil erosion. In Erosion Productivity and Erosion Prediction Workshop, 5th Australian Soil Conservation Conference, Western Australia, 1990.

Wischmeier, W.H., and D.D. Smith. (1978). Predicting rainfall erosion losses - a guide to conservation planning. US Department of Agriculture. Agriculture Handbook No. 537. US Government Printing Office, Washington, DC.

5. Field Plots and Catchments

C.Carroll, L.Merton, and P.Burger.

Principal Research Scientists, Research Assistant and Research Assistant, Queensland Department of Natural Resources, Emerald, Qld.

5.1 Aim

The objectives of the field plot and catchment research were to determine, under natural rainfall:

1. runoff, sediment losses, and sediment erodibility of topsoil and spoil material;
2. the effect of slope gradient and vegetative cover on infiltration, runoff and sediment loss;
3. runoff, sediment loss and salt levels leaving catchments under a range of topographic and vegetative conditions.

5.2 Introduction

There has been very little research conducted on erosion from open-cut coalmine rehabilitation from natural rainfall, either in Australia or overseas. The region's variable rainfall is a major limitation to successful rehabilitation in central Queensland. Annual rainfall can range from 200 mm to 1400 mm/year, with a long-term median of 588 mm/year. In this environment the challenge is to find, and adopt, rehabilitation strategies that enhance infiltration, minimise runoff and erosion, and maximise vegetative growth.

Vegetative cover on agricultural and pastoral land has been shown to greatly reduce runoff and erosion from sloping lands (Carroll *et al.* 1995, 1997, Ciesiolka 1987). However, the impact and role of vegetation on mine rehabilitation land has not been extensively studied, particularly on the steeper slopes found on mine sites.

In 1992 a field study commenced at the Curragh, Oaky Creek and Goonyella coal mines in central Queensland. The three sites were selected to represent a range of topsoil and spoil material in the region. Sediment erosion, runoff, and water quality were measured at two scales; plot (0.01 ha) and small catchment (0.1 to 1.2 ha) (Figure 5-1 and Figure 5-2).

The field plots and catchments provide 'real' data and relationships under natural rainfall for a limited number of sites, with the field (Section 4) and laboratory (Section 3) rainfall simulation study providing sufficient data for results to be extrapolated with confidence to other coal mines in central Queensland.

Planning, design, construction and installation of monitoring equipment were completed in March 1993 on the plot study. The catchments were constructed and fully instrumented a year later in March 1994.

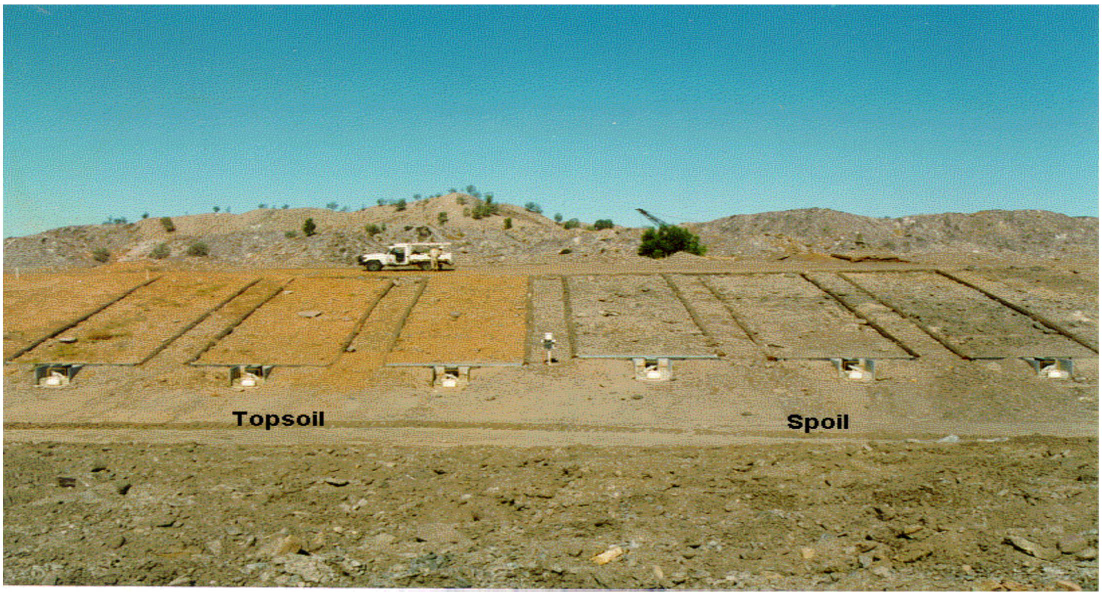

Figure 5-1 The field erosion plots on topsoil and spoil at Oaky Creek mine.

Figure 5-2 Runoff and erosion measuring apparatus for an angle of repose catchment at Oaky Creek mine.

5.3 Methods and Materials

5.3.1 Plots

Sediment and runoff were measured from three slope gradients (10, 20, and 30%). Each slope had pasture and tree treatments imposed on topsoil and spoil material. On the 20% slope, topsoil and spoil plots were left bare as a comparison with other vegetative treatments. A total of 14 plots, 0.01 ha (20m x 5m) in size were monitored at each mine. The number and layout of the plots was the same at each of the three mine-sites.

Runoff was measured using a tipping bucket (Figure 5-3). Sediment was measured as two components: bedload and suspended sediment in runoff. Bedload was deposited in troughs and was weighed after each rainstorm event. A small sample of runoff was collected from one side of the tipping bucket and collected in a 20L plastic drum. This sample was used to determine suspended sediment, pH and electrical conductivity of the runoff water.

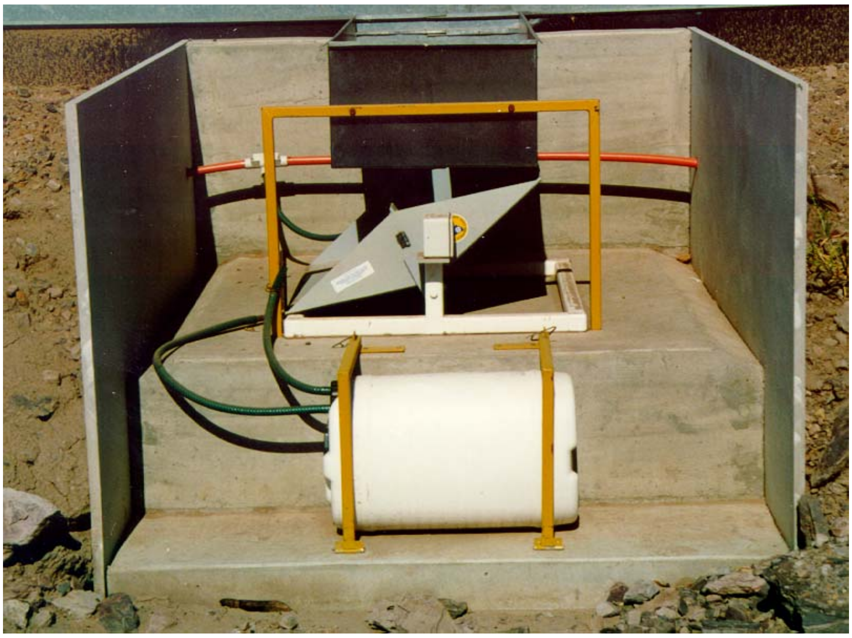

Figure 5-3 The tipping bucket and sampling apparatus for measurement of runoff, suspended load and water quality from a field plot at Oaky Creek mine.

5.3.2 Pasture & Tree Treatments

A mixture of pasture and tree species was sown on the plots (Table 5-1).

Curragh

Buffel grass (*Cenchrus ciliaris*) established well on topsoil and Rhodes grass (*Chloris gayana*) on spoil. Pasture legume species, Wynn cassia, Amiga stylo and Verano stylo did not establish on either material. Tree establishment was poor on both materials. On topsoil, poor tree establishment and low survival rates were initially caused by low sporadic rainfall, and then later in the study, by competition from buffel grass that invaded the plots.

Table 5-1 Pasture and tree species sown on field plots.

	Botanical Names	Common Name	Rate (kg/ha)
Pasture	*Cassia rotundifolia*	Wyn Cassia[1]	30
	Stylosanthes hamata	Amiga Stylo[2]	30
	Stylosanthes hamata	Verano Stylo[2]	3.0
	Bothriochloa insculpta	Creeping Bluegrass	4.0
	Cenchrus ciliaris	Biloela Buffel	4.0
	Chloris gayana	Rhodes Grass	4.0
Trees	*Casurina glauca*	Sheoak	
	Branchychiton rupestris	Narrow-leaf bottle tree	
	Acacia holosericea		
	Acacia salicina	Sally Wattle	
	Acacia saligna	Golden Wreath Wattle	
	Acacia harpophylla	Brigalow	
	Eucalyptus crebra	Narrow-leaf Ironbark	
	Eucalyptus drepanophylla	Grey Ironbark	
	Eucalyptus tereticornis	Blue Gum	
	Eucalyptus citriodora	Lemon-scented Gum	

1. Legume innoculant (group m) applied.
2. Legume innoculant (verano Stylo) applied.

Oaky Creek

Buffel grass (*Cenchrus ciliaris*) established best on topsoil and Rhodes grass (*Chloris gayana*) on spoil. Trees established best on the spoil material, particularly *Eucalyptus populnea, Eucalyptus citridora, Acacia holosericea, and Casuarina glauca*. In contrast, there was poor tree establishment on the topsoil material, due initially to low infiltration, and high runoff losses, and then later to competition from buffel grass.

Goonyella

Buffel grass (*Cenchrus ciliaris*) established best on topsoil and Rhodes grass (*Chloris gayana*) on spoil, only after a series of irrigations were applied in the summer of 1994/95. Establishment was poor on both materials prior to irrigation. After irrigation, trees established best on the spoil material, particularly *Eucalyptus populnea, Eucalyptus citridora, Eucalyptus crebra, Acacia holosericea, Acaia Saligna, Acacia harpophylla*, and *Casuarina glauca*. In contrast when irrigation was terminated, there was poor tree survival rate on the topsoil as a result of low infiltration and high runoff losses from rainfall.

5.3.3 Catchments

Three typical rehabilitated catchments of different size (0.41, 0.58, 0.91 ha) were monitored at Curragh. The top-half of the contoured catchments was laid with topsoil and sown with buffel grass, and on the lower half a mixture of tree species were sown on spoil material. Two catchments were monitored at Oaky Creek (1.2 and 0.5 ha), where spoil was left at the angle-of-repose. Three catchments were monitored at Goonyella (0.48, 0.55, 0.66 ha).

A concrete trapezoidal flume (45 degrees), with a 30 cm throat (Figure 5-2) was constructed at the exit of each catchment to measure runoff and erosion. Bedload was deposited in a 5 m^3 capacity silt trap in front of the flume. A sample of suspended sediment was collected every three minutes at the outlet of the flume with an ISCO sampler. The samples were used to determine electrical conductivity and pH of runoff. An electronic water level sensor and mechanical chart recorder were used to measure flow height in the flume.

5.4 Results and Discussion

5.4.1 Curragh

Average annual median rainfall for Blackwater (1895 to 1994) is 567 mm. During the study only 1996/97 had higher annual rainfall (694 mm) than the long-term median rainfall (Figure 5-4). Just three months produced most of the annual rainfall in the first two years of the study. During the study, 10% of the daily rainfall was >50 mm/day, with no daily rainfall >100mm/day. In contrast, long-term rainfall records show 5% of daily rainfall is >100 mm/day.

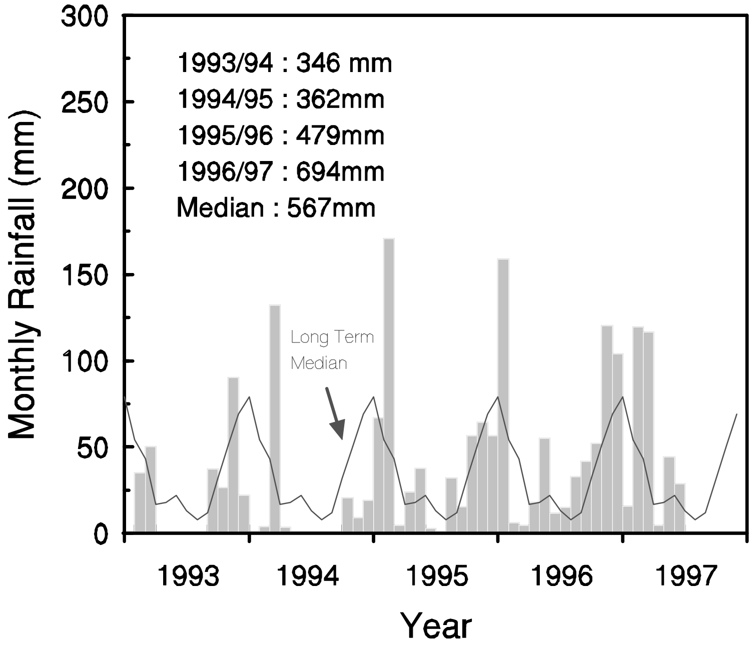

Figure 5-4 Curragh monthly rainfall (1993-97) and long-term rainfall compared.

The soil at Curragh is a montmorillonite clay (CEC = 60 $cmol_{(+)}/kg$) which has good structure and cracks on drying. In contrast, the spoil material crusts hard when dry, and has a fine sand to silty clay loam texture, with a moderately high exchangeable sodium percentage (ESP) and dispersion ratio (Figure 5-5 and Table 5-2).

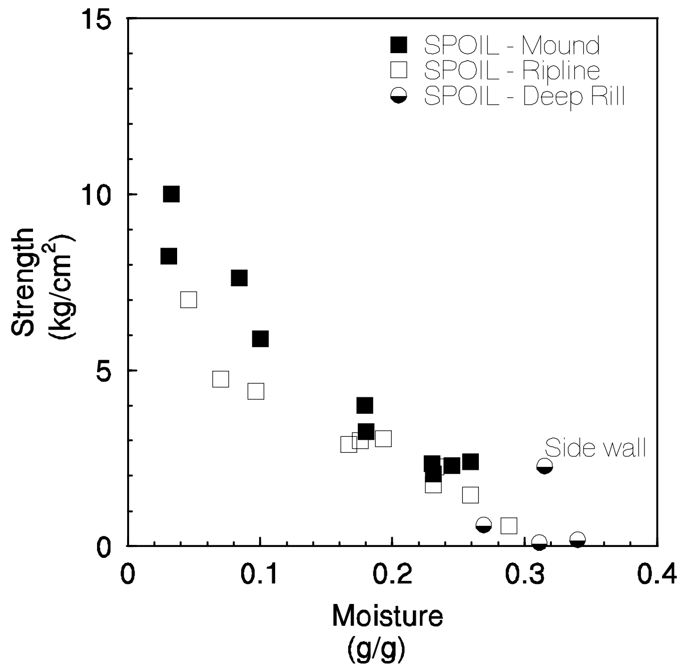

Figure 5-5 Spoil strength for a range of moistures measured using a pocket penetrometer.

Table 5-2 Chemical analysis for Curragh topsoil and spoil material for 1993 and 1996.

Material	EC mS/cm	Cl mg/km	ESP %	Org. C %
Soil 1993	0.434	219	7	1.9
Soil 1996	0.166	17	4	1.3
Spoil 1993	0.613	519	28	1.13
Spoil 1996	0.670	596	31	0.7

Organic carbon has declined and electrical conductivity has more than halved since the topsoil was laid in 1992. The decline in electrical conductivity is associated with a decline in chloride. Before mechanical stripping, chloride was present in the soil at around 60 cm. When stripped, inverted and replaced, the chloride layer is redistributed on the 'new' soil surface. Following successive rainfall the chloride is leached down the soil profile.

5.4.1.1 Field Plots

Topsoil was more erodible than spoil. Consequently more sediment was transported per unit volume of runoff. Although runoff from spoil had a lower sediment concentration, runoff volume was more than double, which resulted in spoil having an overall greater sediment loss than topsoil (Table 5-3).

Table 5-3 Total runoff, sediment loss, sediment concentration, erodibility (MUSLE) and average electrical conductivity of runoff. Curragh 20% bare plots (1993-97). Rainfall 2505 mm.

Material	EC (mS/cm)	Runoff (mm)	Sediment Conc. (g/l)	Sediment Loss (t/ha)	Erodibility (MUSLE *K*)
Topsoil	0.21	495	192	954	0.29
Spoil	0.40	1047	107	1119	0.15

When the spoil is dry a hard dispersive crust forms, which results in low infiltration and large runoff losses. 83% of daily rainfall was lost as runoff (runoff coefficient (c) 0.83) on the spoil, and consequently pasture and tree establishment was poor on this media.

Topsoil initially had a relatively high level of runoff, however once buffel grass (*Cenchrus ciliaris*) established, infiltration increased and runoff decreased (Figure 5-6). In the final year of the study (1997), the topsoil-pasture plot on the 20% slope had half the number of runoff events and just 27 mm runoff, compared with 462 mm runoff from the spoil-pasture plot, where there was little pasture growth. Figure 5-6 shows the development of these trends over the 1993 –96 period, though does not include the 1997 data just described.

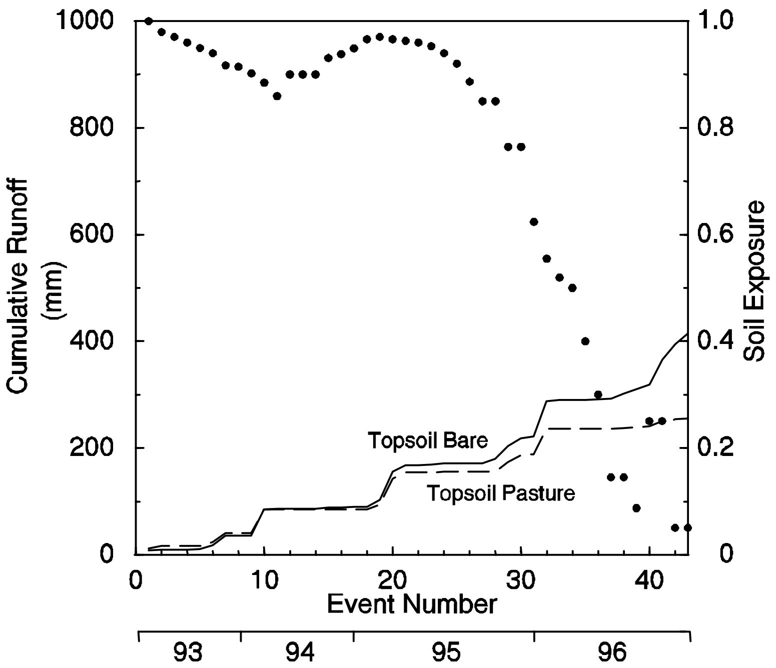

Figure 5-6 Cumulative runoff for Curragh mine topsoil-bare and pasture plots, with soil exposed to rainfall on pasture plot. Soil exposure is indicated by the dotted line.

The low infiltration rate on the spoil is also reflected in the calculated Curve Number. Curve Number is an infiltration parameter used in daily runoff/water balance models, the higher the curve number, the lower the infiltration. On topsoil, there was a 14 unit reduction in curve number where was a dense cover of buffel grass (>75% cover) (Table 5-4). In contrast, for spoil with little pasture established, the Curve Number was very high (96), indicating extremely low infiltration.

Table 5-4 Reduction in curve number on topsoil material with a change in surface vegetation. Topsoil bare, pasture and tree plots on 20% slope.

Vegetative Cover (%)	Number	Curve Number 2
0	49	89.9
<25	42	89.1
25 - 50	10	87.4
50 - 75	9	81.3
>75	13	75.7

Curve Number is an infiltration parameter used in daily runoff/water balance models, the higher the curve number, the lower the infiltration.

5.4.1.2 Window of erosion risk

Topsoil erosion rates were high until there was sufficient pasture cover to prevent erosion. Figure 5-7 shows that soil erosion rates were similar on both the bare and pasture topsoil plots on the 20% slope, when vegetative cover was low. However, by the end of the study when there was a dense sward of buffel grass, soil erosion was 3.1 t/ha on the topsoil-pasture plot, compared to 444 t/ha soil erosion where the soil had no vegetative cover, a 99% reduction in erosion rates where buffel grass was established.

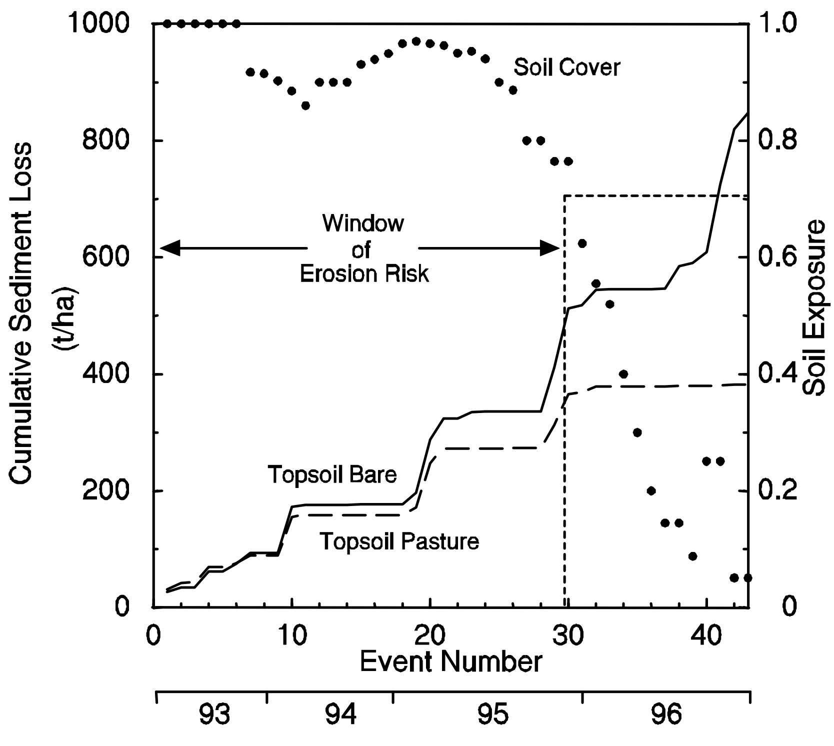

Figure 5-7 Cumulative sediment losses from Curragh mine topsoil-bare and pasture plots (20% slope), with soil exposed to rainfall on pasture plot. Soil exposure is indicated by the dotted line.

Slow tree growth and little soil protection led to a wider 'window of erosion risk' when trees were grown. Erosion rates only declined on the tree plots when weed species began to colonize the plots and provide extra surface cover.

5.4.1.3 Slope

The lowest erosion rate recorded during the study was on the 10% topsoil pasture plot. The pasture plot on 10% slope had just 0.7 t/ha sediment movement in the final year of the study, compared with 3.1 and 48 t/ha respectively from the equivalent treatment on 20% and 30% slopes. On the 30% slope, where rills were present, sediment concentration was almost ten times higher (84 g/l) than the 10% slope (9 g/l), where rills were absent (Table 5-5), despite both treatments having similar levels of buffel grass cover (85% cover).

Table 5-5 Vegetative cover, runoff, sediment concentration and sediment loss from Curragh mine topsoil pasture plots on 10, 20, 30% slopes (1996/97). Rainfall 694 mm.

Slope (%)	Cover (%)	Runoff (mm)	Sediment conc. (g/l)	Sediment loss (t/ha)
10	85	8.3	8.7	0.7
20	87	26.9	11.5	3.1
30	84	57.1	83.8	47.8

On the spoil material, pasture established poorly, with only the 10% plot achieving a sparse layer of Rhodes grass (*Chloris gayana*). Once again the 10% slope had the least runoff and sediment loss, and rills were less pronounced. However, runoff, sediment concentration and sediment loss were similar from the 20% and 30% slopes (Table 5-6). Loch (1997) found rills showed a rapid decline in sediment concentration on steeper slopes as the supply of sediment becomes exhausted.

Table 5-6 Vegetative cover, runoff, sediment concentration and sediment loss from Curragh mine spoil pasture plots on 10, 20, 30% slopes (1996/97). Rainfall 694 mm.

Slope (%)	Cover (%)	Runoff (mm)	Sediment conc. (g/l)	Sediment loss (t/ha)
10	34	405	29	116
20	4	462	97	448
30	4	461	99	456
20 bare	0	425	115	489

On the spoil material, where flow concentrated, there was a tendency for rills to cut deeper rather than wider. The spoil material had low cohesive strength at the bottom of rills where the material was wettest. Consequently, when flow concentrated, this weak layer of material was easily eroded, resulting in deepening rather than widening of rills.

5.4.1.4 Catchments

Catchments A, B, C respectively had 158, 62, and 92 mm total runoff, which was 11, 4 and 7% of the total rainfall during the three year study (Table 5-7). Erosion rates from the rehabilitated catchments were consistently lower than rates measured from the plot study. Sediment concentrations from the catchments were equivalent to concentrations from the topsoil-pasture plot on the 10% slope. Average sediment loss was 1.7, 1.0, 1.3 t/ha/year from the catchments A, B, C respectively. Electrical conductivity of the runoff was <0.139 mS/cm, lower than the background level 0.3 mS/cm measured in the surrounding creeks in the area (Figure 5-8).

Table 5-7 Average electrical conductivity, runoff, sediment concentration, total and average sediment loss from Curragh catchments (1994-1997). Rainfall (1374 mm)

Catchments	Average EC (mS/cm)	Total Runoff (mm)	Sediment Conc. (g/l)	Total Sediment Loss (t/ha)	Average Sediment Loss (t/ha/yr)
A	0.116	158	3.2	5.0	1.7
B	0.136	62	4.7	2.9	1.0
C	0.139	92	4.2	3.9	1.3

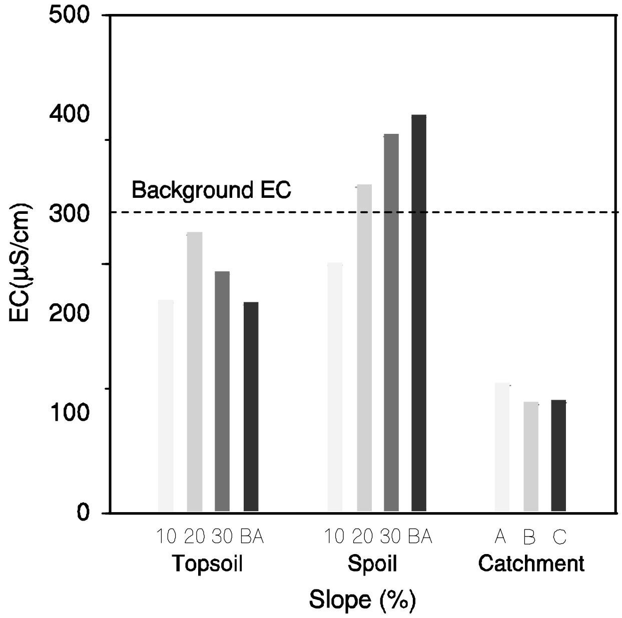

Figure 5-8 Average electrical conductivity of runoff from Curragh mine topsoil and spoil pasture plots on 10, 20, and 30% slopes. Plus, bare (BA) topsoil and spoil plots on 20% slope, and catchments A, B, C.

Most runoff and sediment is likely to be generated from the spoil area on the lower-half of the catchments where infiltration rates are low, and where trees are sown. Buffel grass and vegetative cover have begun to established on the spoil areas in the catchments, predominantly in the channels above contour banks, and where topsoil has deposited in rip-lines.

On a similar spoil at Blackwater mine, there is evidence to suggest that when infiltration is enhanced and chloride is leached out of the surface, then vegetative growth can be maintained and a spoil/soil humus layer can develop. If this should occur in the catchments, vegetative growth and infiltration will be further enhanced, and runoff and sediment loss reduced.

5.4.1.5 Topsoil and Spoil Comparison

Topsoil is more erodible than spoil. However, topsoils have better fertility, soil structure, and infiltration characteristics, resulting in better vegetative growth than on the spoil material. Vegetation, particularly grass cover, protects the soil from rainfall impact which disrupts and detaches soil aggregates and causes macropores to block, infiltration to decline, and runoff and erosion to increase. The presence of even low levels of vegetation has clearly improved soil infiltration capacity, as shown by the reduction in Curve Number (2) and runoff coefficient.

Infiltration of rainfall into topsoil is further enhanced when vegetation dries and cracks the soil. For example, out of a 118 mm rainfall event, 97% of rainfall infiltrated where cracks had formed and there was a dense cover of buffel grass (topsoil-pasture plot on 20% slope). In contrast, on bare topsoil and spoil material 60% and 34% of the rainfall infiltrated.

Topsoil is in limited supply at the Curragh site; consequently it is important that this valuable resource is protected when it is at most risk of erosion when there is little vegetative cover.

5.4.1.6 Establishment of surface cover to minimize 'window of erosion risk'

The region's rainfall is extremely variable, with annual rainfall ranging from 200 mm to 1400 mm. During the study, only one year had annual rainfall greater than the long-term median rainfall. It is therefore important, in such a variable rainfall environment, that rehabilitation practices enhance vegetative growth by maximizing infiltration and minimizing runoff losses. By minimizing runoff losses, off-site movement of sediment and pollutants are reduced. Once a dense sward of buffel grass established on the topsoil pasture plots, runoff and erosion rates declined by up to 99%. In contrast, vegetative growth was very poor on the spoil material, where a hard cohesive crust formed which resulted in low infiltration and high runoff and erosion rates throughout the study.

The greatest 'window of erosion risk' occurs before vegetation is established. It is during this period of high erosion risk that rills form, particularly on the steeper slopes, and once formed the rills persisted even when there is a dense cover of grass. Therefore, vegetative cover should be established quickly to prevent rills forming and avoid any additional costs in repairs and recontouring of rehabilitated areas.

5.4.1.7 Slope and Rill Erosion

Buffel grass clearly reduced both runoff and soil erosion on all topsoil plots. The lowest soil erosion rate was on the pasture plot on the 10% slope, though on the steeper slopes erosion was strongly dominated by rilling. On the 30% slope there was 48t/ha soil erosion in the final year of the study, despite the presence of a dense stand of buffel cover (>85%). Ripping initially protected steeper gradients by ponding rainfall, slowing overland flow and enhancing infiltration.

The steeper slopes (20% and 30%) showed extremely high rates of erosion, and rehabilitation of these steeper slopes clearly carries higher risks of failure due to the potential for high initial soil losses. If slopes of 20% and 30% were to be rehabilitated, emphasis would need to be placed on rapid establishment of vegetative cover and before rills are formed.

Vegetation has greatly reduced soil erosion, particularly on lower slope gradients. However, on steeper slopes and on rill susceptible soils like at Curragh, there is a need for vegetation that will give a high proportion of contact cover and relatively large units of vegetation. Stoloniferous species that are in contact with large areas of the soil would be best suited to resist rill erosion.

There is little chance of successful rehabilitation on the spoil material at Curragh. The material has low infiltration rates and high runoff and erosion rates. On the rehabilitated catchments, tree and pasture establishment has occurred where ripping of the spoil material has left deep depressions, which slows runoff and enhances infiltration. Colonization of the spoil area by understorey vegetation has been slow, but now after 5 years, buffel and Rhodes grass have begun to establish on the spoil area.

5.4.1.8 Rehabilitated catchments

Data collected from the Curragh rehabilitated catchments show that current practices are achieving acceptable levels of sediment loss and water quality. Sediment and water quality from the Curragh rehabilitated catchments is similar to background levels measured in surrounding creeks. Electrical conductivity from the catchments averages <0.139 mS/cm compared with typical background levels in surrounding creeks of 0.3 mS/cm. All three catchments have a dense cover of buffel grass on the topsoil areas, with evidence of grass establishing on the spoil areas within the catchments.

5.4.2 Oaky Creek

5.4.2.1 Plots

During the four year plot study (1993-97) there was 2162 mm rainfall at Oaky Creek. On the bare topsoil plot 49% (1050 mm) of the rainfall was lost as runoff. In contrast, bare spoil had 29% runoff (Table 5-8). Topsoil consequently had greater sediment loss than spoil, despite both materials having similar sediment concentrations. Greater infiltration on the spoil resulted in better tree establishment and survival than on the topsoil material.

However, runoff and sediment loss declined on topsoil, once buffel grass established. On the pasture-topsoil plot on the 20% slope, there was a seven-fold reduction in sediment loss when compared with the bare plot. Over 40% of the erosion on the pasture-topsoil plot occurred in the first year of the study, before buffel grass had fully established, highlighting the greatest window-of-erosion risk in mine rehabilitation.

On the topsoil-pasture plots, the greatest erosion occurred on the 10% slope where there was little surface roughness (Table 5-9a). In contrast, on the spoil-pasture plots the least runoff and sediment loss was on the 20% slope, where surface roughness was greatest, and where rip lines remained intact throughout the study. The 10% spoil-pasture plot had the greatest runoff and erosion, caused by the formation of a chemical crust, and low surface roughness on the plot (Table 5-9b). The chemical weathering resulted in high erosion rates and electrical conductivity (up to 4.75 mS/cm) (Table 5-10a). High EC levels were measured on topsoil plots where erosion stripped topsoil away and exposed the spoil material below (Table 5-10b). Generally, the average EC of runoff from topsoil-pasture plots was equivalent to background levels recorded in surrounding creeks (0.3 mS/Cm) (Figure 5-9 and Table 5-10a-b). An exception was the topsoil-bare plot where there was no vegetative cover. In contrast, spoil runoff generally had higher average EC than background levels.

Table 5-8 Total runoff, sediment loss, sediment concentration, and average annual sediment loss from Oaky Creek mine topsoil and spoil bare plots, 20% slope (1993-97). Total rainfall 2162 mm.

Material	Total Runoff (mm)	Sediment Conc. (g/l)	Total Sediment Loss (t/ha)	Ave. Sediment Loss (t/ha/yr)
Topsoil	1050	49	514	128
Spoil	623	51	318	79

Table 5-9 Total runoff, sediment loss and average annual sediment loss from Oaky Creek topsoil *(a)* and spoil *(b)* pasture plots at 10, 20, and 30% slopes (1993/97). Total rainfall 2162 mm.

(a) Topsoil pasture plots

Slope (%)	Ave. Cover (%)	Total Runoff (mm)	Total Sediment Loss (t/ha)	Ave. Sediment Loss (t/ha/yr)
10	30	898	140	35
20	42	778	72	18
30	20	717	236	59

(b) Spoil pasture plots

Slope (%)	Ave. Cover (%)	Total Runoff (mm)	Total Sediment Loss (t/ha)	Ave. Sediment Loss (t/ha/yr)
10*	21	789	325	81
20	25	216	31	8
30	19	503	102	25

*Weathering and crust formation

Table 5-10 Electrical conductivity of runoff from Oaky Creek spoil *(a)* and topsoil *(b)* pasture plots at 10, 20, and 30% slopes, and 20% bare plot (1993/97)

(a) Spoil pasture plots

Slope	EC (mS/cm)		
(%)	Lowest	Mean	Highest
10*	0.106	1.700	4.750
20	0.053	0.421	0.997
30	0.069	0.494	1.036
20 Bare	0.147	0.967	2.180

* Weathering and crust formation.

(b) Topsoil pasture plots

Slope	EC (mS/cm)		
(%)	Lowest	Mean	Highest
10	0.036	0.145	0.633
20	0.028	0.200	1.359
30	0.048	0.244	0.608
20 Bare	0.131	0.699	1.450

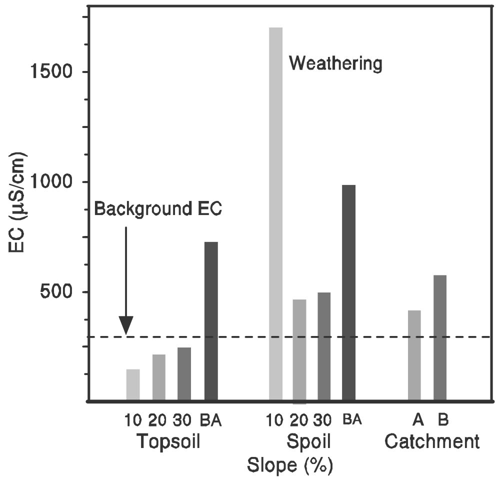

Figure 5-9 The electrical conductivity (EC) of runoff from field plots at Oaky Creek compared to background levels in local creek.

5.4.2.2 Catchments

Substantially less runoff and sediment loss and better water quality were recorded from the angle-of-repose catchments when compared with the plots (Table 5-11 and Figure 5-9). During the study just 0.4% and 1.6% of rainfall was lost as runoff from catchments A and B, respectively. Although, runoff and sediment movement off the angle-of-repose slopes may be significant, a low proportion is finding its way out of the catchments. Most of the runoff infiltrates into the spoil and the sediment deposits in large depressions along the catchment valley. It was observed that most of the recorded runoff and sediment movement was produced from the area immediately in front of the catchment outlets.

Table 5-11 Runoff, sediment concentration, sediment loss from Oaky Creek angle-of-repose catchments (1994-1997). Rainfall (1581 mm)

Catchments	Total Runoff (mm)	Sediment Conc. (g/l)	Total Sediment Loss (t/ha)	Ave.Sediment Loss (t/ha/yr)
A	7	12	0.9	0.3
B	26	93	24	8

5.4.3 Goonyella

Subsidence occurred on some plots during the study, causing slumps and large cracks to appear, which resulted in an incomplete data set on sediment loss and runoff. Slumping began on the topsoil plots on the 10% slope in March 1994, and cracking on 30% slope in December 1994. The topsoil plots on the 10% and 30% slopes never reliably functioned after this, despite repairs being continually conducted on the plots. The most reliable data, over the study, were collected from the topsoil and spoil plots on the 20% slope and from the spoil plots on three slopes.

5.4.3.1 Field Plots

Study results indicated that spoil was slightly more erodible than topsoil, with sediment concentration more than double that from topsoil. However, topsoil had double the runoff, and hence had slightly larger total sediment movement than the spoil material (Table 5-12).

Once buffel grass established on the topsoil, infiltration improved and runoff and sediment loss declined (Figure 5-10). As with the Curragh and Oaky Creek sites, the greatest 'window-of-erosion-risk' was before there was sufficient vegetative cover (>30% cover) to prevent erosion. Once a dense sward of buffel established, soil erosion was reduced dramatically.

The topsoil and spoil materials at Goonyella are both hard setting (Figure 5-11). However, tunnel erosion (piping) tends to develop on the spoil due to the dispersive nature of the material (Table 5-13).

Initially, very little runoff was generated on the spoil material with preferential movement of rainfall into the spoil via pipes. Only 2% of rainfall became runoff in the first two years of the study. Runoff began to increase after 500 mm cumulative rainfall, with 18% percent runoff (runoff coefficient = 0.18) in the final two years of the study (Figure 5-12).

In contrast, runoff was very high on the topsoil material at the start of the study (runoff coefficient = 0.75), with a slight reduction (0.5) late in the study, attributed to cracks appearing on the plot.

Spoil erodibility (K) also increased during the study (Figure 5-13). In the first two years spoil erodibility was 0.03, calculated on a rainstorm event basis using the MUSLE (Onstad and Foster, 1975). In the final two years, spoil erodibility increased more than six-fold to 0.19.

The increase in erodibility corresponded with an increase in electrical conductivity at the spoil surface (Figure 5-14), a result of wetting and drying cycles causing salts to concentrate at the spoil surface. Electrical conductivity of the spoil began to decline after 1995, once vegetation established on the tree and pasture plots. Where there was no vegetation, EC continued to increase.

Table 5-12 Total runoff, sediment loss, sediment concentration, and average annual sediment loss from Goonyella topsoil and spoil bare plots, 20% slope (1993-97). Total rainfall 1798 mm.

Material	Total Runoff (mm)	Sediment Conc. (g/l)	Total Sediment Loss (t/ha)	Ave. Sediment Loss (t/ha/yr)
Topsoil	598	58	345	86
Spoil	255	123	314	78

Table 5-13 Chemical analysis of Goonyella mine soil and spoil material plots 1993 and 1996.

Material	pH	EC mS/cm	Cl mg/kg	ESP %
Soil 1993	7.6	0.32	394	11
Soil 1996	7.2	1.92	1138	8
Spoil 1993	8.0	2.32	3299	38
Spoil 1996	7.3	5.52	9583	37

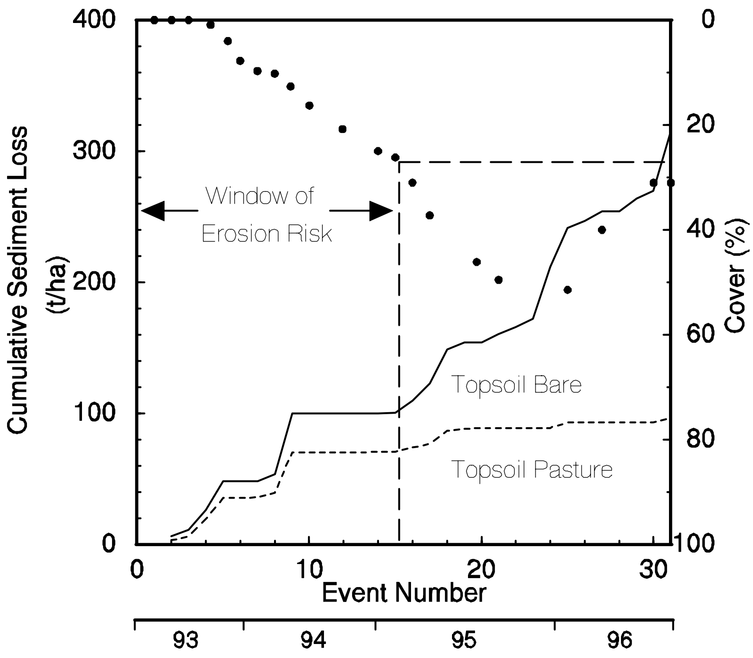

Figure 5-10 The relationship between cumulative topsoil sediment loss from bare and pasture plots on 20% slope (1993-96) and the percentage of pasture cover, indicated by the dotted line.

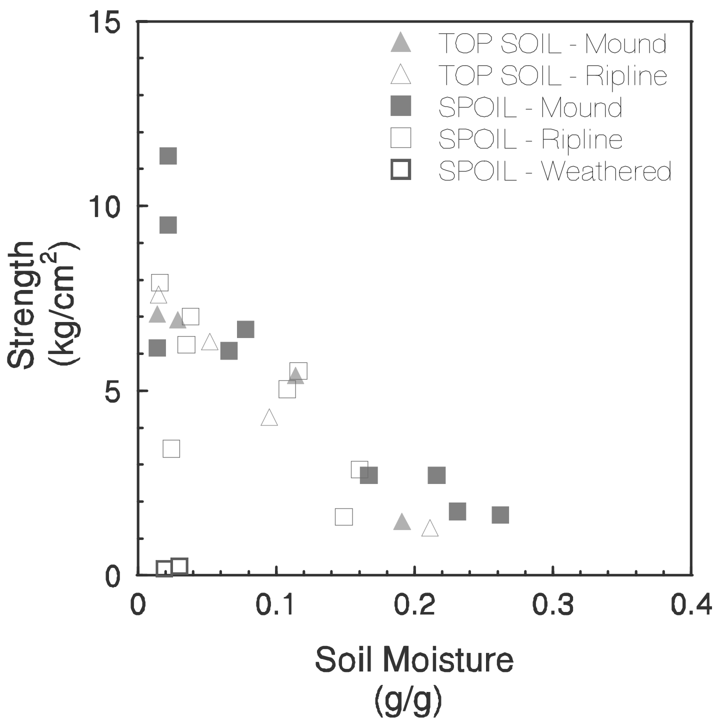

Figure 5-11 Goonyella topsoil and spoil strength across a range of moisture conditions.

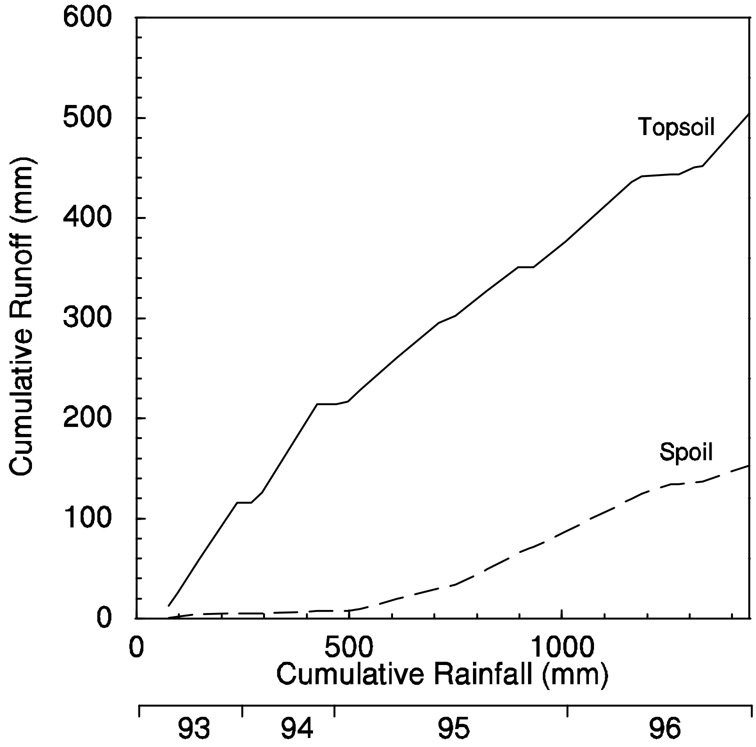

Figure 5-12 Cumulative rainfall and runoff from Goonyella mine bare topsoil and spoil plots on 20% slope, (1993-96).

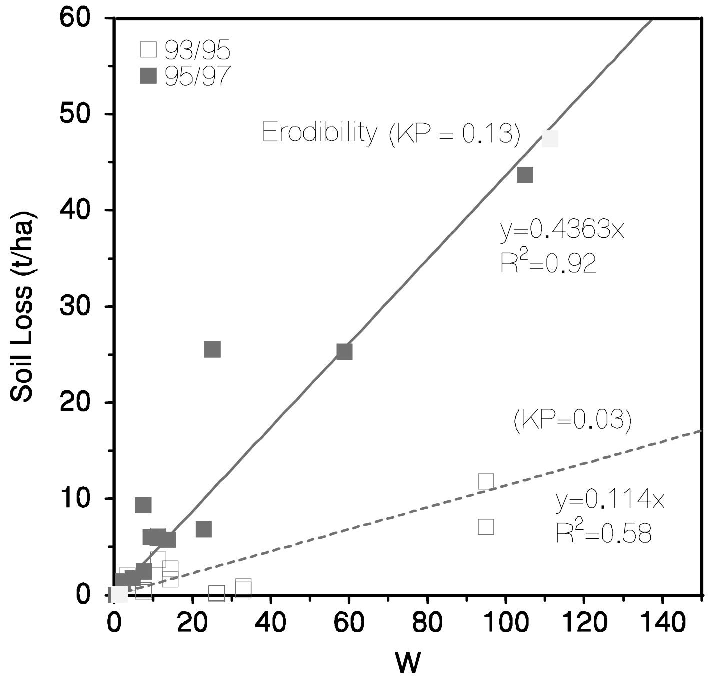

Figure 5-13 Goonyella spoil soil loss versus rainfall and runoff energy (MUSLE *W*), with spoil erodibility and practice factor (MUSLE *KP*) calculated from the Modified Universal Soil Loss Equation (MUSLE).

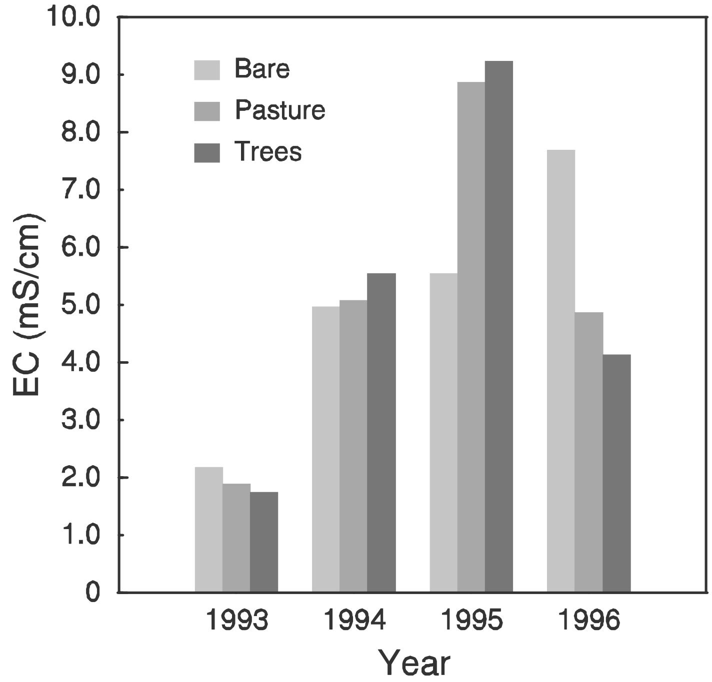

Figure 5-14 Electrical conductivity of Goonyella in-situ spoil material on bare, pasture and pasture plots on 20% slope, (1993-96)

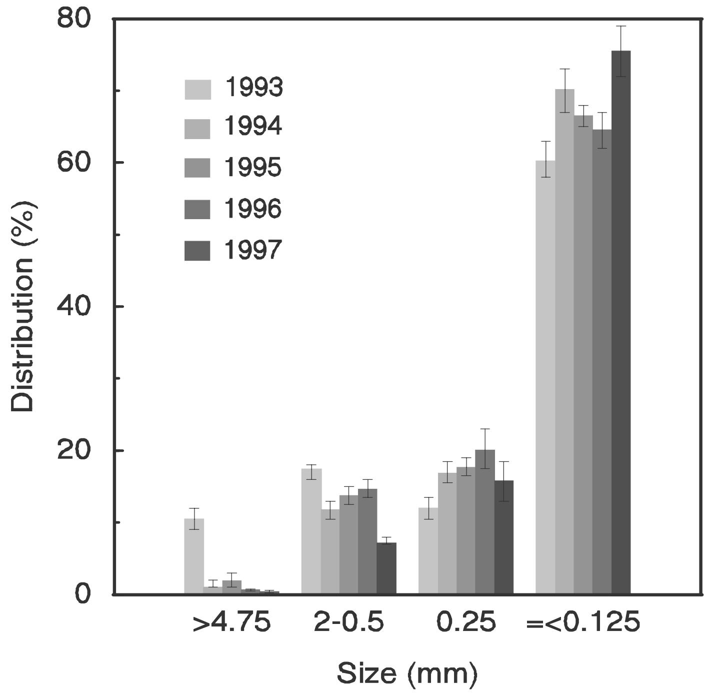

Figure 5-15 Particle size analysis of bare spoil at Goonyella mine (1993-96).

5.4.3.2 Catchments

Buffel grass quickly established on the catchments, which resulted in low sediment concentrations (<6 g/l), and average annual soil loss <4t/ha/year (Table 5-14). Average electrical conductivity of runoff leaving the catchments was lower than background levels recorded in local creeks, and substantially lower than the spoil plots. The use of topsoil, and pasture vegetation on the plots, and contoured rehabilitation reduced electrical conductivity of runoff to environmentally acceptable levels (Figure 5-16).

Table 5-14 Runoff, sediment concentration, sediment loss from Goonyella catchments (1994-1997). Rainfall (1268mm)

Catchments	Total Runoff (mm)	Sediment Conc. (g/l)	Total Sediment Loss (t/ha)	Ave.Sediment Loss (t/ha/yr)
A	140	6	8	2.7
B	212	6	12	4.0
C	164	4	7	2.3

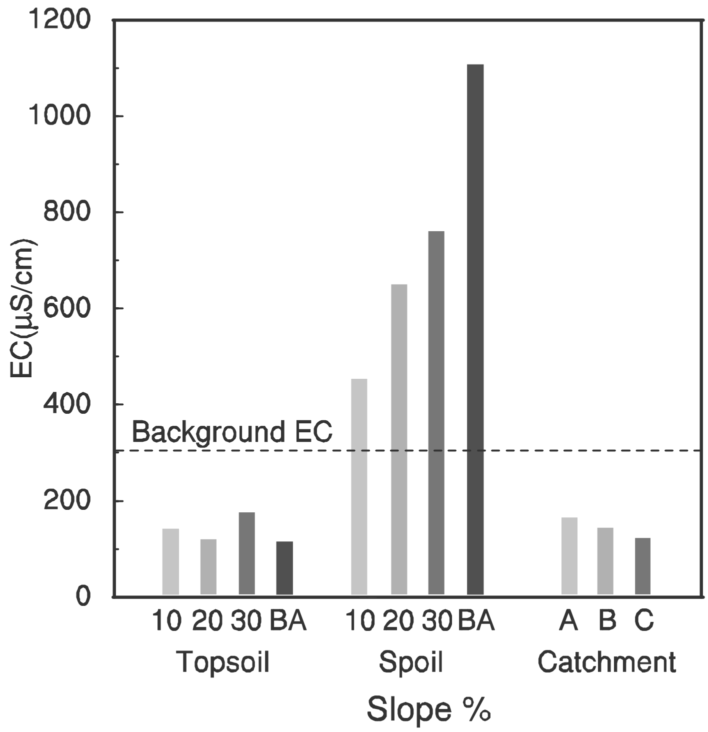

Figure 5-16 Average electrical conductivity of runoff from Goonyella topsoil and spoil pasture plots on 10, 20 and 30% slopes. Plus, bare (BA) topsoil and spoil plots on 20% slope, and catchments A, B, and C.

5.5 Summary

5.5.1 Curragh

The use of topsoil and vegetative cover on low slopes minimised runoff; sediment and salt transport at the Curragh mine. A hard dispersive crust formed on spoil and caused low infiltration rates, and large amounts of runoff and sediment movement. Spoil is not conducive to establishment of vegetation. Runoff leaving rehabilitated catchments had electrical conductivity levels lower than local creeks.

5.5.2 Oaky Creek

Surface roughness and grass cover reduced runoff and sediment loss on both spoil and topsoil material at Oaky Creek. The impact of slope gradient on erosion was modified by ripping, creating a greater surface roughness than on the lower slope. The spoil material had greater infiltration rates and lower runoff and sediment loss than topsoil. However, chemical weathering and crust formation on spoil reduced the rainfall infiltration rate, and increased runoff, sediment loss and the electrical conductivity of runoff. Catchment runoff, sediment loss and water qualities (EC) were lower than from the spoil plots.

5.5.3 Goonyella

Both the topsoil and spoil material at Goonyella is hard setting. Vegetation only established on the plots after irrigation, with pasture growth best on the topsoil and tree growth on the spoil. Once pasture cover established on the topsoil, erosion, and the EC of the runoff water, were reduced, particularly on the lower gradient slopes of the rehabilitated catchments.

References

Carroll, C., Halpin, M., Bell, K., and Mollison, J. (1995). The effect of furrow length on rain and irrigation induced erosion on a vertisol in Australia. *Australian Journal of Soil Research.* 33: 833-50.

Carroll, C., Halpin, M., Burger, P., Bell, K., Sallaway, M. M., and Yule, D. (1997). The effect of crop type, crop rotation and tillage practice on runoff and soil loss on a vertisol in central Queensland. *Australian Journal of Soil Research.* 35:925-39.

Ciesiolka, C.A.A. (1987). Catchment management in the Nogoa watershed. Research Project Compeltion Report. AWRAC Research Project.

Loch, R. J. (1997). Effects of vegetation, slope gradient, and time since rehabilitation on runoff and erosion., Curragh Simulator Study, June 1996. Project Report.

Onstad, C.A., and Foster, G.R. (1975). Erosion modeling on a watershed. *Transactions ASAE* 18: 288-292.

6. A Solute Transport Model for the prediction of salt release from eroding postmining landscapes.

M. Short[a], H.B. So[a] and B. Kirsch[b]

[a]Post-graduate student and Associate Professor of Soil Physics, School of Land and Food & Center for Mined Land Rehabilitation, The University of Queensland, St Lucia, Q 4072

[b]Environmental Officer, Norwich Park Mine, Dysart, Qld. Previously Research Officer, The University of Queensland.

6.1 Aims

The aims of the solute transport modeling component of the PLPEWC project are to:

i. Predict the potential solute release with runoff water from the reconstructed landscape; and

ii. Ascertain the potential rates for solute accumulation or depletion at the surface.

6.2 Introduction

No commercially available package is adequately equipped to achieve the aims of the solute transport modeling component of the PLPEWC project. In addition, no published research yet correctly incorporates a suitable combination of physical processes that can yield the correct simulation for most of the overburden materials subject to the prevailing storm intensities of the Bowen Basin region. Furthermore, a model is useful and 'site portable' if its parameters are identifiable, independent and easily optimized. Meaningful comparison between sites can then be made, and parameter estimation from site/material properties can be attempted. This feature is not generally inherent in the traditional model formulations employed in most solute modeling packages. To remedy this situation, this project has developed a model together with an experimental methodology that can overcome these hurdles.

This research is currently confined to model the surface zone and its response to the hydrological forces acting at the surface. It is reliant upon the primary assumption that a one dimensional mechanistic continuum model can represent the very complex field surface layer. It does not attempt to answer problems that require the accurate simulation of subsurface flows at larger scales. These problems are necessarily three-dimensional and require very detailed subsurface data. Various commercial packages are already available for the purpose of simulating the subsurface movements. (e.g. MODFLOW).

The development of the prediction tool for solute movement, for this project component, entailed 3 key parts:

- Identification of the pertinent physical processes, which then enables the construction of a model that yields a satisfactory description of reality and, at the same time, possesses identifiable parameters;
- Development of experimental methods for acquiring calibration data and development of algorithms for finding optimal parameters; and
- Development of a PC program, with model and parameter data base, for real time simulation.

6.3 The Method

6.3.1 Strategy and Model Formulation

In order that the project objectives are met, there is no choice but to choose a mechanistic description for the movement of the water and solute in the direction perpendicular to the ground surface. For this purpose, the Richards and the convection-dispersion transport equations, for water and solute respectively, were chosen. (The equations were appropriately modified to account for physical processes particularly pertinent to our application.)

Furthermore, for practical reasons, the model is restricted to one spatial dimension. This causes a calibrated model to (i) be restricted to a physical region that is uniform in material, surface geometry, and surface boundary conditions, or (ii) be representative of an average condition for a region in which those attributes vary significantly.

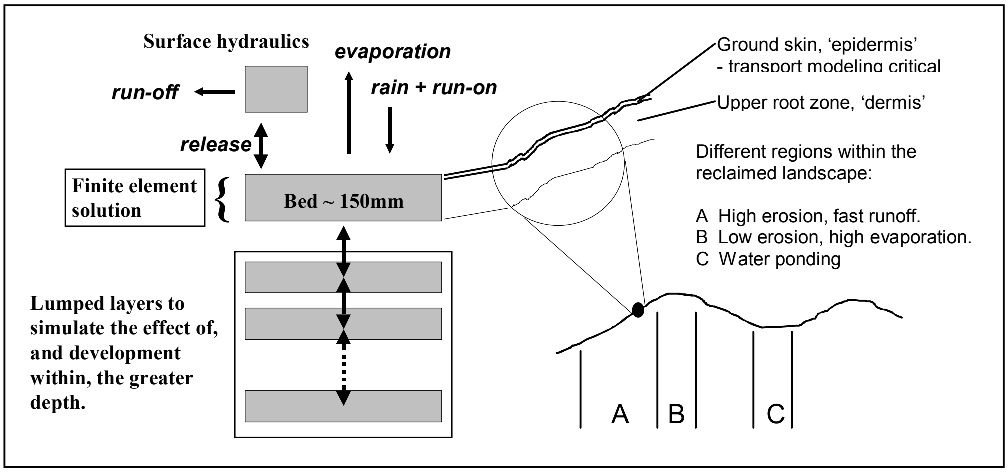

Figure 6-1 The physical model representation.

The water and solute movement within the 'epidermis' (ground skin) and 'dermis' (upper root zone) is simulated using a computational finite element method. The effects of deep drainage and/or subsurface water sources can be simulated with block element layers. The surface boundary conditions are discussed further in later sections of this report.

A more detailed mathematical description of the model is given in Appendix 2.

Before simulation, the model is calibrated for a particular site. This entails the value definition of various model parameters. These parameters specify: the constitutive relationships involving water content-tension, water content-conductivity and solute dispersivity; the solute retention model; boundary transfer relationships involving the surface hydraulic seal, solute release and evaporation; surface discharge laws; the erosion formula; and miscellaneous field effects. The parameters are site specific and may change from site to site.

Of the parameters, the 'Basic Material Parameters' (Figure 6-2) specify the fresh material's hydrological and solute transport properties. These parameters are optimally calibrated for a given material, in its unconsolidated state, from laboratory experiments and are material specific. Provision for modified field behavior (biological influence, structural development, heterogeneity, surface complexity) is made by the remaining group of parameters. These remaining parameters are obtained from existing literature or data, automatically provided by the SALTRO program, or are simply user specified.

Ultimately, the basic material parameters will be inferred from an existing parameter library where simple relationships with easily measured or identified material attributes allow the use of interpolation formulae. This approach is the same taken by the laboratory erosion workers in the PLPECW project where erodibility was regressed against other material properties or attributes.

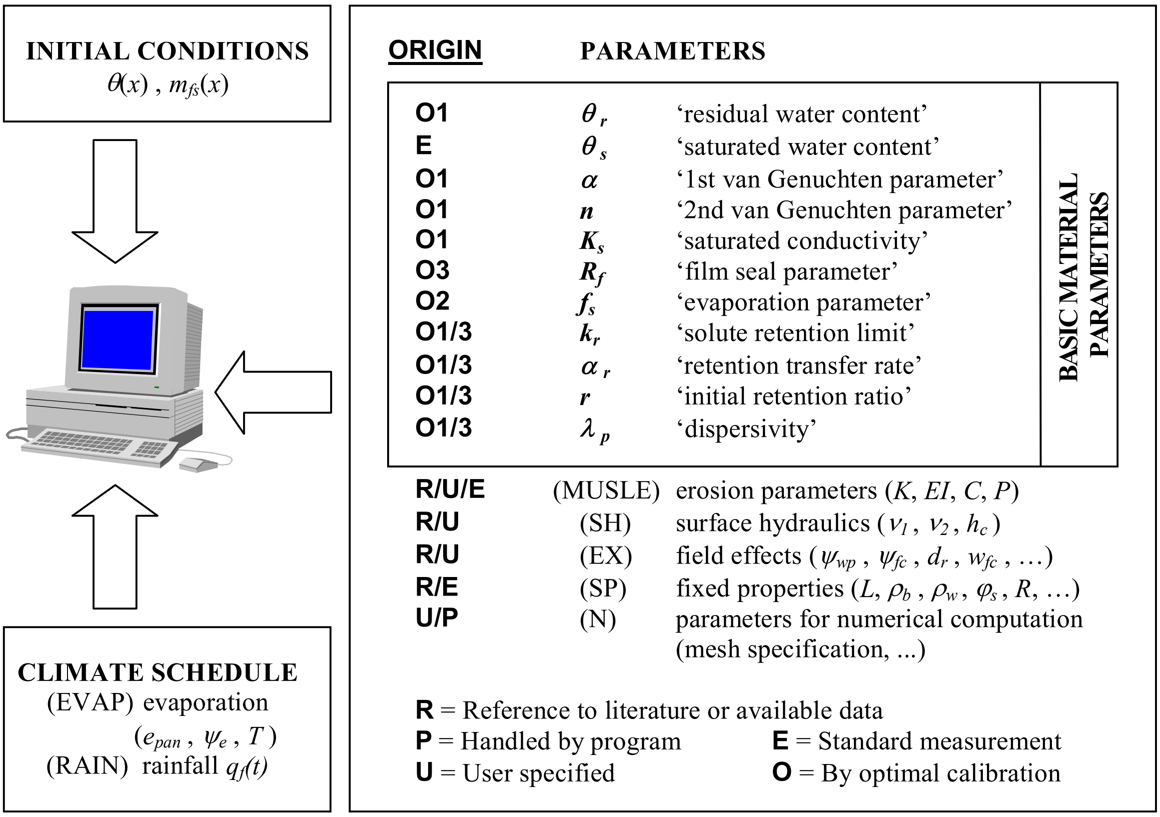

Figure 6-2 SALTRO Input.

The user must specify model parameter values, the climate, and the initial conditions, before the simulation can begin. The parameter origin refers to the method by which the parameter is obtained. (The numbers on the 'O' origin indicate the optimization step in the calibration process.)

The model is, in essence, an idealized mathematical description of the immediate surface layer ('epidermis' + upper root zone) and its behavior in response to the surface boundary conditions imposed by the environment. The user specifies the environment by defining a series of periods in which pan evaporation, material air-dry limit, rainfall intensity, and mean temperature are given.

6.3.2 Model Solution and Programming

For the simulation and the computational solution of the equation system, the Galerkin finite element method, a proven and robust weighted residual technique, is employed. The source code is written in C / C++ and has been verified against the analytical solution of special cases. A summary of this method is provided by Appendix 3.

As illustrated in Figure 6-3, real time output from this calculation are runoff hydrographs, chemical release hydrographs, cumulative chemical release, and the evolution of the water and chemical profiles.

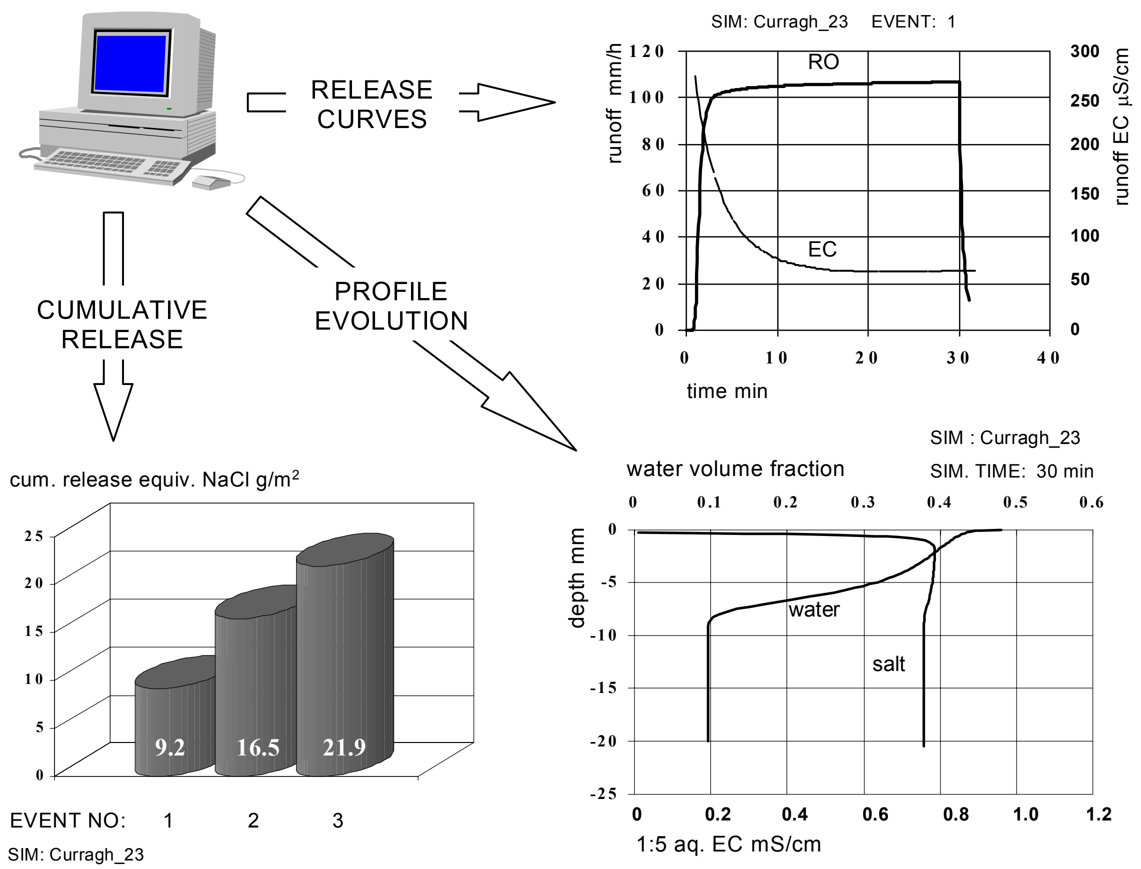

Figure 6-3 SALTRO Output

6.3.3 Basic Material Parameter calibration

Ultimately, a database of the basic material parameters, for various sites, will be available. For a sufficiently large database, parameters for new sites can be determined by interpolation methods. In the early stages however, experiment and optimal calibration of the model is necessary. This section outlines the procedure for the latter recourse.

The data for the determination of the basic material parameters are collected from three laboratory experiments described below. The materials were thoroughly mixed, sieved to 10mm, and loosely packed.

6.3.3.1 Calibration Experiments

1. <u>'Tub Experiment'</u>

The tub trial is employed to provide data against which the model is run, to determine the optimal in-bed parameters, which are those prefixed by **O1** (hydraulic) and **O1/3** (solute) in Figure 6-4a. The trial provided a data time series, which is equivalent to measurement repetition. This trial requires approximately 0.02m^3 or 30kg of material.

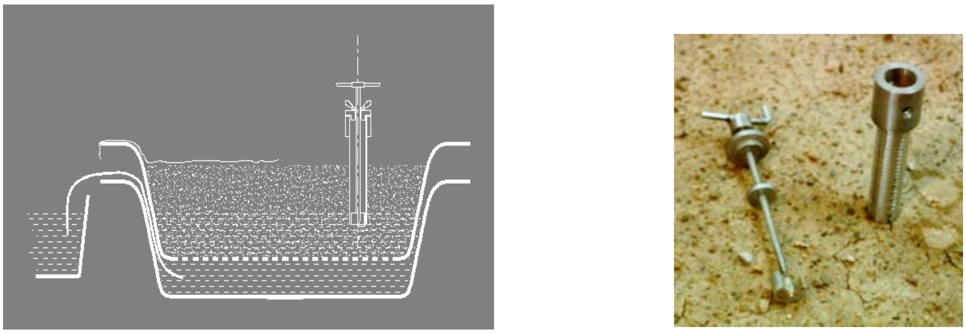

Figure 6-4 Equipment used in 'Tub Experiment'

a. Diagram of the laboratory apparatus used for the determination of 'in-bed' solute transport parameters.

At time zero, a layer of well mixed oven dry material is laid above a well mixed and totally saturated layer, of the same material, in a plastic tub. A constant water head is maintained at the base of the tub and the surface is kept sealed (gladwrap). The plot was cored to track the transport of water and solute. The results distinctly reveal the transport of both quantities.

b. The high resolution coring tool

The tool is 30mm in diameter. The sheath or tube (right) is constantly lowered as the collecting tool (left) retrieves the subsamples at 5mm depth resolution. Testing showed this tool to recover subsamples at their target depths within a maximum of 30% mixing.

A custom coring tool, (Figure 6-4b), was fabricated for the coring. Its diameter was sufficient to provide large enough subsamples at target depth increments of 5mm for moisture and EC measurements, but not large enough to cause unacceptable disturbance to the on-going experiment.

2. <u>Evaporation experiment</u>

Complex geometry, thermal buffering and surface radiation properties all cause the evaporation rate from the saturated material surface to differ from the pan evaporation rate. The evaporation parameter, being the ratio between the two rates, accounts for this deviation.

In order to determine the evaporation parameter for the material, the parameter prefixed by **O2** in Figure 6-2, an evaporation trial is conducted. This entails running the model against the evaporative loss data from a drying bed that was initially saturated. The only data required is weight changes with time. Approximately 0.01m^3 or 12kg of material is required for this trial.

3. Flume experiment

Laboratory tilted flume bed with rainfall simulator trials, that are conducted for the determination of material erodibilities, also provide the necessary runoff data that enable the calibration of the solute and hydraulic film seal basic material parameters. The utilized data is, specifically, the water ponding time and the solute release curve. The film seal parameter (**O3**, Figure 6-2) is optimized against the ponding time. As the rainfall intensities are very large the hydrograph reveals little information within the degree of measurement error involved. The solute release data augments the tub trial data for the optimization of the solute parameters (**O1/3**, Figure 6-2).

The 3m x 0.4m x 0.15m flume bed and oscillating rainfall simulator at the Erosion Process Laboratory University of Queensland has been employed for this purpose. The laboratory research of PLPEWC (C. Walker and G. Sheridan) has already developed a large data set for most of the materials. The flume bed requires approximately $0.2m^3$ or 300kg of material.

6.3.3.2 Calibration Method

Put simply, the computational model is run against the data until the model output and experimental data show the best agreement, (error sum minimized). An acceptable gradient method is chosen for the optimization procedure; a modified Newton-Raphson procedure using the techniques of Gauss and Marquart is employed, the details of which are provided in Appendix 4.

6.3.4 Model validation

Model validation will be achieved in three ways:

1. Comparison of model simulation with laboratory flume bed core data for three materials. These materials being overburdens from Curragh, Oaky Creek, and Goonyella. The beds were subjected to at least three rainfall wetting and drying period cycles. (A moderated glasshouse climate was used for the drying.) Note that flume bed cores are not used as part of the model calibration.
2. Correspondence between water retention parameters and laboratory pressure plate data, and also the model hydraulic conductivity function and data from laboratory outflow experiments.
3. Comparison of the model simulation with PLPEWC field catchment data. (The model is run for these site materials under the catchment's climate record.)

6.4 Results and Discussion

6.4.1 Model Output

An example of the principle output from the SALTRO program is illustrated in Figure 6-3. The real time simulation can at any time produce the profiles of water and solute. During rainfall events, hydrographs and solute release curves can be generated and total solute release is calculated.

Of particular interest to the environmental planner would be the salt profile and cumulative salt runoff after worst case and best case climate scenarios.

6.4.2 Theoretical model development

For the first approximation, the method of Wallach and Shabtai (1992*)* was employed. The Richards equation and the standard convection dispersion equation (CDE) with linear equilibrium sorption were combined with the surface boundary conditions for the simulation. Erosion was assumed as zero, and quite arbitrary constitutive relations are used to close system. Provision was made for surface sealing, a necessary feature for the types of material and rainfalls that are dealt with. A simulation program, written in standard C for DOS, and called WST (water solute transport), was written. When attempts were made to calibrate this early model against the tilted flume cycle data, using the WST program, two problems became apparent:

1. The model could not simulate the experimental solute release curve.
2. The unsystematic method of manually varying a large number of parameter values until (subjective) agreement was maximized, was too time consuming and led to a parameter set of dubious significance.

The first problem was symptomatic of a model that failed to adequately describe the important physical processes. The second problem was related to parameter indentifiability, or rather lack thereof. The following two subsections separately discuss how these problems were overcome.

6.4.2.1 Identification of the pertinent physical processes

The first problem was the inability of WST to match the observed solute release curve, which, in the case of the eroding media under study, reached a steady rate well above zero, as indicated by the experimental data points in Figure 6-5. The traditional method where accelerated solute dispersion is introduced within the surface zone, (to account for enhanced viscous dispersion due to rainfall impact), failed to shift the predicted curve to match the experiment. Whilst a greater total transfer was achieved, the predicted curve still exhibited an excessively rapid decay. Increasing the (equilibrium) sorption flattened the curve, but not nearly to the extent required.

Variations in surface process modeling were studied with WST. The transfer mechanism by which solute is transported from the material water to the surface water was explored. Traditionally a ‘film diffusion model’ is employed, where

net salt transfer rate = film diffusion coefficient x *concentration difference*

Considering the relatively small scale of any possible existing laminar boundary layer to the material surface geometry, the net infiltration, and the probable extension of the surface turbulence into the larger pores of the material, this law should rather be considered as an approximation to the viscous transfer of the solute. Furthermore, perfect mixing between the surface and soil waters at the boundary is a reasonable assumption. (For perfect mixing the film coefficient in this first order kinetic law is infinite.) However, even perfect mixing was unable to yield a good match to the solute release curve behavior.

Modeling of the surface hydraulics was also considered. Instead of assuming fast run off, surface discharge was faithfully represented by a non-zero surface water pond head and by employing traditional surface flow formulae. This variation did not affect the solute release curve significantly. The effect of saline run-on into the surface pond water was also studied. This variation was also found to have an insignificant effect on the curve.

At this stage the exclusion of an important process became apparent. Data from the PLPEWC laboratory erosion studies (C. Walker, G. Sheridan) shows a strong correlation between *sediment yield (erosion)*, *EC of fresh material* and *total solute released in the runoff water*. The implied process is that solute is trapped in surface aggregates or particles at the surface and is not immediately transportable. During an erosion process, these pieces of material relinquish their solute content to the runoff water. The incorporation of the erosion process, by the Lagrangian formulation of the transport equations and modified boundary transfer relationships, together with a solute retention mechanism, enabled the new model to finally simulate the experimental solute release curve (Figure 6-5). The appropriate computer program was denoted WST3Y.

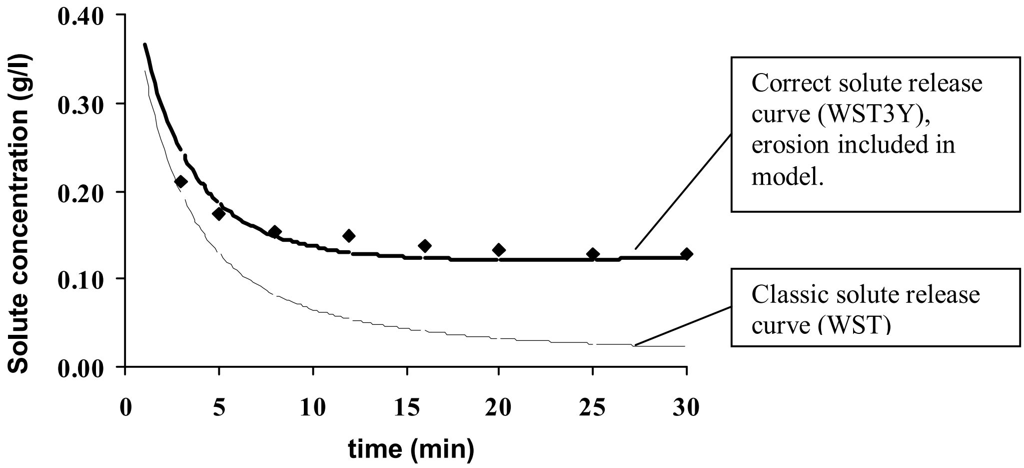

Figure 6-5 Solute release curves.

Solute concentration, in g/l of NaCl equivalent, in runoff water from tilted flume subject to nominal 100mm/h x 30 min event. The bed is fresh Curragh overburden. The points are measured data. The bottom faint curve is the classic rapid depletion exhibited by traditional fixed matrix models. The bold top curve is the model simulation that includes the erosion process.

Featured in the dimensionless model is the 'erosion effect number', E, which is a measure of the relative magnitude of rate of erosion to the hydraulic flow rates. The higher this number, the more important is erosion for the prediction of runoff water quality. A value of zero corresponds to the traditional fixed matrix model and small values are generally indicative of more sandy materials (or erosion resistant materials of course).

The way solute retention is modeled is of critical importance. Whilst equilibrium sorption enabled WST3Y to simulate the solute release curve, it failed as a satisfactory mechanism in two respects. Firstly, as solute retention is increased for the purpose of the release curve simulation, transport retardation is necessarily increased as well. That is, WST3Y would significantly underestimate the transport of the solute within the material. Secondly, there is no provision for any mechanism that can deliver a net migration of solute to the surface during a wetting and drying cycle, a phenomena that has been experimentally observed.

The problems were mostly overcome when the solute retention was modeled with a non-equilibrium mechanism. Although a mobile-immobile water model is most appropriate for interpretation of the actual process occurring in most of the overburdens, a three-parameter non-equilibrium sorption model was instead chosen for SALTRO. (Refer Appendix 2.) This model is advantageous by its less committed physical interpretation, and is better suited for simulating the effects of wetting-drying cycles.

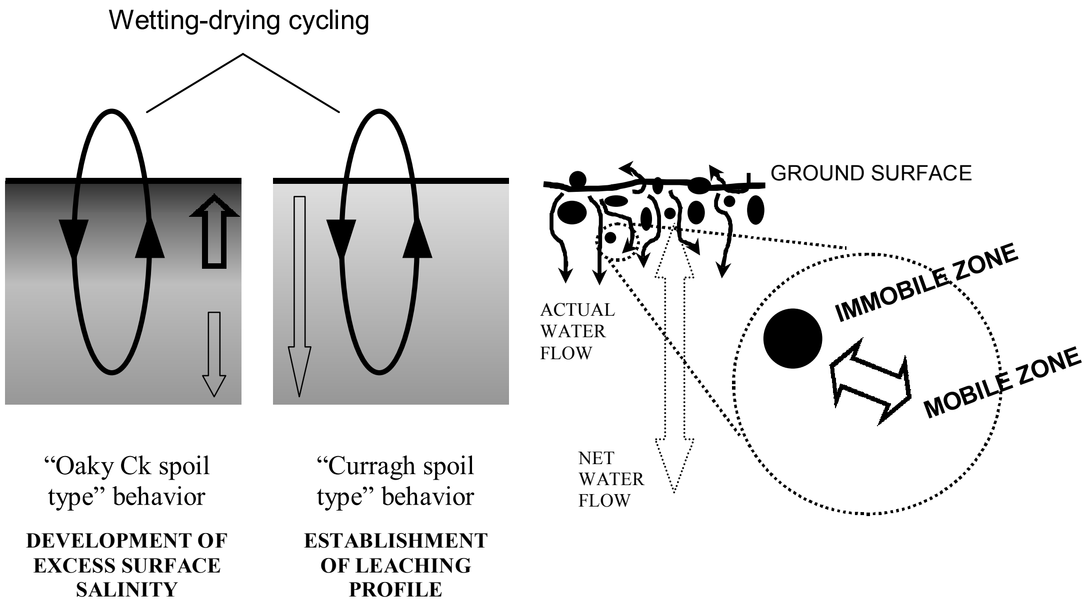

Figure 6-6 Pertinent solute transport processes

The hydrological behavior and the nature of the non-equilibrium exchange of solute between regions of varying mobility, are key factors in determining the susceptibility of the material to surface salinity.

The SALTRO solute transport model retains the traditional viscous solute dispersion. This provides the mechanism for solute release in the case of zero erosion. (Only this term allows for net upward flux of solute during infiltration.)

6.4.2.2 Parameter identifiability

In a model, the basic material parameters must be considered as independent meaningful properties of the material (site), if the model is to progress beyond a curve fitting exercise. It is desirable that these parameters ultimately be related to simple measured material properties and prescribed conditions. Hence the model becomes truly portable. Practically, parameter identifiability is synonymous with model usability. Mathematically, parameter identifiability corresponds with a dominant and distinct minimum of the objective function for model-data agreement in parameter space and the insensitivity of the optimal parameter vector to data perturbation.

The basic material parameter set of WST3Y was too large and redundancy among these parameters lead to very poor identifiability. Hence, this model was of little practical value for the purpose of comparing materials and applying it to new sites. The model formulation in SALTRO has largely overcome this problem with a reduced and expedient formulation.

It is only recently that optimization methods in the field of unsaturated hydrology have been developed. This work adopted the 'inverse modeling approach' (Kool, Parker, and van

Genuchten, 1987), extended the method for our purpose, and incorporated it into the calibration routine of SALTRO.

6.4.3 The SALTRO computer program.

By incorporating the research outcomes of this project component, the SALTRO program was developed to serve as a site water management planning aid and also as a valuable tool in rehabilitation planning in terms of surface salinity management.

As an end product, SALTRO takes the form of a program with a graphical user interface that runs on Windows95/98/NT (win32). It contains principle modules that:

i. simulate the water and solute transport and boundary cross-over (infiltration, evaporation, solute release) in real time for given parameters and climate schedule;

ii. derive the optimal basic material parameters from the calibration data, and ultimately;

iii. derive the model parameters by interpolation of other sets with easily measured material properties and site attributes.

All of the source code is in C/C++ (with Borland 5.0 OWL).

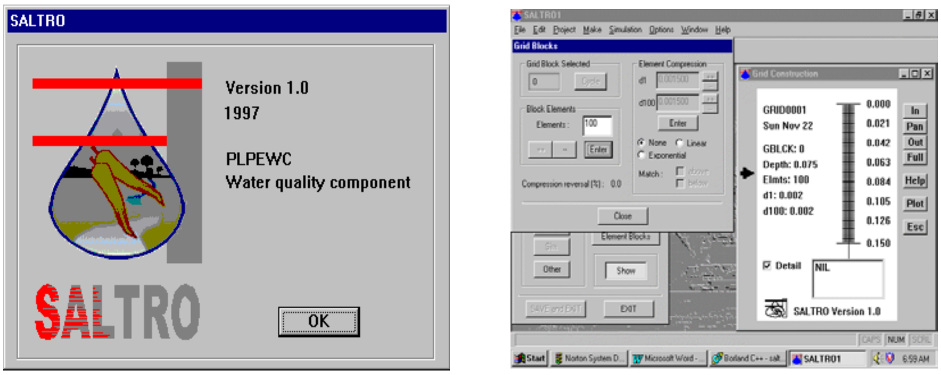

Figure 6-7 Elements of the SALTRO program

The program is compiled for win32. Its principle modules include all the necessary preprocessing tasks (run scheduling, parameter/input definition, grid construction), the solver engines, calibration routines, and custom graphical output presentation. Efforts are made to make this program as user friendly as possible.

6.5 Summary

The pertinent physics involved in the release of salt from an eroding surface material has been identified and a model, that both yields a satisfactory simulation and possesses an identifiable parameter set, has been developed.

It is expected that a working program of SALTRO and a limited library of material parameters will be available at the end of 1998 and will be provided to all the participating mines and ACARP. Due to the original aspect and fast track development of much of this research, there remains a little more work before a satisfactory product is attained that is fit for release and routine use.

Note: Work will continue beyond 1998, as funding permits, to complete a larger library of basic material parameters for all participating mines. Updates will be provided to all participating mines and ACARP, as results become available.

Acknowledgements

The support from ACARP, BHP Australia Coal Ltd, Callide Coalfields Pty Ltd, Capricorn Coal Management Pty Ltd, Curragh Qld Mining Ltd, MIM Holdings Ltd, and Pacific Coal Pty Ltd is gratefully acknowledged.

References

Kool, J.B., Parker, J.C., and van Genuchten, M.T. (1987). Parameter estimation for unsaturated flow and transport models – A review. *Journal of Hydrology*. 91: 255-293.

Wallach, R. and Shabtai, R. (1992). Modeling surface runoff contamination by soil chemicals under transient water infiltration. *Journal of Hydrology*. 132: 263-281.

7. Field Erosion Survey

A.Grabski[a], B. Kirsch[b], M. Short[a] and H.B. So[a]

[a]Research Officer, Post-graduate student and Associate Professor of Soil Physics, School of Land and Food & Center for Mined Land Rehabilitation, The University of Queensland, St Lucia, Q 4072

[b]Environmental Officer, Norwich Park Mine, Dysart, Qld. Previously Research Officer, The University of Queensland.

7.1 Aims

The objectives of the Field Erosion Survey (FES) was to characterize the severity of erosion within existing postmining rehabilitated landscapes, and to catalogue those features of the landscape which are considered to have a significant impact upon the erosion process. This survey is designed as a simple and robust methodology and an inexperienced environmental officer should be able to use it with relative ease. Data and soil samples have been collected by students on vacation work from eight minesites with a broad a range of alternative rehabilitation strategies, and this should allow the effectiveness of existing rehabilitation practices to be determined. Analysis of these samples is continuing at the University of Queensland (constrained by limited availability of funds) and results should be completed within the next few months and will be made available to all participating mines, as they become available.

7.2 Methods and Materials

Once landscapes have been successfully revegetated, erosion tends to be dominated by rills and gullies and accordingly the survey methodology tends to reflect this. The FES consists of 3 broad components:

1. **Classification of Erosion** according to Australian Soil and Land Survey Handbook.
2. **Field transects** to measure gully dimensions, ground cover and to collect soil samples.
3. Collection of **reclamation history** and long term **rainfall records.**

7.2.1 Classification of erosion

At each site the severity of the erosion was classified according to the following guidelines:

Ref: McDonald, R.C., Isbell, R.F., Speight, J.G., Walker, J., and Hopkins, M.S. (1990). "*Australian Soil and Land Survey - Field Handbook 2nd*" ed. pp92-95, Inkata Press, Melbourne.

7.2.1.1 State of Erosion

The erosion in the study area was categorized as:

A - Active

S - Stabilized

P - Partly stabilized

7.2.1.2 Sheet Erosion

This is the relatively uniform removal of the soil from an area without the development of conspicuous channels. Indicators of sheet erosion include soil deposits in downslope sediment traps (fence lines, farm dams), and pedestaling, root exposure or exposure of subsoils.

0 – ***None***: no sheet erosion

1 - ***Minor***: indicator may include shallow deposits in downslope sediment traps. Often difficult to asses as evidence may be lost with cultivation, pedoturbation (profile inversion by soil fauna), or revegetation.

2 - ***Moderate***: partial exposure of roots, moderate deposits in downslope sediment traps

3 - ***Severe***: loss of surface horizons, exposure of subsoil, pedestaling, root exposure, substantial soil deposits in downslope sediment traps.

7.2.1.3 Rill Erosion

A rill is a small channel up to 0.3m deep.

0 – ***None***: no rill erosion

1 - ***Minor***: occasional rills

2 – ***Moderate:*** common rills

3 – ***Severe:*** numerous rills forming corrugated ground surface

7.2.1.4 Gully Erosion

A gully is a channel more than 0.3m deep.

0 – ***None:*** no gully erosion

1 - ***Minor:*** gullies isolated linear, discontinuous, restricted to primary or minor drainage lines

2 - ***Moderate:*** gullies linear, continuous, and restricted to primary or minor drainage lines

3 - ***Severe:*** gullies are continuous or discontinuous, and either branch away from primary drainage lines and on to footslopes, or have multiple branches within primary drainage lines

7.2.1.5 Tunnel Erosion

Removal of subsoil by water while surface soil remains relatively intact.

0 – ***None****:* no tunnel erosion

1 – ***Present:*** tunnel erosion present

7.2.2 Field Transects

The selection of representative sites is critical to the success of the field erosion survey. Areas were selected that were isolated from external drainage and run-on effects, that is, they were contained within clearly defined catchments. For example if a particular slope was subjected to runoff from a road at its top end, then that slope was not suitable for the survey.

7.2.2.1 Gully Dimensions

Three 100m long transects were established across the study slope, at distances equivalent to 1/4, 1/2, and 3/4 of the slope length, from the bottom of the slope (Figure 7-1). The depth, width, and shape (Figure 7-2) of each gully **(>15cm deep)** encountered along each transect was recorded upon survey data sheet 1 *(see* Appendix). Total slope length and slope angle was also recorded. The total soil loss from the slope can be estimated from the total volume of gullies, assuming each transect represents a portion of the slope length.

We became aware that this aspect can be improved and in the future, transects will be selected at 1/6, 1/2 and 5/6 distance up the slope (each transect will represent 1/3 of the slope length). Where greater accuracy is required, a greater number of transects will be used. For more accurate estimation of soil loss, both rills and gullies will be recorded.

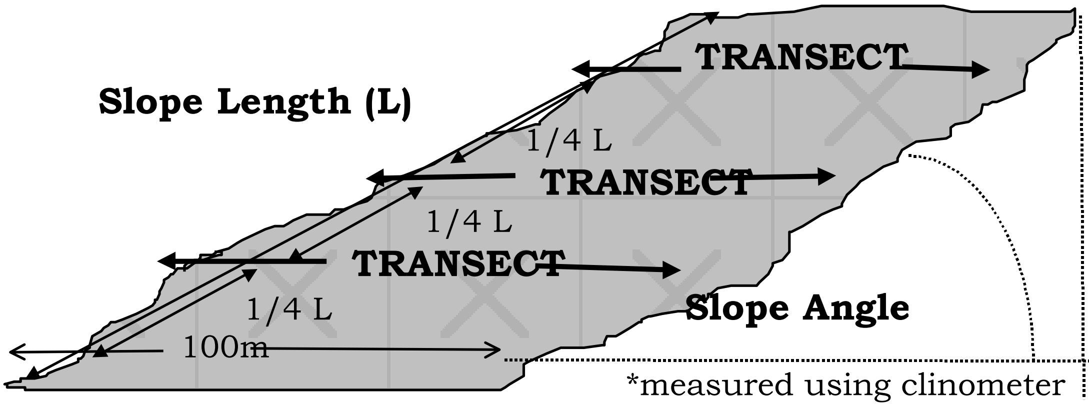

Figure 7-1 Field erosion survey transects for assessing the extent of gullying on rehabilitated slopes.

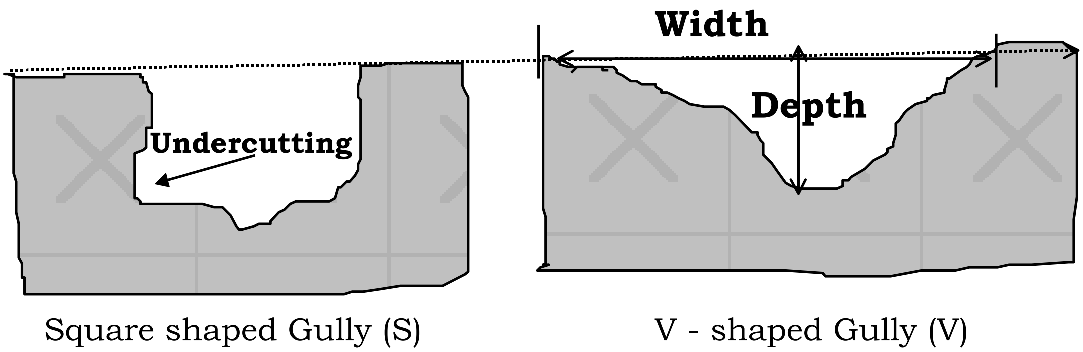

Figure 7-2 Guidelines for assessment of gully dimensions for the field erosion survey.

7.2.2.2 Ground Cover

Ground cover reduces the erosivity of rainfall by the interception of raindrops, and by protecting the surface from overland flow. Cover is therefore very important for controlling erosion. This survey only measured "total cover", which includes those aspects of the landscape which directly intersect with the soil surface, for example, low vegetation, litter, and rocks. **Observation on rocks should be done separately.**

Total cover was assessed visually within systematically sampled quadrats of 1m x 1m square, and was assigned a class according to the following specifications:

Class 1: 0-10% of soil covered	(Bare soil; very low cover)
Class 2: 10-25% of soil covered	(Low cover)
Class 3: 25-50% of soil covered	(Moderate cover)
Class 4: 50-75% of soil covered	(High cover)
Class 5: 75-100% of soil covered	(Very high cover eg heavy pasture)

To avoid problems associated with the subjectivity associated with multiple operators classifying cover independently of one another, a visual system of rated examples of total cover were used to "calibrate" field survey staff (Appendix 5). To further reduce the subjectivity of the cover estimations a single photograph was made of the ground surface within the quadrat area.

The gross form of the vegetation present at each site was visually assessed and recorded on the survey data sheet (Appendix 5). Figure 7-3 diagrammatically illustrates the layout of the areas used for cover assessment between the transect lines.

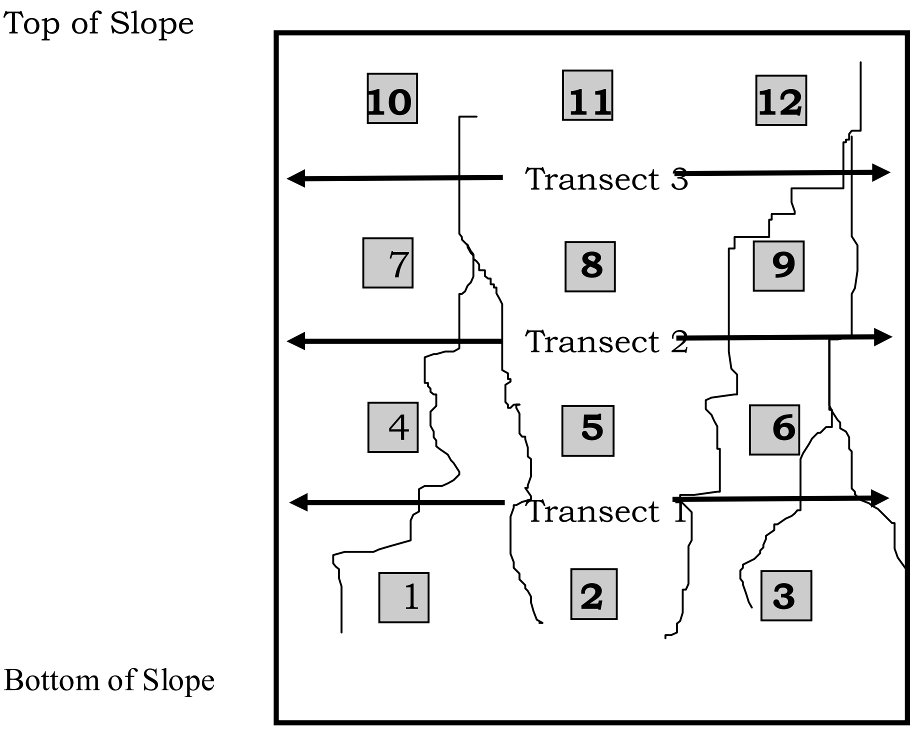

Figure 7-3 The layout of the areas used for cover assessment quadrats between the transect lines.

7.2.2.3 Collection of soil samples

A similar quantity of soil/spoil samples should be collected from each of 10 locations along each transect using a suitable tool (spade, auger etc). Where conditions along the transect are very variable, the samples should be bulked for sections that are similar. These samples are to be analyzed in the laboratory for properties that are relevant to the erosion process such as pH, EC, CEC, cations, organic carbon, soil texture, and dispersibility.

7.2.3 Reclamation History and Long Term Rainfall Records

7.2.3.1 Reclamation History

All available records of the reclamation strategies used at the site were transcribed onto data sheets, including:

- dates of reshaping, seeding, irrigation, formation of erosion control structure;
- spoil / soil replacement, and ripping strategies.

7.2.3.2 Rainfall Records

Any rainfall records (daily totals etc) kept at the site were collected by the survey participants to enable the potential "erosive history" of the site to be assessed.

7.3 Results and Discussion

The field erosion survey has been carried out at Blair Athol, Norwich Park, German Creek, Goonyella-Riverside, Peak Downs, Saraji, Blackwater and Moura. Initial results have been compiled, however analysis of the full data set will not be carried out until the remaining laboratory analyses are completed in the coming months.

7.4 Summary

The field erosion survey component of the project has developed a suitable methodology for the semi-quantitative and qualitative assessment of the success of postmining reclamation practices in terms of erosion stability. A total of eight minesites participated in the survey. Results from the complete dataset are yet to be analyzed. No conclusions can be drawn from this work at this stage, but it does appear that it will be suitable as a simple and rapid survey method to assess erosion stability as an indicator of a mine's performance in the rehabilitation of its postmining landscape.

References

McDonald, R.C., Isbell, R.F., Speight, J.G., Walker, J., and Hopkins, M.S. (1990). *Australian Soil and Land Survey Field Handbook.* 2nd ed. pp92-95, Inkata Press, Melbourne.

8. Catchment Evolution Model

Garry Willgoose

Associate Professor of Hydrology, Department of Civil, Surveying and Environmental Engineering & Center for Site Rehabilitation and Remediation, The University of Newcastle, Newcastle, NSW.

8.1 Aims

The aim of this component of the PLPEWC project was to develop a computer package for integrated erosion and hydrology assessment that could be used in conjunction with the mine design and management computer packages currently used by the industry. Originally, it was anticipated that the main package that the software would be integrated with was the ARGUS rehabilitation design tool developed by ACIRL, running only on Silicon Graphics computers. During the project this scope was expanded to include a range of other mine management packages, and it was decided to port the package to the WinTel platform.

Software for meeting these objectives already existed within the group at The University of Newcastle and had been demonstrated at the Ranger Uranium Mine. The main difficulty with it was that these pieces of software were (1) not integrated together so that they were difficult to use, (2) somewhat immature so they could not be used by non experts without considerable caution and (3) did not include software for interfacing with mine management packages. To meet this objective a number of intermediate objectives for the project were identified:

- An easy to use interface that could be used by a non-expert needed to be developed that integrated the existing pieces of software and other pieces of software that were needed to interface to existing mine management packages were developed.
- Extra capabilities had to be added to the existing software to address rehabilitation design issues that were specific to the surface mining coal industry.
- An easy to access environmental database specific to the Queensland coal mines needed to be developed from data collected in other parts of the project.

8.2 Introduction

At the beginning of the project ACIRL was completing development of their ARGUS rehabilitation design package which they were using in-house as well as attempting to commercialize. It was recognized that an environmental assessment package would substantially enhance the capabilities of this package. At that stage all rehabilitation tools were based on road design packages and used cross sections along a line to simulate landforms. ARGUS departed from this approach by adopting a digital terrain map that bypassed the limitations of road cross-section type approach.

Around the same time workers at The University of Newcastle were demonstrating the capabilities for mine site rehabilitation of the then new digital terrain map based hydrology and erosion models that had been developed, models called DISTFW and SIBERIA respectively. Their work demonstrated the applicability of models based on digital terrain maps but also highlighted that a major stumbling block to routine applications of these tools was in their lack of integration into a single tool and their lack of a friendly user interface.

One further advantage of the SIBERIA model was the ease with which the hydrology and erosion analysis could be automated using it. This arose from SIBERIA being a landscape evolution model, which simulated the evolution of landforms over time under the action of runoff and erosion. Because the landform evolves over time and SIBERIA needs to analyze the runoff and erosion over time, the development of SIBERIA had entailed the development of fast automated means of landform analysis, eliminating the manual drawing of catchment boundaries, drainage paths etc required in traditional hydrology and erosion analyses.

Finally, SIBERIA was able to simulate the cumulative effect of erosion over a range of design time-scales ranging from 1 year to 1000 years. For instance, it has recently been demonstrated in a separate project that SIBERIA can effectively model gully development on two mine waste dump in the Northern Territory over time-scales from 1 year to 40 years.

This project aimed to tightly integrate these capabilities into a single user package. It also aimed to target this tool at environmental officers, mine planners and other personnel involved in the mine planning process and so integrate rehabilitation design and environmental assessment into mine planning from the very earliest stages. It is believed that this would result in substantial cost savings to the industry.

8.3 Results and Discussion

8.3.1 The Environmental Assessment and Modeling System (EAMS) Package

The EAMS package was developed by integrating a number of existing packages that had been developed at The University of Newcastle with a graphical user interface. The key capability of these packages that made them unique and suitable for this project was that they used digital terrain maps (DTMs), the basis of all modern mine management packages and mapping systems. This use of DTMs was the key aspect that allowed them to be integrated with the mine management packages. The existing packages were:

- **SIBERIA**: A grid DTM based long-term erosion model.
- **DISTFW**: A grid DTM based hydrology model.
- **DISCRETE**: Conversion from irregularly spaced elevation DTM to a grid DTM.

These packages were extended to facilitate their integration and a variety of other packages were developed as part of the project including:

- **CONVERT**: Conversion from DXF AutoCAD file format and automated identification of contour banks

The interface involved the development of software for the GUI including menus, dialogs, etc, system calls to trigger the running the individual pieces of software and code required to provide the glue between the various components of the package.

Since the project originally envisioned that the package would be integrated with ACIRL's ARGUS package (which only ran on SGI UNIX workstations) the software was developed using MOTIF, a widely used UNIX GUI development environment. At a late stage of the project it was decided to port the application to the WinTel environment. Since MOTIF is not supported under Windows this necessitated a complete rewrite of the package from the ground up. It was decided to use the newly developed open GL/GLUT environment for this port as they had close similarities to MOTIF and provided operating system independence for the software. This work was done late in the project and allowed us to substantially modify the interface to address some usability concerns we had developed during the testing of the original MOTIF interface.

As part of the porting to the Windows environment the opportunity was taken to port from the Macintosh a suite of codes optimized for visualization and manipulation of digital terrain maps. This program was necessary because the original plan used ARGUS for visualization of the simulation results, which was not possible for Windows because ARGUS did not run in this environment. This package combined a variety of existing programs with new capabilities of specific use for mine site assessment into a package called EAMS-Viewer.

In total, including the viewer package, this part of the project has involved the writing of about 24,000 lines of Fortran and C code.

EAMS can output peak discharges, mean erosion and deposition depth, sediment yield, the spatial pattern of the erosion, deposition and yield, risk of gully erosion, and the predicted long-term change in the shape of the landform as a result of erosion and deposition. The design process using EAMS is outlined in Figure 8-1.

The novel aspects of the EAMS are:

- Its ability to predict the spatial pattern of the process interactively. This interior detail allows modification of the rehabilitation design to remove localized problem areas. This is a significant advance over traditional sub-catchment based erosion models which can only provide catchment average soil/spoil loss and ignore local effects.
- The use of DTMs eliminates the laborious process of manually defining catchment boundaries, one of the main stumbling blocks to more widespread use of existing erosion models.
- Automatic hydrology and erosion analysis of landforms with contour banks (Gyasi-Agyei and Willgoose, 1996).
- An environment assessment on a particular design can be carried out in several minutes and the interface is simple enough to be used by a non-expert.

Figure 8-2 shows an example output from EAMS.

8.3.2 Erosion/Hydrology Database

As part of the EAMS package, an easy to access hydrology and erosion database needed to be developed. The hydrology and erosion data used in this component of the work was the rainfall simulator data collected at each of the mine sites, the natural rainfall data collected from the plots installed at Curragh, Oaky Creek and Goonyella, and the field plots installed at these three mines.

The analysis of the hydrology data was carried out with the DISTFW DTM based hydrology model. This model was integrated with the NLFIT nonlinear parameter estimation package, which allowed a) estimation of the model parameters, their reliability and the reliability of model predictions, b) statistical testing of the significance of interplot variability of the hydrology and erosion parameters at any given mine site, c) statistical testing of the effect of vegetation and time effects on hydrology and erosion parameters, d) statistical testing of the spatial variation of hydrology and erosion parameters from mine site to mine site and e) statistical testing of the effect of the different data collection strategies (i.e. rainfall simulator versus plots). The results from this work are discussed below.

The parameter estimation process for EAMS is a four-stage process, which is outlined in Figure 8-3. The four stages are:

1. Calibration of the DISTFW rainfall-runoff model.

2. Calibration of the erosion event model.
3. From the calibrated rainfall-runoff model, determination of the peak discharge-area relationship.
4. From the calibrated rainfall-runoff model, the erosion event model and a rainfall record simulation of a long-term erosion record and from that the mean annual erosion rate.

Due to the drought in the early stages of the project it was some time before any data was available for the plots and catchments at the 3 detailed study mine sites. Accordingly, to keep the project on track, much greater use has been made of the rainfall simulator results than originally anticipated. The detailed sites have been used to check that the simulator data is not biased in some form or other.

8.3.3 Bowen Basin Rainfall Analysis

The pluviograph records for a number of sites in the Bowen Basin were examined to see if there was any effect on erosion rates from changes in the rainfall characteristics across the Bowen Basin (Gyasi-Agyei and Willgoose, 1998b). The pluviograph records across the Bowen Basin are quite short and the records did have a sufficient common period to allow a direct comparison of records. The alternative approach adopted was to calibrate a rainfall model to the data and compare the parameters of the model. While this approach does not completely address potential difference in the rainfall record due to differing length records, the parameters of the model adopted (Gyasi-Agyei and Willgoose, 1997, 1998a) do to a large extent reflect the underlying statistical characteristics of the rainfall extremes rather than the year by year variability.

The result of this analysis confirmed that there was little systematic variation of rainfall extremes across the Basin and that it was satisfactory in Step 4 of the calibration outlined above to use the best record available in the Basin, which was the QDNR records measured at Emerald.

8.3.4 The Effect of Vegetation on Hydrology and Erosion

Figure 8-4 shows the effect of vegetation on a number of the hydrology parameters at the Curragh mine. The increase in roughness that comes from vegetation is clearly shown in Figure 8-4a where the kinematic wave speed parameter decreases with time. This figure suggests that the roughness increases by about a factor of 10 from unvegetated to 100% vegetated. For the infiltration parameters the results are less clear cut. There appears to be no significant effect on the initial loss by vegetation (Figure 8-4b). The continuing loss, however, increased from 0.5 mm/hr for 0% vegetation to 30mm/hour for 100% vegetation (Figure 8-4c). Careful comparison of these results with the bare plots at 20% slope confirm that these results do not appear to be as a result of changes in the spoils since the bare plots did not change over the period 1994-1997. There appears to be no relationship between these results and slope suggesting that these results are independent of slope.

8.3.5 Variability of the Hydrology of Soils and Spoils

A key component in the statistical testing of the variability of the hydrology of the soils and spoil is the use of compatibility plots. These plots indicate the region in the parameter space that the parameters will lie in with a given probability, given the data that the parameter estimation was carried out on. An example will demonstrate the usefulness of this technique.

Figure 8-5 shows the three hydrographs from the three rainfall simulator trials at German Creek for the rainfall simulator trials on spoil (Gyasi-Agyei, *et al.*, 1995f). Figure 8-6a shows the corresponding compatibility plot for two of the infiltration parameters for the three simulator trials, roughly corresponding to the initial (y axis) and continuing losses (x axis). The ellipses indicate the region that the parameters lie within with 95% probability (i.e. there is 5% chance they lie outside the ellipse). Since the ellipses for plots 1 and 2 overlap, the region of overlap indicates a range of values that the parameters lie within with 5% chance of error. Likewise, there is overlap between Plots 1 and 3. Thus we can say with 5% chance of error that the infiltration parameters for Plots 1 and 2 are not significantly different and the parameters for Plots 1 and 3 are not significantly different. However, because the ellipses for Plots 2 and 3 do not overlap, so there are no parameters that satisfy both Plots 2 and 3, we can say that the infiltration parameters for Plots 2 and 3 are statistically significantly different. This analysis quantifies the observation in Figure 8-5 that there are differences between the measured hydrograph, but it is not clear how important they are.

Finally Figure 8-6b shows the compatibility regions for spoil and topsoil for the site. These ellipses take into account the variability between each plot and parameterize the range of the parameters that might be expected for the German Creek site. What this plot shows is that for German Creek there is a significant difference between the spoil and topsoil infiltration properties because there is no overlap between the ellipses. The fact that the difference is mostly in the vertical direction indicates that the difference is due to the initial loss (the y-axis) changing between the two materials. It also shows that the continuing loss may vary from 0 to 4.5 mm/hour and the sorptivity (initial loss) from 0 to about 13.5 mm/hour$^{0.5}$.

8.3.6 Site Specific Variability

The characterization of the site-specific variability of hydrology properties has been carried out with the compatability analyses for each of the mine sites. The rainfall simulator data that was collected by DNR for each of the mine sites for the unvegetated condition was used to carry this out. The details of this work are reported in Arkinstal, *et al.*, (1994a-c) and Gyasi-Agyei, *et al.*, (1995a-h, 1996a-c). A summary discussion was presented in Willgoose, *et al.*, (1996).

The general conclusions are:

- There is little difference between plots in the routing of water (the speed at which water runs off). This is consistent with them all being smoothed before testing.
- The interplot variability of infiltration losses is less for soils than for spoils. That is, soils tend to be more uniform than spoils.
- Spoils tend to display pockets of atypical material. If these atypical materials are excluded from analysis then spoils show less variability than soils. This suggests that there is more likelihood of localized unpredictable behavior in spoils than in soils. The cause of these pockets of atypical material is not known but the parameters are consistent with variations in compaction.
- Initial losses are typically less for spoils compared with soils, by up to 50%, and the initial loss for the spoils and soils are typically significantly different.
- There is no obvious trend for continuing loss.

8.3.7 Bowen Basin Variability

A detailed discussion of the variability of the Bowen soils and spoils is provided in Gyasi-Agyei and Willgoose (1997a). Figures 8-7 and 8-8 shows the compatibility plots for the runoff routing and infiltration parameters for all the rainfall simulator test sites the Bowen Basin spoils and soils.

It has not been possible to relate these results to material properties because of the variability of the spoils and an inability to reconcile data provided by QDNR and UQ with the exact sites tested by the simulator. As already discussed, there is considerable, and sometimes statistically significant, variation in hydrology and erosion parameters from plot to plot even on one mine site so it not surprising that reliable regressions between material properties and hydrology and erosion properties have been difficult to obtain when it is not possible to guarantee the exact location of material samples.

The general conclusions from these analyses are that:

- The runoff routing properties for all of the mines and all soils and spoils are the same. As mentioned in the previous section this is consistent with all of the plots being constructed by the same method, having the same surface roughness and the same degree of rilling.
- For the infiltration parameters of the topsoils there is considerable scatter in the parameters. There are only a few results that appear to be clustered together. Three clusters can be identified, namely, (1) Oaky Creek and Peak Downs with low initial loss, (2) Newlands and Saraji with medium initial loss and (3) Curragh, Gregory and Moura with high losses. It is unclear what, if any significance this clustering has and what it is related to.
- The infiltration parameters of the spoils for almost all the mines are clustered around a region that has low continuing loss and medium initial loss. The outriders, with very much higher infiltration are Blackwater (with high continuing loss) and Goonyella (with high initial loss).

8.3.8 Variability of Spoil and Soil Erodibility

As part of the EAMS database development the last step is to determine the SIBERIA erodibility for use within EAMS. While the erodibility cannot be directly compared with that derived from USLE, the relative effects should be about the same (i.e. the ratio of erodibility at two mines should be about the same). Also because the calibration process for the erosion model does not use NLFIT, we are unable to calculate compatibility regions so we are unable to make comments about the statistical significance of the differences between the erodibilities. The erodibilities for EAMS are included in the database of the EAMS software and we do not present them here. We will only highlight some of the more notable results. The erodibilities in the discussion below are the aggregate result of the intrinsic soil/spoil erodibility for a given discharge and differences due to differences in the runoff properties. Some conclusions are:

- For the soils, the erodibility results vary from a low of 0.000034 (Blackwater) to a high of 0.0007 (German Creek) and 0.002 (Norwich Park). More typically, however, most results are in the range of 0.0001 to 0.0003. The Blackwater result is due to the high infiltration capacity of the soil so that runoff is small. The Norwich Park result is due to high soil erodibility and runoff, while the German Creek result follows from a combination of a moderately high runoff and erodibility.

- For the spoils, the erodibility results vary from a low of 0.000039 (Norwich Park) to a high of 0.00095 (Saraji). In comparison with the soils, the spread of the results is much more uniform from low to high. The low results arise from spoils that have high infiltration and thus low runoff rather than from spoils with an intrinsically low erodibility.

These results are incorporated into the Version 1 database as part of the EAMS software (Gyasi-Agyei and Willgoose, 1997a). A variety of other issues to do with the parameterization of the erosion process, which we have found to be important in other projects, will be addressed in later versions of the database as time permits. Generally speaking, however, the Version 1 database is likely to be conservative with predicted erosion rates being higher than what will actually occur. Later versions of the database will address some of the conservative assumptions made in its derivation.

8.3.9 Comparison between the Rainfall Simulator and the Installed Plots

Final analyses for the results of this part of the work are not yet complete but preliminary work with the Curragh data with the compatibility plots suggest that the results obtained from the rainfall simulator trials and the Curragh plots for different slope are not significantly different for the 0% vegetation cover case.

Note : The EAMS software is complete and will be distributed once the IP agreement are signed between ACARP, The University of Queensland and the University of Newcastle, as per agreement at the February 1998 steering committee meeting.

References

Arkinstal M, Willgoose G R, Loch R and Pocknee C. (1994a). Calibration of DISTFW parameters for the QDPI rainfall simulator for Tarong, Research Report 095.04.1994, Department of Civil Engineering and Surveying, The University of Newcastle, Australia, Callaghan.

Arkinstal M, Willgoose G R, Loch R and Pocknee C. (1994b). Calibration of DISTFW parameters for the QDPI rainfall simulator for Wandoan, Research Report 094.04.1994, Department of Civil Engineering and Surveying, The University of Newcastle, Australia, Callaghan.

Arkinstal M, Willgoose G R, Loch R and Pocknee C. (1994c). Calibration of DISTFW parameters for the QDPI rainfall simulator for Oaky Creek, Research Report 093.04.1994, Department of Civil Engineering and Surveying, The University of Newcastle, Australia, Callaghan.

Gyasi-Agyei Y and Willgoose G R. (1995a). "Prediction of the evolution of post-mining landforms due to erosion", Annales Geophysicae Supplement II, 13, Hamburg, May, 1995, p C454.

Gyasi-Agyei Y and Willgoose G R. (1997a). Calibration of SIBERIA parameters for 15 mine sites using runoff and erosion data obtained from the QDPI rainfall simulator, Research Report 146.05.1997, Department of Civil, Surveying and Environmental Engineering, The University of Newcastle, Callaghan, NSW.

Gyasi-Agyei Y and Willgoose G R. (1997b). "A hybrid model for point rainfall modelling", Water Resources Research, 33(7), pp 1699-1706.

Gyasi-Agyei Y and Willgoose G R. (1998a). "Generalisation of a hybrid model for point processes: Rainfall example", Water Resources Research, in press.

Gyasi-Agyei Y and Willgoose G R. (1998b). Point rainfall modelling within Central Queensland, Research Report, Department of Civil, Surveying and Environmental Engineering, The University of Newcastle, Australia, Callaghan, in preparation.

Gyasi-Agyei Y and Willgoose G. R. (1996). "Evaluation of the use of contour banks as post-mining rehabilitation control option using a digital terrain based rainfall-runoff-erosion models", Holzmann H and Nachtnebel H P (Ed), Application of Geographic Information Systems in Hydrology and Water Resources Management, HydroGIS '96, Vienna, Austria, 16-19 April, 1996, pp 143-150.

Gyasi-Agyei Y, Willgoose G R, Pocknee C and Loch R. (1995b). Calibration of the DISTFW parameters for the QDPI simulator, Blackwater Mine, Research Report 124.11.1995, Department of Civil, Surveying and Environmental Engineering, The University of Newcastle, Australia, Callaghan.

Gyasi-Agyei Y, Willgoose G R, Pocknee C and Loch R. (1995c). Calibration of the DISTFW parameters for the QDPI simulator, Blair Athol Mine, Research Report 123.11.1995, Department of Civil, Surveying and Environmental Engineering, The University of Newcastle, Australia, Callaghan.

Gyasi-Agyei Y, Willgoose G R, Pocknee C and Loch R. (1995d). Calibration of the DISTFW parameters for the QDPI simulator, Callide Mine, Research Report 122.11.1995, Department of Civil, Surveying and Environmental Engineering, The University of Newcastle, Australia, Callaghan.

Gyasi-Agyei Y, Willgoose G R, Pocknee C and Loch R. (1995e). Calibration of the DISTFW parameters for the QDPI simulator, Curragh Mine, Research Report 121.11.1995, Department of Civil, Surveying and Environmental Engineering, The University of Newcastle, Australia, Callaghan.

Gyasi-Agyei Y, Willgoose G R, Pocknee C and Loch R. (1995f). Calibration of the DISTFW parameters for the QDPI simulator, German Creek Mine, Research Report 120.11.1995, Department of Civil, Surveying and Environmental Engineering, The University of Newcastle, Australia, Callaghan.

Gyasi-Agyei Y, Willgoose G R, Pocknee C and Loch R. (1995g). Calibration of the DISTFW parameters for the QDPI simulator, Gregory Mine, Research Report 119.11.1995, Department of Civil, Surveying and Environmental Engineering, The University of Newcastle, Australia, Callaghan.

Gyasi-Agyei Y, Willgoose G R, Pocknee C and Loch R. (1995h). Calibration of the DISTFW parameters for the QDPI simulator, Moura Mine, Research Report 118.11.1995, Department of Civil, Surveying and Environmental Engineering, The University of Newcastle, Australia, Callaghan.

Gyasi-Agyei Y, Willgoose G R, Pocknee C and Loch R. (1996a). Calibration of the DISTFW parameters for the QDPI simulator, Goonyella Mine, Research Report, Department of Civil, Surveying and Environmental Engineering, The University of Newcastle, Australia, Callaghan.

Gyasi-Agyei Y, Willgoose G R, Pocknee C and Loch R. (1996b). Calibration of the DISTFW parameters for the QDPI simulator, Peak Downs Mine, Research Report, Department of Civil, Surveying and Environmental Engineering, The University of Newcastle, Australia, Callaghan.

Gyasi-Agyei Y, Willgoose G R, Pocknee C and Loch R. (1996c). Calibration of the DISTFW parameters for the QDPI simulator, Saraji Mine, Research Report, Department of Civil, Surveying and Environmental Engineering, The University of Newcastle, Australia, Callaghan.

Willgoose G R and Gyasi-Agyei Y. (1995). "New technology in hydrology and erosion modeling for mine rehabilitation", APCOM XXV Application of Computers and Operations Research in the Mineral Industries, Brisbane, 10-12 July

Willgoose G R, Gyasi-Agyei Y, Loch R and So B. (1996). "Plot hydrology and erosion experimental data: Scaling issues, land and mine rehabilitation", Water and the Environment, 23rd IEAust Hydrology Conference, Hobart, 21-24 May, 1996, pp 97-102.

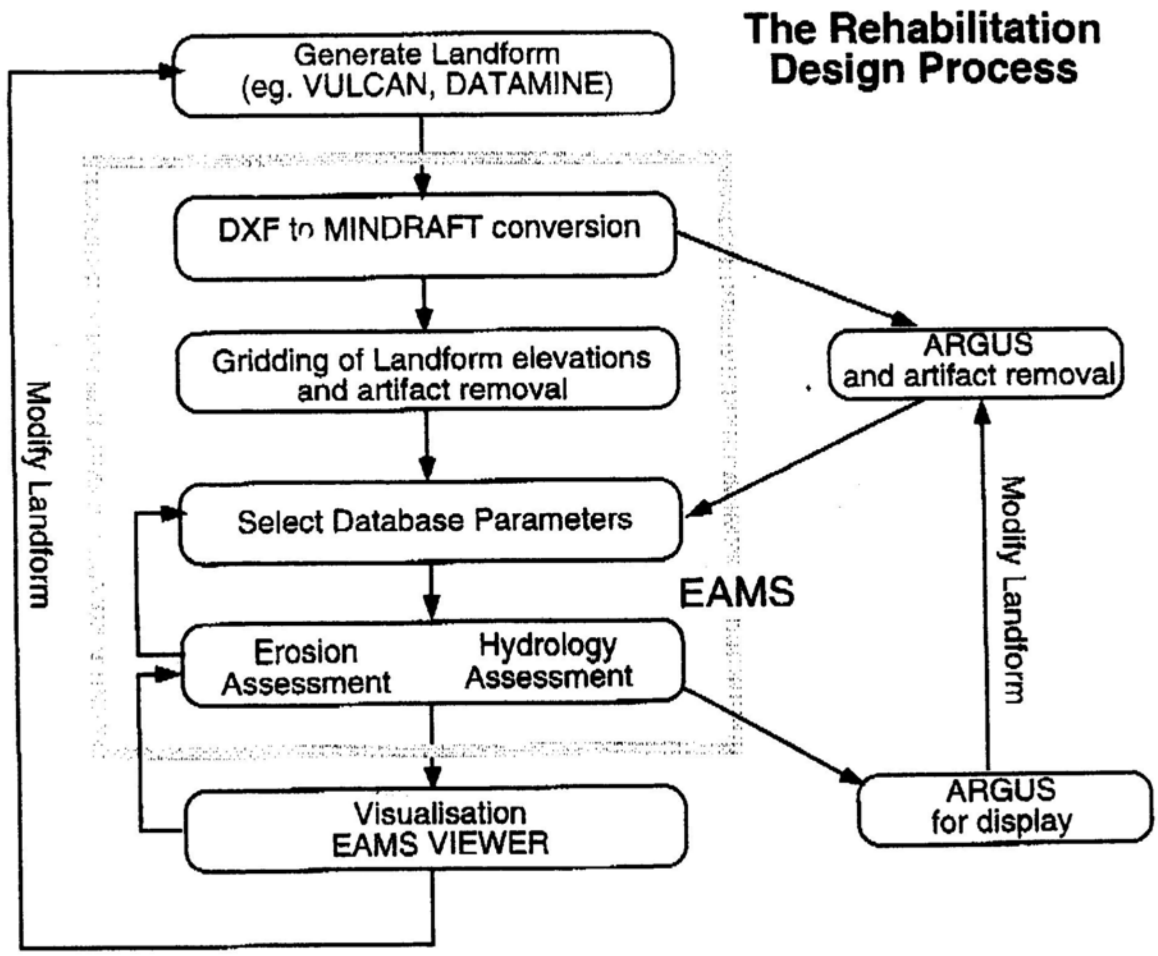

Figure 8-1: The computer aided design process based on EAMS indicating the iterative process of design, assessment, visualisation and design modification. Heuristics based on USLE and vegetation analysis feed into the design process in a separate loop.

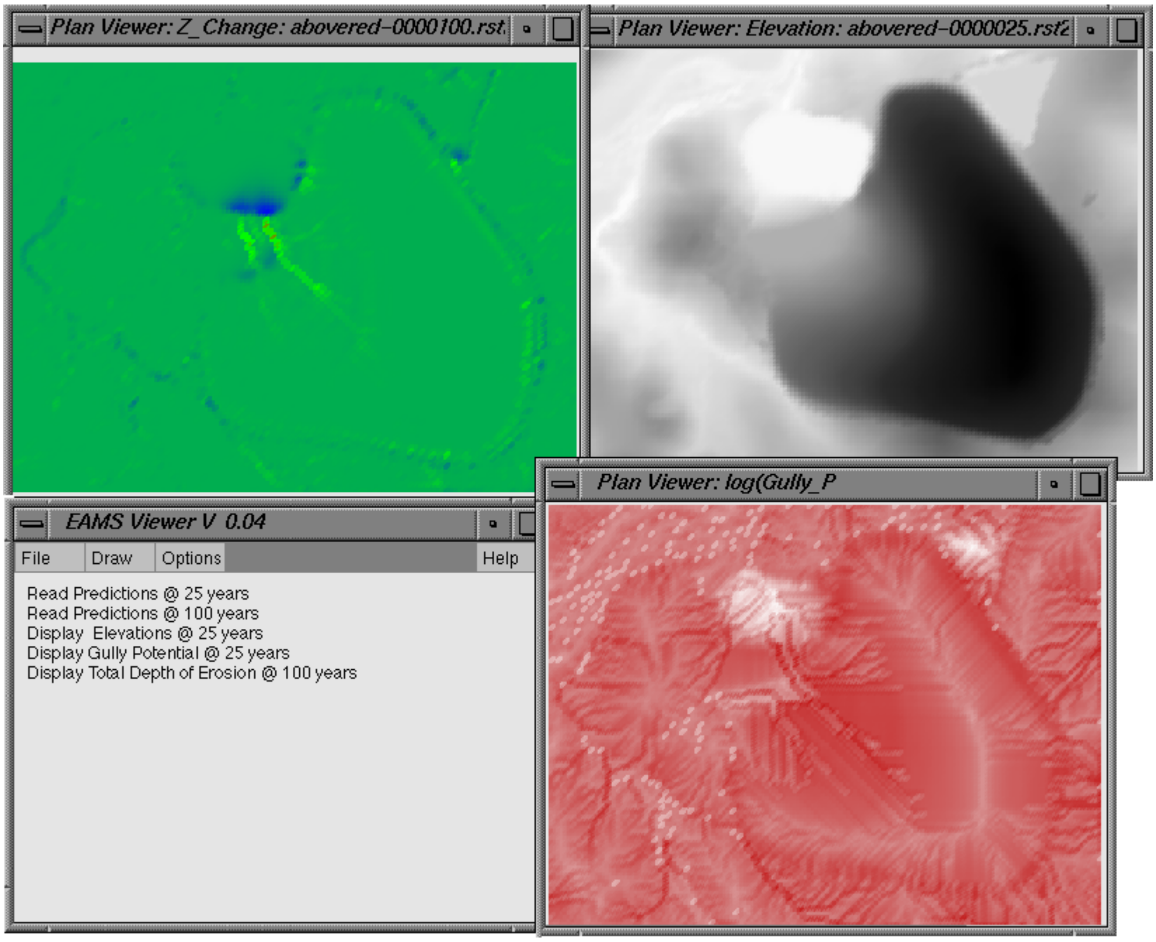

Figure 8-2: EAMS output for the 1000 year predictions for the above-grade proposal at Ranger Uranium Mine displayed in ARGUS (a) elevations increasing with increasing darkness (b) slope increasing with increasing darkness and (c) erosion and deposition depths, white indicates no erosion or deposition with increasing darkness for increasing erosion or deposition. Computer display is in colour, black and white is used here for reproduction.

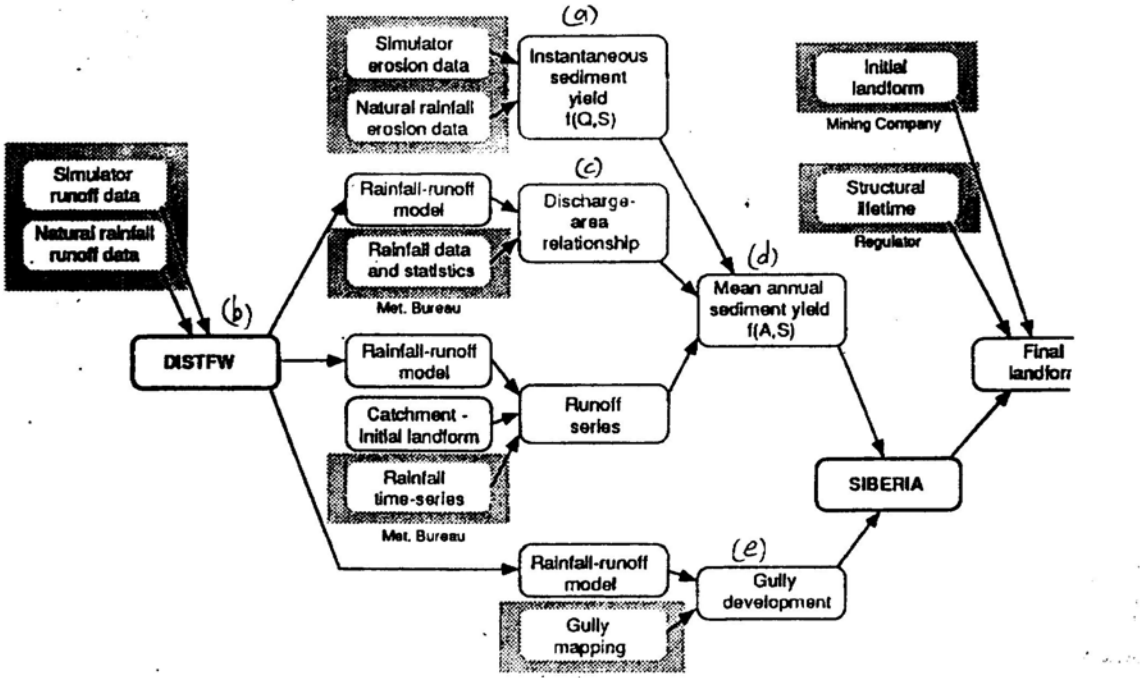

Figure 8-3: The EAMS calibration process indicating the central importance of the simulator and natural rainfall plots to the calibration of the (a) event erosion model (b) hydrology model, (c) the peak discharge-area curve and (d) the mean annual erosion rate. The figure also indicates the possibility of gully prediction in (e) but the type of data for calibration of this model has not been collected in this project.

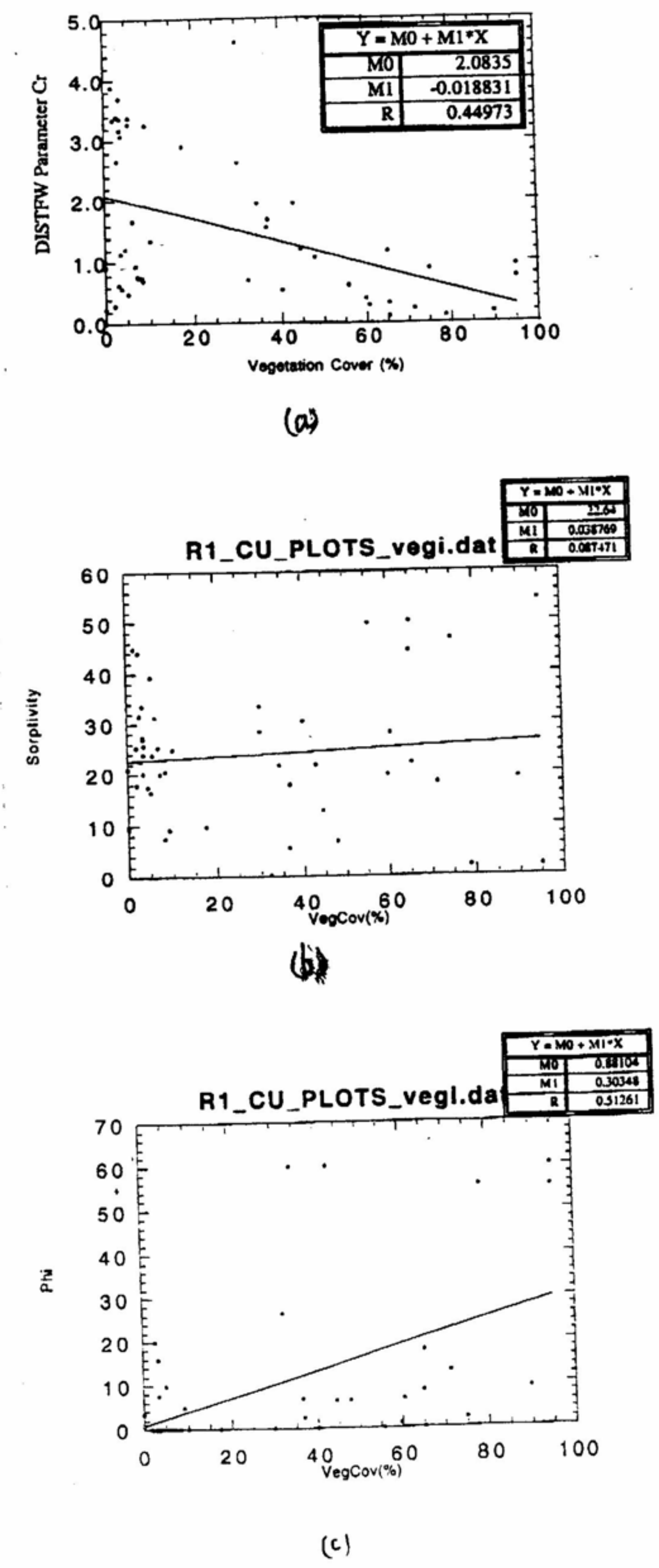

Figure 8-4: The effect of vegetation on the parameters of the hydrology model as determined from the natural rainfall plots at Curragh using the data from all plots from 10% to 30%. (a) Kinematic wave coefficient (roughly inversely proportional to surface roughness) versus vegetation, (b) Initial loss parameter versus vegetation, and (c) continuing loss parameter versus vegetation.

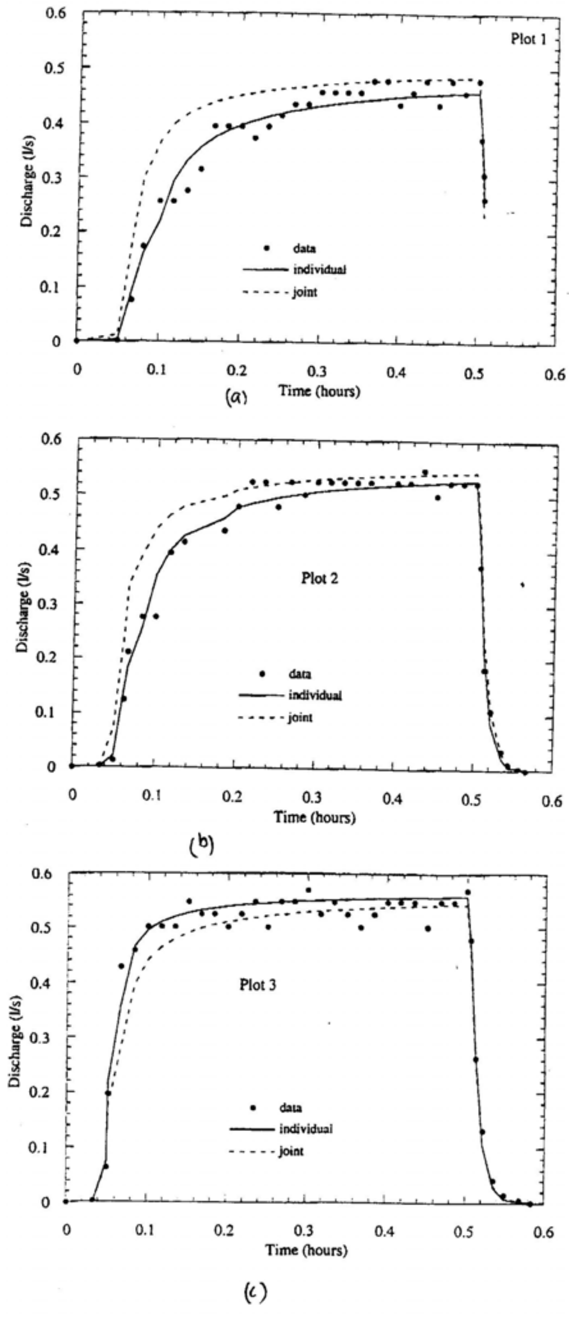

Figure 8-5: Fitted hydrographs with the hydrology model for the 1994 rainfall simulator trials at German Creek on the spoil for the 3 plot replicates (a), (b) an (c). The solid lines are the best fit hydrograph for each hydrograph individually and correspond to the confidence limits in Figure 6a. The dotted lines are the best fit when the hydrology parameters are constrained to be the same for all three of the plots, and correspond to the confidence limits in Figure 6b.

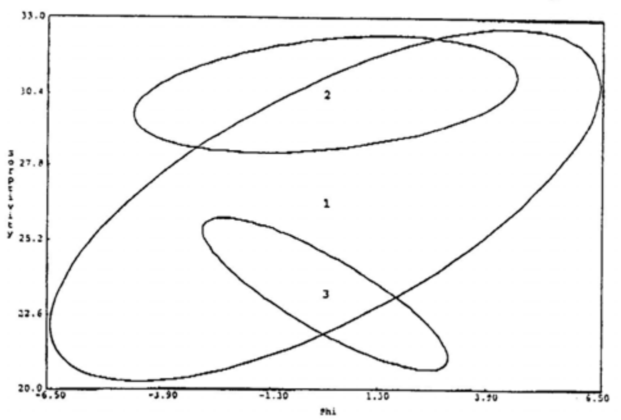

(a)

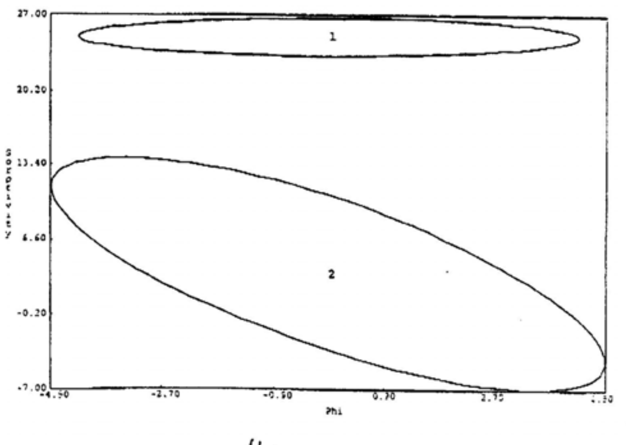

(b)

Figure 8-6: The 95% confidence limits for the infiltration parameters for the plot data displayed in Figure 5 for German Creek. (a) the confidence limits when each of the plots is fitted independently, the best fit parameter set is at the centre of the ellipse, the numbers correspond to the plot numbers in Figure 5, (b) the confidence limits for the three plots when the parameters are constrained to be the same for all three of the plots, 2 corresponds to the German Creek soil data, and 1 corresponds to the German Creek spoil data and corresponds to the data in plot (a).

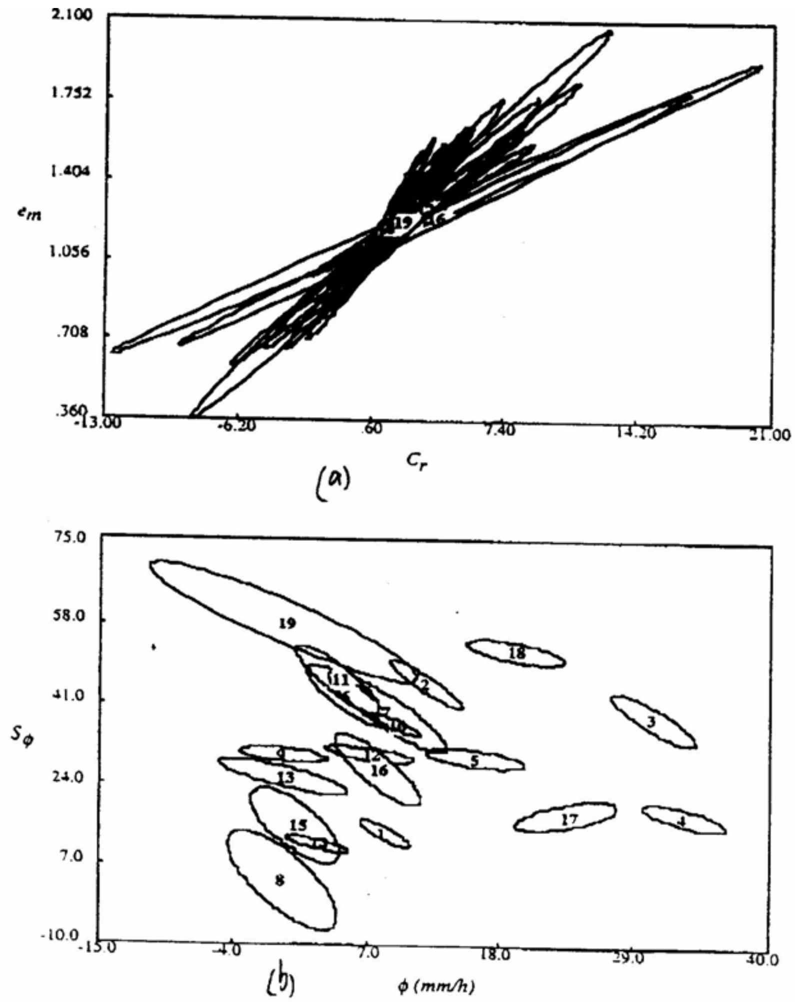

Figure 8-7: The 95% confidence limits for the (a) kinematic wave routing parameters and (b) the infiltration parameters for all of the rainfall simulator data collected for top soils in the Project.

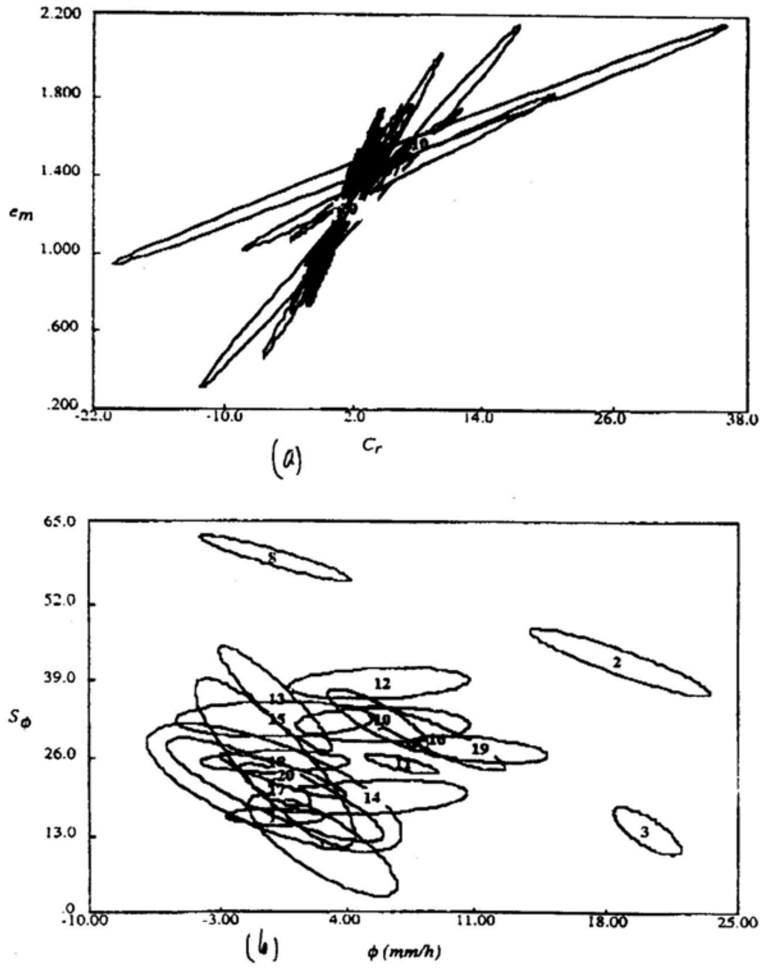

Figure 8-8: The 95% confidence limits for the (a) kinematic wave routing parameters and (b) the infiltration parameters for all of the rainfall simulator data collected for spoils in the Project.

APPENDIX 1: MUSLE K-factor calculation - Field Rainfall Simulation Data

MINE	MATERIAL	plot no	Rain Intensity (mm/h)	Duration (min)	EI 30 (metric)	LS	CP	Q (mm)	q (peak) (mm/h)	Soil loss (t/ha)	K (metric)	K (avg metric)
BW	SPOIL	4	118.8	30	212.3	1.04	0.61	37.2	88.1	5.8	0.06	0.09
		3	118.8	30	212.3	1.02	0.61	34.0	74.2	11.5	0.12	
BW	SOIL	1	118.8	30	212.3	1.05	0.41	30.2	87.8	14.7	0.23	0.22
		2	118.8	30	212.3	0.96	0.41	31.1	83.9	12.9	0.22	
	(TW)	5	118.8	30	212.3	1	0.41	34.8	93.1	33.6	0.51	0.47
	(TW)	6	118.8	29	205.3	0.996	0.41	34.7	100.3	27.4	0.43	
BW	M/S SPOIL (RAW)	7	119.1	30	213.4	1.49	0.41	45.4	102.0	41.7	0.38	0.38
	(TW)	8	118.8	30	212.3	1.43	0.41	42.8	96.9	41.4	0.41	0.33
	(TW)	9	118.8	30	212.3	1.3	0.41	40.1	96.9	23.0	0.26	
	(RAW)	10	118.8	30	212.3	1.55	0.41	44.5	103.8	43.4	0.39	
CAL	SPOIL	1	109.4	30	180.0	1.6	0.66	49.7	109.4	43.4	0.24	0.22
		2	109.4	30	180.0	1.51	0.66	48.9	105.7	33.3	0.20	
		3	109.4	30	180.0	1.53	0.66	46.0	98.6	36.6	0.22	
CAL	SOIL	4	109.4	30	180.0	1.37	0.60	33.8	89.4	56.5	0.48	0.51
		5	109.4	30	180.0	1.48	0.60	35.4	91.5	65.3	0.50	
		6	109.4	30	180.0	1.46	0.60	35.5	88.1	69.0	0.54	
CUR	SPOIL	3	117.9	30	209.3	3.007	0.53	47.1	110.2	38.5	0.13	0.13
CUR	SPOIL	4	117.9	30	209.3	3.08	0.53	53.6	118.3	40.8	0.13	
	(TW)	9	117.9	30	209.3	1.99	0.53	50.9	114.9	30.2	0.15	0.20
	(RAW)	10	117.9	30	209.3	2.125	0.53	48.1	109.4	27.4	0.13	0.18
	(RAW)	11	117.9	29	202.3	2.15	0.53	48.8	113.6	46.4	0.22	
	(TW)	12	117.9	30	209.3	2.1	0.53	52.6	102.0	53.3	0.25	
		15	100.3	30	151.4	0.65	0.53	43.6	101.4	21.6	0.43	0.39
		16	102.0	30	156.6	0.783	0.53	43.6	104.8	22.0	0.35	

CUR	SOIL	1	108.2	30	176.3	3.04	0.37	37.2	94.2	79.9	0.49	0.49
		2	108.2	30	176.3	3.115	0.37	35.0	93.2	80.5	0.49	
		5	117.9	30	209.3	2.116	0.37	42.9	107.8	111.9	0.82	0.80
		6	106.1	30	169.6	2.28	0.37	38.2	100.0	95.4	0.78	
		7	117.9	30	209.3	2.26	0.37	40.1	106.0	97.3	0.69	0.88
		8	117.9	30	209.3	1.6	0.37	40.3	108.9	107.9	1.08	
		13	102.0	36	187.9	0.937	0.37	42.1	90.1	38.4	0.70	0.67
		14	100.3	30	151.4	0.753	0.37	31.4	87.8	21.8	0.64	
GC	SPOIL	1	102.7	29	153.5	1.28	0.67	33.9	92.4	17.1	0.15	0.17
		2	114.0	30	195.6	1.82	0.67	41.2	104.5	24.2	0.12	
		3	114.0	30	195.6	1.75	0.67	47.3	107.3	47.5	0.23	
GC	SOIL	7	120.0	30	216.7	1.93	0.68	56.3	117.7	112.5	0.42	0.40
		8	122.0	24	179.2	1.96	0.68	48.1	118.0	86.5	0.38	
GC	SAND	4	102.7	29	153.6	2.09	0.58	27.4	131.6	451.1	2.95	2.53
		5	102.7	35	185.3	2.24	0.58	24.4	114.1	307.3	1.75	
		6	102.7	30	158.9	2.26	0.58	37.2	158.6	573.4	2.90	
GYA	SPOIL	1	110.4	30	183.4	0.72	0.47	35.2	103.1	13.0	0.26	0.26
		3	101.1	30	153.8	1.96	0.47	27.6	89.2	18.6	0.17	0.16
		4	101.1	30	153.8	1.96	0.47	19.8	80.0	13.9	0.14	
		7	109.4	30	180.0	2.33	0.47	23.4	86.2	23.5	0.17	0.16
		8	109.4	30	180.0	2.22	0.47	35.5	98.5	24.2	0.16	
GYA	SOIL	2	110.4	35	214.0	0.8	0.63	41.7	91.5	8.1	0.09	0.09
		5	101.1	30	153.8	1.8	0.63	36.3	88.3	23.6	0.16	0.14
		6	101.1	30	153.8	1.89	0.63	36.6	97.6	21.5	0.13	
		9	109.4	30	180.0	2.36	0.63	43.4	107.8	69.9	0.29	0.30
		10	93.2	30	130.8	2.36	0.63	33.6	80.0	52.7	0.31	
OC	SPOIL	4	102.4	30	157.8	2.45	0.64	33.7	88.8	25.2	0.12	0.13
		5	102.4	30	157.8	2.21	0.64	32.4	91.5	18.4	0.10	
		6	102.4	30	157.8	1.94	0.64	39.1	95.1	19.9	0.11	
		7	102.4	30	157.8	2.12	0.64	36.2	91.6	31.3	0.17	
		8	102.4	30	157.8	2.2	0.64	na	na	22.4	na	

OC	SOIL	1	102.5	30	158.2	2.14	0.66	44.3	99.0	68.7	0.32	0.25
		2	102.5	30	158.2	2.3	0.66	43.3	95.2	41.8	0.19	
		3	102.4	30	157.8	2.34	0.66	47.5	102.0	58.8	0.24	
TAR	S/S SPOIL	1	100.0	33	165.6	1.14	0.66	47.6	100.3	36.3	0.30	0.21
		2	100.0	30	150.5	1	0.66	32.6	80.9	15.9	0.19	
		3	100.0	33	165.6	1.08	0.66	35.9	84.1	14.0	0.14	
TAR	LITHOSOL	4	100.0	30	150.5	0.783	0.44	35.9	86.3	24.2	0.53	0.29
		5	100.0	30	150.5	0.9	0.44	27.1	72.0	13.6	0.30	
		6	100.0	30	150.5	0.819	0.44	23.4	62.2	16.0	0.41	
veg study 95		9	122.0	30	224.0	1.35	1.00	57.4	119.9	34.5	0.12	
		10	117.0	30	206.0	1.43	1.00	49.7	107.5	29.9	0.11	
TAR	KRASNOZEM	7	100.0	35	175.6	1.26	0.05	25.2	69.3	33.9	4.60	5.84
		8	100.0	35	175.6	0.81	0.05	29.5	76.2	35.6	7.08	
	loose plot	9	100.0	35	175.6	0.76	0.05	23.9	77.3	49.9	11.27	
WAN	SPOIL	1	103.0	30	159.6	0.81	0.59	42.6	96.3	9.2	0.13	0.13
		2	103.0	30	159.6	0.76	0.59	38.0	95.4	8.6	0.14	
		3	121.7	30	223.0	0.79	0.59	53.0	119.6	10.6	0.11	
WAN	SOIL	4	121.7	30	223.0	0.81	0.48	39.5	112.0	11.4	0.16	0.22
		5	111.7	30	187.9	0.77	0.48	38.5	105.2	14.5	0.25	
		6	112.0	30	188.7	0.81	0.48	33.6	103.7	14.1	0.24	
BA	S/STONE SPOIL	1	74.8	30	84.2	0.658	0.69	28.9	66.2	3.5	0.09	0.09
		2	74.8	30	84.2	0.731	0.69	32.2	74.2	3.5	0.08	
		3	74.8	30	84.2	0.831	0.69	29.6	68.2	4.6	0.10	
BA	TOPSOIL	4	81.0	30	98.7	0.728	0.75	30.1	76.6	20.4	0.40	0.42
		5	81.0	30	98.7	0.592	0.75	32.5	79.2	20.1	0.46	
		6	81.0	30	98.7	0.648	0.75	30.8	70.2	18.7	0.41	
BA	CLAY TOPSOIL	7	86.1	30	111.6	1.82	0.39	20.5	69.4	30.1	0.49	0.47
		8	86.1	30	111.6	2.12	0.39	20.4	63.9	31.6	0.45	

		9	86.1	30	111.6	2.17	0.39	23.4	75.6	36.7	0.48	
GRE	PERMIAN SPOIL	1	89.5	30	120.6	1.25	0.62	26.1	73.2	4.4	0.06	0.09
		2	89.5	30	120.6	0.905	0.62	25.1	74.3	4.7	0.09	
		3	89.5	30	120.6	1.06	0.62	34.6	84.3	10.4	0.14	
GRE	TOPSOIL	4	90.1	30	122.2	0.661	0.49	24.6	70.7	9.8	0.31	0.28
		5	90.1	30	122.2	1.14	0.49	27.2	76.9	13.4	0.24	
		6	90.1	30	122.2	1.13	0.49	31.2	79.0	16.8	0.28	
MOU	ROCKY SPOIL	1	94.0	30	133.0	2.52	0.61	29.0	80.9	9.1	0.05	0.09
		2	94.0	30	133.0	2.65	0.61	28.7	75.3	15.2	0.09	
		3	94.0	30	133.0	2.52	0.61	32.7	88.3	20.9	0.12	
MOU	BLACK EARTH	4	91.0	30	124.7	1.79	0.40	27.5	82.6	35.2	0.48	0.40
		5	91.0	30	124.7	1.77	0.40	24.4	81.5	22.3	0.32	
		6	91.0	29	120.6	1.75	0.40	30.0	82.3	28.7	0.39	
MOU	YELLOW SPOIL	7	91.4	30	125.6	1.44	0.54	35.1	82.6	10.1	0.11	0.13
		8	91.4	30	125.6	1.56	0.54	35.5	86.9	13.6	0.14	
		9	91.4	30	125.6	1.48	0.54	31.7	79.8	11.7	0.13	
NEW	ALLUVIAL SAND	1	97.0	29	136.8	1.29	0.58	27.7	82.5	12.5	0.15	0.14
		2	97.0	41	193.4	1.3	0.58	37.1	83.7	13.8	0.12	
		3	97.0	30	141.5	1.41	0.58	31.3	83.6	13.6	0.14	
NEW	CLAY TOPSOIL	4	97.0	55	259.5	1.25	0.24	21.4	64.1	12.1	0.26	0.25
		5	97.0	56	264.2	1.35	0.24	25.0	65.5	9.9	0.19	
		6	97.0	55	259.5	1.37	0.24	26.1	61.4	16.0	0.30	
NEW	GREY MUDSTONE	7	102.2	30	157.2	1.35	0.71	21.1	83.4	2.9	0.03	0.03
		8	102.2	30	157.2	1.14	0.71	30.1	79.9	4.0	0.04	
		9	102.2	30	157.2	1.72	0.71	30.6	84.4	4.1	0.03	

NP	TERTIARY SPOIL	1	95.6	30	137.5	1.72	0.49	36.5	100.0	7.9	0.07	0.08
		2	95.6	30	137.5	1.61	0.49	27.8	82.4	7.3	0.08	
		3	95.6	30	137.5	1.61	0.49	32.3	92.1	7.5	0.08	
	added mesh	4	95.6	40	183.4	1.68	0.49	23.7	70.1	5.3	0.05	
NP	PERMIAN SPOIL	5	83.4	30	104.7	1.59	0.72	31.0	74.6	3.0	0.03	0.02
		6	83.4	30	104.7	1.95	0.72	27.3	68.8	2.7	0.02	
		7	83.4	35	122.2	1.31	0.72	29.3	73.0	2.2	0.02	
NP	SANDY TOPSOIL	8	101.6	29	150.2	1.61	0.70	42.9	102.2	154.7	0.94	0.94
		9	101.6	30	155.4	1.45	0.70	40.0	98.7	137.6	0.95	
PD	TERTIARY SPOIL	1	90.6	30	123.5	0.943	0.55	30.2	77.4	8.3	0.15	0.11
		2	90.6	30	123.5	1.04	0.55	13.1	53.0	4.2	0.09	
		3	90.6	30	123.5	1.06	0.55	17.1	58.0	4.2	0.09	
PD	PERMIAN SPOIL	4	76.5	30	88.1	0.878	0.62	30.7	71.4	3.6	0.08	0.09
		5	98.4	30	145.6	1.09	0.62	34.3	90.7	6.2	0.07	
		6	98.7	30	146.6	0.823	0.62	42.5	99.0	7.8	0.11	
PD	TOPSOIL	7	98.7	30	146.6	0.693	0.71	39.2	91.3	11.2	0.17	0.16
		8	98.7	30	146.6	0.803	0.71	46.7	105.9	13.8	0.16	
		9	91.8	30	126.9	0.834	0.71	39.0	91.5	11.0	0.15	
SAR	TERTIARY SPOIL	1	80.2	30	96.7	0.46	0.53	30.5	79.6	4.7	0.21	0.20
		2	80.2	30	96.7	0.46	0.53	29.9	76.9	3.3	0.15	
		3	80.2	30	96.7	0.456	0.53	31.7	81.6	5.8	0.25	
SAR	TOPSOIL	4	86.7	30	113.2	0.453	0.69	32.9	80.0	2.5	0.08	0.08
		5	86.7	30	113.2	0.456	0.69	25.8	73.0	2.6	0.09	
		6	86.7	30	113.2	0.441	0.69	29.4	77.1	2.6	0.09	

APPENDIX 2: SALTRO Model (1D dimesionless)

Transport equations:

local time rate of change in quantity density + flux divergence – generation = 0

Water transport: Water flux law (Darcy Buckingham law): Co-ordinate transformation: (x=0 fixed to ersosion surface)

$$\frac{D}{Dt}\beta\theta + \frac{\partial q}{\partial x} - W = 0, \quad q = -K\frac{\partial \psi}{\partial x} \qquad \frac{D}{Dt} \equiv \frac{\partial}{\partial t} - v_e E \frac{\partial}{\partial x}$$

Water potential:

$$\psi = \psi_m + \psi_p - \cos(s)\int_0^x \beta \, dx \qquad \xi_0 \equiv \xi|_{x=0}$$

Surface water recharge (Hortonian excess):

$$q_r = q_f - q_{ev} + v_e E \beta_0 \theta_0 - q_0$$

(q_f includes rain + runon)

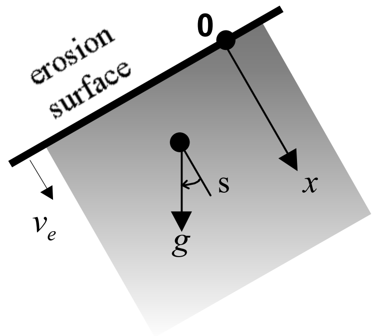

Evaporation:

$$q_{ev} = \frac{f_s \cdot e_{pan} \cdot (\exp(\phi\psi_0) - \exp(\phi\psi_e))}{(1 - \exp(\phi\psi_e))}$$

$$\phi = \frac{gLM}{RT}$$ (evaporation energy co-efficient)

Surface hydraulic seal:

$$q_0 = \frac{1}{R_f}(\psi_- - \psi_0)$$

Surface boundary condition:

$\theta_- = \theta_-(\psi_-)$ governs the surface boundary condition :

$\theta_- < \theta_s \Rightarrow q_0 = q_f - q_{ev}$ (flux boundary condition)

$\theta_- \geq \theta_s \Rightarrow \psi_- = h$ (value boundary condition)

Surface water model:

$$\frac{dh}{dt} = q_r - q_h(h), \quad q_h = v_1 (h - h_c)^{v_2}$$

Water content – matric water potential relation (van Genuchten's formula):

$$S_e = \left(1 + (-\alpha\psi_m)^n\right)^{-m} \quad m = 1 - \tfrac{1}{n} \qquad S_e = \frac{\theta - \theta_r}{\theta_s - \theta_r}$$

Water conductivity relation (Mualem – van Genuchten prediction formula):

$$\beta K = K_s S_e^{0.5}\left(1 - (1 - S_e)^{\frac{1}{m}})^m\right)^2$$

The Erosion Effect Number (EEN):

$$E = \frac{\rho_w a_0}{K_{S0} g \rho_b}$$

Material – spacial co-ordinate transformation:

$$z = \int_0^x \beta \, dx, \quad \beta = 1 + \frac{\partial u}{\partial x} = \frac{\rho_b}{\rho_s \theta_S} = \frac{\rho_b (1+e)}{\rho_s}$$

Material expansion relation:

$\beta = \beta(S_e)$ (time invariant)

Solute transport equation:

$$\frac{D}{Dt}\left(\varphi\beta(\theta - \theta_r)\right) + \frac{Dm_{ps}}{Dt} + \frac{Dm_{rs}}{Dt} + \frac{\partial J}{\partial x} - \Phi = 0$$

Solute flux law (viscous transport only):

$$J = \varphi q - \lambda_p |q| \frac{\partial \varphi}{\partial x}$$

Solute retention model:

$$\frac{Dm_{rs}}{Dt} = \alpha_r \left(k_r m_{fs} - m_{rs}\right) \qquad m_{fs} = \varphi\beta(\theta - \theta_r) + m_{ps}$$

$$r = \left.\left(\frac{m_{rs}}{m_{fs}}\right)\right|_{t=0}$$ (initial retention ratio)

$m_{ps} = 0 \Leftarrow \varphi < \varphi_s$ (instantaneous buffering by precipitated solute)

$m_{ps} \geq 0 \Leftarrow \varphi = \varphi_s$

$m_{ps} > 0 \Rightarrow \varphi = \varphi_s$

Solute release:

$$J_r = v_e E \cdot \left.\left(\varphi\beta(\theta - \theta_r) + m_{ps} + m_{rs}\right)\right|_0 - J_0$$

Perfect mixing condition:

$$\varphi_h = \varphi_0$$

Surface water solute balance:

$$\frac{d(\varphi_h h)}{dt} = J_r - J_h + J_{ro} \qquad J_h = \varphi_h q_h$$

In practice, for SALTRO, material expansion is ignored, $\beta \equiv 1$

In the case of fast runoff $h \equiv 0$

DIMENSIONING:

$$\breve{x} = xL \qquad \breve{t} = \frac{tL\rho_w}{K_{S0} g}$$

$$\breve{\psi} = \psi g L \qquad \breve{h} = hgL \qquad \breve{m}_w = \rho_w \beta\theta \qquad \breve{m}_{fs/rs/ps} = m\rho_w$$

$$\breve{K} = KK_{S0} \qquad \breve{W} = \frac{WK_{S0} g}{L} \qquad \breve{\Phi} = \frac{\Phi K_{S0} g}{L} \qquad \breve{\lambda}_p = \lambda_p L \qquad \breve{\alpha}_r = \frac{\alpha_r K_{S0} g}{\rho_w L}$$

$$\breve{v}_e = \frac{v_e a_0}{\rho_b}$$

NOMENCLATURE

t time

x spatial co-ordinate (in material space)

s	slope angle from horizontal
g	gravitational acceleration
v_e	erosion velocity (in material space)
E	erosion effect number
m_W	water content
q	water flux density
q_r	surface water charge rate (Hortonian excess)
q_f	rain + run-on water load rate
q_{ev}	evaporation rate
q_h	surface discharge rate
e_{pan}	pan evaporation
f_s	evaporation parameter
ϕ	evaporation energy coefficient
R_f	film seal parameter
W	water source density (in material space)
K	water conductivity (in material space)
K_S	saturated water conductivity (in material space)
K_{S0}	standard water conductivity (usually K_S)
ψ	water potential – units of specific energy
ψ_m	matric water potential
ψ_p	over pressure water potential
ψ_e	air dry water potential
h	surface pond head
h_c	depression storage head
z	spatial co-ordinate
β	material expansion (Jacobian of matrix displacement)
u	material displacement
ρ_b	material bulk density (in material space)
ρ_s	material solid density
ρ_w	condensed water density
θ	volumetric water fraction
θ_r	residual water content
θ_s	saturated water content
θ_S	volumetric material solid fraction
e	void ratio
φ	solution concentration (mass ratio)
φ_h	surface water concentration
φ_s	saturation concentration
m_{fs}	free solute density

m_{ps}	precipitated solute density
m_{rs}	retained solute density
J	solute flux density
J_r	released solute rate
J_{ro}	run-on solute influx
J_h	discharged solute rate
Φ	solute source rate
λ_p	solute dispersivity
α_r	retention transfer rate
k_r	solute retention limit
r	initial retention ratio
L	characteristic length
a	erosion rate (in material space)
a_0	standard erosion rate (lab erosion for nominal 100mm/h x 30min simulated storm @ 20deg)
M	water molecular mass
R	universal gas constant
T	effective environmental Kelvin temperature

m_{ps}	precipitated solute density
m_{rs}	retained solute density
J	solute flux density
J_r	released solute rate
J_{ro}	run-on solute influx
J_h	discharged solute rate
Φ	solute source rate
λ_p	solute dispersivity
α_r	retention transfer rate
k_r	solute retention limit
r	initial retention ratio
L	characteristic length
a	erosion rate (in material space)
a_0	standard erosion rate (lab erosion for nominal 100mm/h x 30min simulated storm @ 20deg)
M	water molecular mass
R	universal gas constant
T	effective environmental Kelvin temperature

APPENDIX 3: The finite element method employed by SALTRO

Firstly the equations must be converted to an appropriate formulation. The equation should remain applicable across the entire range of the dependent variable for computational convenience. Furthermore, for computational stability, all coefficients must remain bounded for the usual choice of constitutive realtionships.

The equation is then generically cast as:

$$L(\xi) = 0$$

Example (water transport):

$$L(\psi) = C\left(\frac{\partial}{\partial t} - v_e E \frac{\partial}{\partial x}\right)\psi + \frac{\partial}{\partial x}\left(K\left(\beta \cos(s) - \frac{\partial \psi}{\partial x}\right)\right) - W \qquad \psi_{ng} \to \psi$$

$$C = \begin{cases} \left(\beta + \theta \dfrac{d\beta}{d\theta}\right)\dfrac{d\theta}{d\psi_m}, & \psi \le 0 \\ 0, & \psi > 0 \end{cases} \qquad \psi \in (-\infty, \infty)$$

The soulution is approximated by a finite element construction,

$$\xi' = \sum_{i=0}^{n} \Xi_i(t) \cdot \Lambda_i(x)$$

Galerkin weighted residual method requires that: $\int_\Omega L(\xi') \cdot \Lambda_i d\Omega = 0$ for $i = 0, 1, 2, \ldots, n$

And economical computation requires that the shape functions be chosen such that,

$\xi'(x_i, t) = \Xi_i$ for $i = 0, 1, 2, \ldots, n$

This leads to :

For the example:

$$\sum_{jk}\left\{\frac{d\Psi_j}{dt} C_k U_{ijk} - v_e E \Psi_j C_k V_{ijk} - \cos(s) K_j B_k Y_{ijk} + \Psi_j K_k Z_{ijk}\right\} - \sum_j W_j T_{ij} + [\Lambda_i q]_{\partial\Omega} = 0$$

for $i = 0, 1, 2, \ldots, n$

$$T_{ij} = \int_\Omega \Lambda_i \Lambda_j d\Omega \qquad V_{ijk} = \int_\Omega \Lambda_i \frac{d\Lambda_j}{dx} \Lambda_k d\Omega \qquad Z_{ijk} = \int_\Omega \frac{d\Lambda_i}{dx}\frac{d\Lambda_j}{dx} \Lambda_k d\Omega$$

$$U_{ijk} = \int_\Omega \Lambda_i \Lambda_j \Lambda_k d\Omega \quad Y_{ijk} = \int_\Omega \frac{d\Lambda_i}{dx} \Lambda_j \Lambda_k d\Omega$$

which reduces to an easily inverted linear tridiagonal system :

$$a_i \frac{d\Xi_{i-1}}{dt} + b_i \frac{d\Xi_i}{dt} + c_i \frac{d\Xi_{i+1}}{dt} + e_i \Xi_{i-1} + f_i \Xi_i + g_i \Xi_{i+1} = h_i \qquad \text{for } i = 0, 1, 2, \ldots, n$$

An implicit march in time can be chosen where,

$$\left.\frac{d\Xi}{dt}\right|_v \approx \frac{\Xi_v - \Xi_{v-1}}{t_v - t_{v-1}}$$

APPENDIX 3: The finite element method employed by SALTRO

Firstly the equations must be converted to an appropriate formulation. The equation should remain applicable across the entire range of the dependent variable for computational convenience. Furthermore, for computational stability, all coefficients must remain bounded for the usual choice of constitutive realtionships.

The equation is then generically cast as:

$$L(\xi) = 0$$

Example (water transport):

$$L(\psi) = C\left(\frac{\partial}{\partial t} - v_e E\frac{\partial}{\partial x}\right)\psi + \frac{\partial}{\partial x}\left(K\left(\beta\cos(s) - \frac{\partial\psi}{\partial x}\right)\right) - W \qquad \psi_{ng} \to \psi$$

$$C = \begin{cases}\left(\beta + \theta\dfrac{d\beta}{d\theta}\right)\dfrac{d\theta}{d\psi_m}, & \psi \le 0 \\ 0, & \psi > 0\end{cases} \qquad \psi \in (-\infty, \infty)$$

The soulution is approximated by a finite element construction,

$$\xi' = \sum_{i=0}^{n} \Xi_i(t) \cdot \Lambda_i(x)$$

Galerkin weighted residual method requires that: $\int_\Omega L(\xi') \cdot \Lambda_i d\Omega = 0$ for $i = 0, 1, 2, \ldots, n$

And economical computation requires that the shape functions be chosen such that,

$\xi'(x_i, t) = \Xi_i$ for $i = 0, 1, 2, \ldots, n$

This leads to :

For the example:

$$\sum_{jk}\left\{\frac{d\Psi_j}{dt}C_k U_{ijk} - v_e E\Psi_j C_k V_{ijk} - \cos(s)K_j B_k Y_{ijk} + \Psi_j K_k Z_{ijk}\right\} - \sum_j W_j T_{ij} + [\Lambda_i q]_{\partial\Omega} = 0$$

for $i = 0, 1, 2, \ldots, n$

$$T_{ij} = \int_\Omega \Lambda_i \Lambda_j d\Omega \qquad V_{ijk} = \int_\Omega \Lambda_i \frac{d\Lambda_j}{dx}\Lambda_k d\Omega \qquad Z_{ijk} = \int_\Omega \frac{d\Lambda_i}{dx}\frac{d\Lambda_j}{dx}\Lambda_k d\Omega$$

$$U_{ijk} = \int_\Omega \Lambda_i \Lambda_j \Lambda_k d\Omega \quad Y_{ijk} = \int_\Omega \frac{d\Lambda_i}{dx}\Lambda_j \Lambda_k d\Omega$$

which reduces to an easily inverted linear tridiagonal system :

$$a_i \frac{d\Xi_{i-1}}{dt} + b_i \frac{d\Xi_i}{dt} + c_i \frac{d\Xi_{i+1}}{dt} + e_i \Xi_{i-1} + f_i \Xi_i + g_i \Xi_{i+1} = h_i \qquad \text{for } i = 0, 1, 2, \ldots, n$$

An implicit march in time can be chosen where,

$$\left.\frac{d\Xi}{dt}\right|_v \approx \frac{\Xi_v - \Xi_{v-1}}{t_v - t_{v-1}}$$

APPENDIX 4: Method for finding the optimal basic material parameters in SALTRO

Parameter vector : $\bar{\zeta}$

Optimum parameter vector : $\bar{\zeta}^*$

Objective function to be minimised : $O(\bar{\zeta}) = \sum_{\mu=1}^{n} e_\mu^{\ 2}$

$e_\mu = y_\mu - f_\mu$ $\quad$ y_μ is data

f_μ is model prediction

Gradient methods : $\bar{\zeta}_{i+1} = \bar{\zeta}_i - R_i \bar{q}_i \quad \bar{q}_i = \frac{\partial O}{\partial \bar{\zeta}_i}$ and i is the iteration index.

The method is acceptable, (i.e. $O(\bar{\zeta}_{i+1}) < O(\bar{\zeta}_i)$ for sufficiently small $\|R_i\|$), when R_i is positive definite.

Near $\bar{\zeta}_i$, $\quad O \sim Q_i(\bar{\zeta}) = O(\bar{\zeta}_i) + \bar{q}_i^{\ T}(\bar{\zeta} - \bar{\zeta}_i) + \frac{1}{2}(\bar{\zeta} - \bar{\zeta}_i)^T H_i (\bar{\zeta} - \bar{\zeta}_i)$

where H is the Hessian having the components $H_{\alpha\beta} = \frac{\partial^2 O}{\partial \zeta_\alpha \partial \zeta_\beta}$.

Then Q predicts $\bar{\zeta}^*$ by the stationary condition $\frac{\partial Q_i}{\partial \bar{\zeta}} = \bar{0}$

$\rightarrow$ Newton-Raphson step : $\bar{\zeta}_{i+1} = \bar{\zeta}_i - H_i^{-1} \bar{q}_i$

$$H_{\alpha\beta} = 2\sum_{\mu=1}^{n} \left[\frac{\partial f_\mu}{\partial \zeta_\alpha} \frac{\partial f_\mu}{\partial \zeta_\beta} - e_\mu \frac{\partial^2 f_\mu}{\partial \zeta_\alpha \partial \zeta_\beta} \right] \qquad A_{\alpha\beta} = 2\sum_{\mu=1}^{n} \left[\frac{\partial f_\mu}{\partial \zeta_\alpha} \frac{\partial f_\mu}{\partial \zeta_\beta} \right]$$

Gauss approximation : $H \approx A$

Marquardt method ensures acceptability of method, by choosing,

$R_i = \left(A_i + \lambda_i B_i^2\right)^{-1}$ where $B = diag\left\{ |A_{ii}|^{\frac{1}{2}} \right\}$ for example.

λ_i is adjusted dynamically in the algorithm.

APPENDIX 4: Method for finding the optimal basic material parameters in SALTRO

Parameter vector : $\bar{\zeta}$

Optimum parameter vector : $\bar{\zeta}^*$

Objective function to be minimised : $O(\bar{\zeta}) = \sum_{\mu=1}^{n} e_\mu^{\,2}$

$e_\mu = y_\mu - f_\mu$ $\qquad y_\mu$ is data

f_μ is model prediction

Gradient methods : $\bar{\zeta}_{i+1} = \bar{\zeta}_i - R_i \bar{q}_i \quad \bar{q}_i = \dfrac{\partial O}{\partial \bar{\zeta}_i}$ and i is the iteration index.

The method is acceptable, (i.e. $O(\bar{\zeta}_{i+1}) < O(\bar{\zeta}_i)$ for sufficiently small $\|R_i\|$), when R_i is positive definite.

Near $\bar{\zeta}_i$, $\qquad O \sim Q_i(\bar{\zeta}) = O(\bar{\zeta}_i) + \bar{q}_i^{\,T}(\bar{\zeta} - \bar{\zeta}_i) + \tfrac{1}{2}(\bar{\zeta} - \bar{\zeta}_i)^T H_i (\bar{\zeta} - \bar{\zeta}_i)$

where H is the Hessian having the components $H_{\alpha\beta} = \dfrac{\partial^2 O}{\partial \zeta_\alpha \partial \zeta_\beta}$.

Then Q predicts $\bar{\zeta}^*$ by the stationary condition $\dfrac{\partial Q_i}{\partial \bar{\zeta}} = \bar{0}$

$\rightarrow$ Newton-Raphson step : $\bar{\zeta}_{i+1} = \bar{\zeta}_i - H_i^{-1} \bar{q}_i$

$$H_{\alpha\beta} = 2\sum_{\mu=1}^{n}\left[\frac{\partial f_\mu}{\partial \zeta_\alpha}\frac{\partial f_\mu}{\partial \zeta_\beta} - e_\mu \frac{\partial^2 f_\mu}{\partial \zeta_\alpha \partial \zeta_\beta}\right] \qquad A_{\alpha\beta} = 2\sum_{\mu=1}^{n}\left[\frac{\partial f_\mu}{\partial \zeta_\alpha}\frac{\partial f_\mu}{\partial \zeta_\beta}\right]$$

Gauss approximation : $H \approx A$

Marquardt method ensures acceptability of method, by choosing,

$R_i = \left(A_i + \lambda_i B_i^2\right)^{-1}$ where $B = diag\left\{|A_{ii}|^{\frac{1}{2}}\right\}$ for example.

λ_i is adjusted dynamically in the algorithm.

APPENDIX 5: Field Erosion Survey

Survey Data Sheet 1 - Erosion (Date : / /)

Survey by (Name) : ______________________________ Mine : ____________________
Rehab Site ID and Age : ____
Slope Length (m) : _______ Slope Angle (% or X°) : _______

State of Erosion (A,S,P) : _________ Sheet Erosion (0,1,2,3) :__________

Rill Erosion (0,1,2,3) : ____________ Gully Erosion (0,1,2,3) : __________

Tunnel Erosion (0,1) : _____________

Tansect 1 : 1/4 up slope Transect 2 : 1/2 up slope
Transect 3 : 3/4 up slope (1/6 up slope)
(5/6 up slope)

Distance (m)	Gully Width (cm)	Gully Depth (cm)	Shape (s/v)

....table continues....

Survey Data Sheet 1 - Cover and Vegatation (Date: / /)

**** **Please remember to take photographs of all cover quadrats**

Survey by (Name) : ______________________________ Mine : ____________________
Rehab Site ID and Age : ____

1. Cover (vegetation, rocks, litter, intersecting with soil surface)
Estimate rock cover seperately.

Quadrat #	Cover Class	Quadrat #	Cover class	Quadrat #	Cover Class

2. Vegetation Characteristcs ***** Please note photos useful for future interpretation

Give visually assessed estimates of the following,

Vegetation Form (tick) : None( ) Grass( ) Grass & Trees( ) Trees ( )
Proportion of total vegetation composed of grasses : __________________
Grass species present (common name and or Genus ok) :
____

Tree/shrub species present (common name and or Genus ok) :

____
____
____
____

Tree/ Shrub Stems/ ha : ____
Average Height of trees/shrubs : ______________________________________

What % of the ground is covered by the canopy of
(a) Grasses : _________________ Canopy Height : ____________________
(b) Trees and Shrubs : _________________ Canopy Height : ____________

OTHER COMMENTS (VEGETATION OR EROSION)